Physics – Uspekhi **54** (9) 939 – 974 (2011)

CONFERENCES AND SYMPOSIA

PACS numbers: 01.10.Fv, **01.52.+r**, **01.65.+g**, 14.60.Pq, **14.60.–z**, 25.30.Pt, **26.65.+t**, **28.60.+s**, **29.20.–c**, 29.40.Ka, 32.80.Qk, 32.80.Wr, **42.55.–f**, 87.56.B–, 95.55.Vj, 96.50.sb, 96.50.sh, 96.60.Vg

Forty years of the Institute for Nuclear Research (Scientific session of the Physical Sciences Division of the Russian Academy of Sciences, 22 December 2010)

DOI: 10.3367/UFNe.0181.201109e.0973

On 22 December 2010, the scientific session of the Physical Sciences Division of the Russian Academy of Sciences (RAS), devoted to the 40th anniversary of the Institute for Nuclear Research, RAS, was held at the Institute for Nuclear Research, RAS in Troitsk.

The agenda of the session announced on the website www.gpad.ac.ru of the RAS Physical Sciences Division listed the following reports:

(1) **Matveev V A** (Institute for Nuclear Research, RAS, Moscow) "Introductory word";

(2) **Gavrin V N** (Institute for Nuclear Research, RAS, Moscow) "Contribution of the SAGE results to the understanding of solar physics and neutrino physics";

(3) **Domogatsky G V** (Institute for Nuclear Research, RAS, Moscow) "Baikal neutrino experiment";

(4) **Tkachev I I** (Institute for Nuclear Research, RAS, Moscow) "Observation of the Greisen–Zatsepin–Kuz'min effect at the Telescope Array Observatory";

(5) **Kudenko Yu G** (Institute for Nuclear Research, RAS, Moscow) "Neutrino T2K experiment: the first results";

(6) **Sadykov R A** (Institute for Nuclear Research, RAS, Moscow) "Fields of study of condensed media at the neutron facility at the INR, RAS";

(7) **Zhuikov B L** (Institute for Nuclear Research, RAS, Moscow) "Production of isotopes at the INR, RAS: reality and prospects."

The papers written on the base of reports 1–5 and 7 are published below.

In addition, the paper "High-power diode-pumped alkali lasers" by A M Shalagin is published. The paper is based on the report presented at the scientific session of the General Assembly of the Physical Sciences Division, RAS (13 December 2010) devoted to the 50th anniversary of the laser, the main materials of the session having been published in *Usp. Fiz. Nauk* **181** (8) 867 (2011) [*Phys. Usp.* **54** 837 (2011)]

Uspekhi Fizicheskikh Nauk **181** (9) 973 – 1016 (2011)
DOI: 10.3367/UFNr.0181.201109e.0973

PACS numbers: **01.52.+r**, **01.65.+g**, **14.60.–z**
DOI: 10.3367/UFNe.0181.201109f.0973

Institute for Nuclear Research of the Russian Academy of Sciences turns 40

V A Matveev

The Institute for Nuclear Research (INR), RAS was founded by the USSR Covernment's decision of December 1970 on the initiative of N N Bogoliubov and M A Markov supported by M V Keldysh, the President of the Academy of Sciences of the USSR, with the aim of creating the modern experimental base and pursuing research activities in the fields of the physics of elementary particles, fundamental nuclear physics, the physics of cosmic rays, and neutrino astrophysics.

The director of the Institute from the day of its foundation until 1986 was Academician A N Tavkhelidze.

In 1978, the Institute began to build on the territory of the Scientific Center of the USSR Academy of Sciences in Troitsk, Moscow region, a facility based on a high-current linear accelerator of protons and negative hydrogen ions with the rated energy up to 600 MeV and average beam current up to 0.5 mA. At present, construction of the Center of Neutron

Administration and laboratory wing of INR, RAS in Troitsk.

V A Matveev Institute for Nuclear Research,
Russian Academy of Sciences, Russian Federation
E-mail: matveev@inr.ac.ru

Uspekhi Fizicheskikh Nauk **181** (9) 973 – 975 (2011)
DOI: 10.3367/UFNr.0181.201109f.0973
Translated by M Sapozhnikov; edited by A Radzig

and Isotopic Research and the Proton Therapy Complex is being completed on the base of this facility.

The Institute provided the construction of the Baksan Neutrino Observatory in the Elborus region of the Kabardino-Balkarian Republic in the Northern Caucasus with a set of neutrino telescopes in deep underground laboratories and above-ground large-area facilities for studying extensive air showers and high-energy cosmic rays. In 1978, an underground scintillation telescope, the largest in that time, was commissioned here for studying atmospheric neutrino fluxes penetrating through the thickness of Earth and for searching for neutrino radiation produced during the collapse of massive stars in the Galaxy.

On 23 February 1987, a neutrino signal generated by the explosion of the 1987A supernova in the Large Magellanic Cloud at a distance of about 150 kpc from Earth was first detected with this telescope and simultaneously with three other large-scale neutrino telescopes: Kamiokande-II (Japan), IMB (Irvine–Michigan–Brookhaven) (USA), and the LSD (Liquid Scintillation Detector) Russian–Italian telescope under Mont Blanc, Italy).

In 1991, the construction of the unique Gallium–Germanium Neutrino Telescope with a liquid-metal gallium target of a mass close to 60 t, which has no counterparts anywhere in the world, was accomplished at the underground laboratory (the site depth is 4800 m of water equivalent) of the Baksan Neutrino Observatory. The investigation of solar neutrino fluxes performed by Russian and American scientists for more than 20 years on this telescope [Soviet–American Gallium Experiment (SAGE)] confirmed experimentally for the first time the thermonuclear nature of solar energy and made an important contribution to the discovery of the fundamental phenomenon of neutrino oscillations.

The Institute constructed the world's first stationary deep-sea neutrino telescope in Lake Baikal at a depth of more than 1 km for studying natural high-energy neutrino fluxes and searching for new heavy particles, such as superheavy magnetic monopoles, and neutralinos. Based on this telescope, a project is being developed at present for constructing a deep-sea neutrino telescope with a volume of up to 1 km^3.

The Institute is one of the acknowledged leaders in the investigations of problems of neutrino astrophysics, the physics of superhigh-energy cosmic rays, and studies of interrelations between the physics of elementary particles, astrophysics, and cosmology.

Along with the telescopes mentioned above, the 100-t Collapse scintillation facility located in salt mines in Artemovsk (Ukraine) is well known around the world. This facility was a prototype of the large-scale neutrino Large Volume Detector (LVD) developed in cooperation between the Russian Academy of Sciences and the Instituto Nazionale di Fizica Nucleare (INFN) (Italy) and located at underground Gran Sasso laboratory.

The record-sensitive Troitsk-ν-Mass Setup for searching the mass of an electron antineutrino in precision studies of the decay spectrum of gaseous tritium with a wide-aperture superconducting magnetic spectrometer is also well known in the scientific world. Today, this setup is being modernized to increase its sensitivity to the neutrino mass to a value of better than 1 eV.

The scientific schools of N N Bogoliubov, M A Markov, A N Tavkhelidze, I M Frank, G T Zatsepin, and A E Chudakov have been established at the Institute, and are conducting active studies at present. The impressive advances of theorists at the Institute include, notably, the prediction of the spectrum cut-off for superhigh-energy cosmic rays (the Zatsepin–Kuzmin–Greisen effect), the discovery of the specific features of neutrino oscillations in matter (the Mikheyev–Smirnov–Wolfenstein effect), the theoretical discovery of the monopole catalysis of proton decay (the Rubakov effect), the discovery of the properties of power asymptotics of exclusive processes (the Matveev–Muradyan–Tavkhelidze quark counting formulas), calculations of multiloop radiative effects in quantum chromodynamics (Chetyrkin, Tkachev, Kataev, Larin), the study of the baryon asymmetry of the Universe and, in particular, the consideration of the nontrivial structure of the ground state in the theory of quantized gauge fields (Kuzmin, Rubakov, Shaposhnikov), the study of the orthopositronium problem (Gninenko, Krasnikov), and the investigation of the enigmas of the physics of superhigh-energy cosmic rays (Berezinsky, Kuzmin, Rubakov, Troitsky, et al.)

INR scientists have made an important contribution to the study of rare decays of pions and kaons on the basis of the large Istra facility constructed by them using the beam of the U-70 proton accelerator at the Institute of High-Energy Physics in Protvino, and also to the study of problems of relativistic nuclear physics using the beams of accelerators at the Joint Institute for Nuclear Research (Dubna) and the SPS (Super-Proton Synchrotron) at CERN. Investigations are under way on the parameters of neutrino oscillations in the OPERA (Oscillation Project with Emulsion-tRacking Apparatus, Italy) and K2K (KEK-to-Kamioka, Japan) experiments and cosmic rays in the Caucasus, Tibet, the Transbaikal region, Japan, and the USA.

The Institute for Nuclear Research, RAS began to collaborate with CERN in 1993, taking part in the NOMAD (Neutrino Oscillation MAgnetic Detector) experiments and making a contribution to the construction of an electromagnetic spectrometer. At present, the Institute is actively participating in the CMS (Compact Muon Spectrometer), ALICE (A Large Ion Collider Experiment), and LHCb (Large Hadron Collider beauty) experiments at the Large Hadron Collider (LHC), the NA61 and NA62 experiments at the SPS, and the CAST (CERN Axion Solar Telescope) experiments.

In 2002, INR, RAS founded the International Academician Markov Prize for work that has made an outstanding contribution to fundamental physical studies in the fields of science closely related to the scientific program of the Institute.

In the 40 years since its foundation, the Institute has become one of the leading scientific centers in Russia and the world in the fields of fundamental and applied nuclear physics, one of the pioneers of 'underground and deep-sea neutrino physics', which has actively been developed throughout the world over the last decades.[1]

The scientists of the Institute have obtained fundamental results in the fields of elementary particle and nuclear physics, neutrino astrophysics, theoretical physics, and cosmology.

The 40th anniversary marks a mature age. The Institute and its collective body have big plans of development in accordance with the new challenges of fundamental science and the demands of innovation development of economics in our country — the economics of knowledge.

I would like to wish the collective body of the Institute great new enterprises and scientific discoveries.

[1] More detailed information on INR, RAS is presented on the websites www.inr.ru and www.inr.ac.ru.

PACS numbers: **26.65.+t**, 95.55.Vj, 96.60.Vg
DOI: 10.3367/UFNe.0181.201109g.0975

The Russian-American gallium experiment SAGE

V N Gavrin

1. Introduction

Ever since W Pauli postulated in 1933 the existence of the neutrino, it remains one of the most interesting particles in nuclear physics. The concept of a neutrino in the beta-decay theory, which was developed by E Fermi a year later, proved to be so fruitful that the neutrino was confidently introduced to the family of elementary particles long before its discovery [1].

By 1956, when C Cowan and F Reines with coworkers succeeded to detect the free neutrino for the first time, the characteristics of this particle had been already established for the most part from indirect data obtained in many preceding experiments with natural and artificial beta-decay and K-captured isotopes and in studies of meson–neutrino reactions in accelerators.

The notion of the neutrino based on these studies was in good agreement with all experimental observations until the 1970s–1980s, although the questions of the existence of the neutrino mass and its nature (the Dirac or Majorana neutrino) remained open. In this period, the results of the first solar neutrino experiments were obtained, which led to changing the view of the neutrino and thereby of a number of phenomena in the modern physical picture of the world.

2. The solar neutrino problem

The aim of the first solar neutrino experiment started in the late 1960s was to verify the theory of the structure and evolution of stars, which forms the basis of the Standard Solar Model (SSM) [2].

It was believed that energy in the Sun is produced due to thermonuclear transformation of four protons to an α particle in reaction chains where two positrons and two neutrinos are created. It was also assumed that weakly interacting neutrinos pass through the Sun and reach Earth without any changes.

Thus, the recording of the energy spectrum of neutrinos should give information on conditions under which thermonuclear reactions proceed in the Sun. M A Markov pointed out in 1964: "It is widely accepted that the energy balance of stars like the Sun is supported by nuclear reactions proceeding in the depths of a celestial body. Although this hypothesis looks very plausible, nevertheless, the existence of such processes in the Sun has not been experimentally confirmed to date, and surprises with far-reaching consequences are possible, in principle, here" [3].

Gavrin V N Institute for Nuclear Research,
Russian Academy of Sciences, Russian Federation
E-mail: gavrin@inr.ru

Uspekhi Fizicheskikh Nauk **181** (9) 975–984 (2011)
DOI: 10.3367/UFNr.0181.201109g.0975
Translated by M Sapozhnikov; edited by A Radzig

Indeed, the first solar neutrino flux measurement in the USA with a chlorine detector containing a 610-t chlorine-containing target revealed a considerably smaller number of neutrinos than that predicted by the detailed models of physical processes in the Sun [4]. This experiment was started in the late 1960s and continued until the mid-1980s. In it researchers realized B Pontecorvo's remarkable idea of detecting solar neutrinos by the radiochemistry method by measuring the production rate of ^{37}Ar isotopes in the reaction of neutrino capture by ^{37}Cl nuclei in a chlorine target [5]. Although various SSMs predicted somewhat different rates for the chlorine experiment, the capture rates in all these models considerably exceeded the values observed. This discrepancy became the widely known 'solar neutrino problem', which existed for more than 30 years.

For 20 years, the chlorine experiment remained the only one for detecting solar neutrinos. The chlorine target utilized in this experiment was sensitive solely to the highest-energy neutrinos in the solar spectrum, produced in the decay of ^{8}B nuclei and to a fraction produced in the decay of ^{7}Be. The reactions in which these neutrinos are created make an insignificant contribution to the energy produced in the Sun, while the intensity of these neutrino fluxes strongly depends on the temperature at the center of the Sun. The very low intensity of neutrino fluxes observed in experiments cannot be explained within the framework of the SSM.

As a result, a great number of so-called nonstandard models were constructed in which agreement with the chlorine-experiment result was achieved by introducing some temperature lowering mechanisms at the center of the Sun. However, most of these models encountered problems in describing other measured parameters of the Sun.

An alternative explanation of the discrepancy of the chlorine-experiment results with SSM predictions could be the existence of neutrino oscillations. In the chlorine experiment, neutrinos are detected by the reaction of inverse β-decay and, therefore, the chlorine detector is only sensitive to electron neutrinos. If neutrinos oscillate during their motion from the central regions of the Sun to Earth (and, hence, change their flavor), the chlorine detector can detect only a fraction of their flux.

The idea that neutrinos may oscillate was proposed by Pontecorvo [6] already in the early 1960s, but was not generally accepted because it led to a strong mixing of neutrinos, which was inconsistent with the concepts existing at that time.

In the mid-1980s, measurements of a solar neutrino flux were started in Japan by using a large water Cherenkov detector (the Kamiokande experiment) sensitive to recoil electrons created in elastic collisions of solar ^{8}B-neutrinos with target electrons. As in the chlorine experiment, the measured flux proved to be lower than that predicted by the SSM, and so the existence of the neutrino deficit in the high-energy part of the solar neutrino spectrum was confirmed in the second independent experiment.

To understand whether this deficit is related to solar physics or neutrino physics, the gallium solar neutrino experiment was required. This experiment differs from all other solar neutrino experiments in its high sensitivity to the proton–proton (pp) reaction $p + p \to d + e^{+} + \nu_e$ in which most of the solar energy is generated.

The rate of the p-p reaction is directly related to the solar luminosity and, therefore, it is virtually independent of the model, while the capture rate of the pp-neutrino by Ga nuclei

can be predicted very accurately. Thus, the gallium experiment is the only one providing a direct measurement of the rate of energy generation in the Sun.

3. Gallium experiments

The use of gallium in the radiochemical solar neutrino experiment was proposed by V A Kuzmin back in 1963 [7], even before the first solar neutrino experiments were performed. However, the high cost of gallium, the small amount of its global production, and the absence of reliable technology for extracting and counting single atoms of the germanium ^{71}Ge isotope produced via the capture of neutrinos by a large-tonnage gallium target significantly prevented carrying out the gallium experiment at that time.

Laboratory investigations on the design process of the gallium experiment at the Institute for Nuclear Research (INR) of the Academy of Sciences of the USSR and at the Brookhaven National Laboratory (BNL) in the USA were started almost simultaneously in 1975. Methods for extracting germanium from liquid metal gallium and from the solution of gallium chloride in hydrochloric acid were developed. Considerable advances were achieved in the development of these two methods for a few years. Methods for counting single ^{71}Ge atoms were developed, and the production rates of ^{71}Ge nuclei were calculated and measured in different background processes caused by muons of cosmic rays, α particles from internal radioactive impurities, and fast neutrons from external sources.

The American group chose the method utilizing a gallium chloride solution as the simplest to realize, and made a pilot facility containing 1.3 t of gallium in the gallium chloride solution in hydrochloric acid. In 1981, a proposal to perform a large-scale 50-t gallium experiment was directed to the US Department of Energy. The proposal was considered at a high level and recommended for realization, but was unfunded. Fifteen years later, G T Garvey, Director of the Los Alamos Meson Physics Facility, commented on this financial mishap in the following way: "This happened mainly because, as was found out, a Federal Agency for financing studies of this type was nonexistent, which is a true flaw in the USA system."

At the department headed by G T Zatsepin at INR, laboratory studies on the development of the gallium experiment were also started by using the gallium chloride solution. But when it became clear that our industry could not provide the required purity of 50 t of this solution, it was decided to begin to develop a method for extracting germanium directly from metal gallium because metal gallium is considerably less sensitive to radioactive impurities.

The possibility of extracting extremely small amounts of germanium from metal gallium was first demonstrated by R Davis. Based on the Davis idea, we developed the technology of extracting single ^{71}Ge atoms from many tons of metal gallium. Our first paper in which this method was applied to extracting single ^{71}Ge atoms from 300 kg of metal Ga was published in 1980 [8].

In 1984, G T Garvey sent a proposal to the INR, USSR Academy of Sciences to combine the efforts of the Los Alamos National Laboratory (LANL) in the USA and the INR in investigations of solar neutrinos, in particular, in conducting the gallium experiment. An agreement on the performance of the joint Soviet–American Gallium Experiment using the gallium–germanium neutrino telescope (GGNT) at the Baksan Neutrino Observatory was signed by V A Matveev in 1986. The experiment was called SAGE (Soviet–American Gallium Experiment). The American participants of the experiment were LANL and Pennsylvania State University. Later on, the University of Washington and the National Institute of Standards and Technologies (Gaithersberg) were also involved in the experiment.

In 1986, a pilot facility containing 7.5 tons of metal Ga was created at the INR in Troitsk, at which the procedure of extracting single ^{71}Ge atoms was fine-tuned. The American team was engaged in the development and production of a system for detecting the decay of extracted ^{71}Ge atoms.

In 1984, a German group at the Max-Planck-Institut (Heidelberg) headed by T Kirsten presented a project on the gallium experiment with the use of a gallium chloride solution at the underground Gran Sasso Laboratory in Italy and began to create, with the participation of BNL, the Western-European Collaboration, which was called GALLEX (GALLium EXperiment).

Thus, two independent gallium experiments appeared, in fact, simultaneously: GALLEX, based on the Ga chloride solution, at the underground Gran Sasso Laboratory, and SAGE, based on metal Ga, at the underground laboratory at the Baksan Neutrino Observatory of the INR.

4. Gallium–germanium neutrino telescope laboratory at the Baksan Neutrino Observatory of the Institute for Nuclear Research, RAS

Solar neutrino experiments were some of the first initiating a new direction of investigations in astrophysics and the physics of elementary particles. These studies required the establishment of underground laboratories providing a considerable lowering of the muon background of cosmic rays (by a few million times), and special low-background materials for protecting detectors from the radiative emission of the environment. The Baksan Neutrino Observatory was founded for the development of these investigations in the USSR.

The Baksan Neutrino Observatory is located in the upper reaches of the Baksan River in the Northern Caucasus at an altitude of 1700 m above the sea level. The underground parts of the observatory are located in the depths of the Andyrchi Mountain massif (3937 m in altitude), which is part of the side branch of the Large Caucasian Ridge. The construction of the observatory was initiated in 1967.

The initial project of the Baksan Neutrino Observatory assumed the construction of a deep underground laboratory containing, according to the program of solar neutrino spectroscopy proposed by G T Zatsepin, a unified complex of three radiochemical neutrino telescopes based on Cl, Li, and Ga and having different sensitivities to neutrinos created in different reactions proceeding in the Sun.

It was proposed that this complex be placed at a distance of 4200 m from the entrance of a horizontal adit where the intensity of cosmic-ray muon fluxes in the depths of the massif reaches its minimum.

Because the acquisition of experimental data in the low-energy part of the spectrum of solar neutrinos became very urgent, it was decided in 1977 to begin first of all with establishing a separate gallium–germanium neutrino telescope laboratory, not waiting for the termination of the adit sinking over the entire projected length.

Because the gallium neutrino experiment can be performed at smaller depths than those required for chlorine

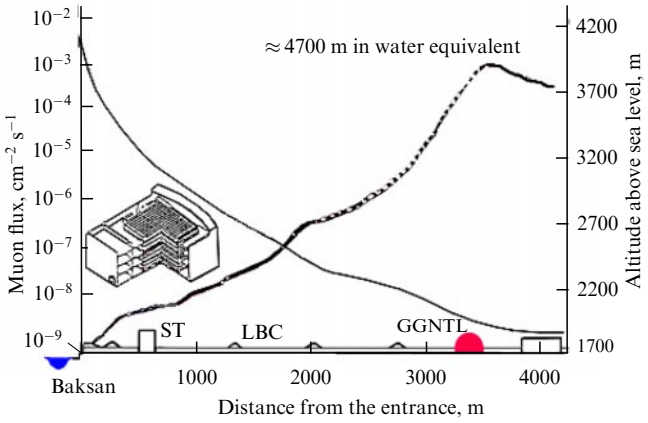

Figure 1. Profile of a mount, the dependence of the muon flux on the adit length, and the schematic arrangement of underground laboratories at the Baksan Neutrino Observatory: ST — scintillation telescope, LBC — low-background chambers, GGNTL — gallium–germanium neutrino telescope laboratory. The insert in the left part of the figure shows the schematic view of the scintillation telescope.

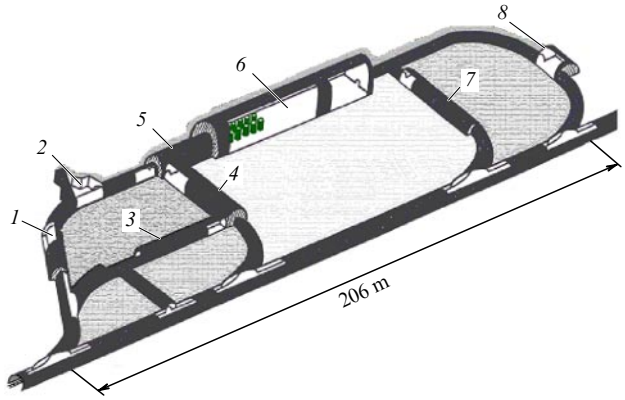

Figure 2. Schematics of the underground compartments of the GGNT laboratory: *1*, *2*, *5*, *7*, *8* — auxiliary compartments; *3* — electric substation compartment; *4* — air-conditioning compartment, and *6* — reactor hall of the GGNT.

experiments [9, 10], the GGNT laboratory facility was placed at a distance of 3600 m from the entrance of an adit (Fig. 1). The thickness of cover rocks over the laboratory is 2100 m, corresponding to 4700 m of the water equivalent. The GGNT laboratory is now second in the world in site depth.

The GGNT laboratory comprises a cylindrical chamber shaft 60 m in length, 15 m in diameter, 12 m in base width, and 10 m in height. To organize work rooms, control panels, and sites for the technological equipment, support metal structures are mounted in the laboratory at different levels. The auxiliary equipment of engineering systems (electric substation, air-conditioning system, air vent aggregate, etc.) is placed in separate rock shafts adjacent to the laboratory (Fig. 2). The temperature of the surrounding rock reaches 38.3 °C.

The laboratory has a forced ventilation system taking fresh air from the adit, and an air vent discharge setup directing the exhaust air to its air line. Laboratory rooms are cooled with an air conditioner. The incoming air is purified in two stages: in the first filter chamber (with FL-1.8 filtering material), the air is purified of dust, and in the second chamber with Petryanov FPP-1.5 filters, it is purified of aerosols contained in air (in particular, the decay products of ^{232}Th and ^{238}U nuclei). Air is directed to each room through separate air lines. A ventilator of the air-flow system produces excess pressure in the laboratory rooms. The exhaust air arrives at the main ventilator placed at the entrance of the auxiliary adit.

Personnel, materials, and equipment are transported by rail using electric battery locomotives, passenger cars, and special platform cars.

The muon flux in the GGNT laboratory was measured with a small telescope of scintillation polystyrene detectors 4 m^2 in area [11]. The global intensity of muon fluxes in the GGNT laboratory was measured to be [11]

$$N_{\text{measured}} = (3.03 \pm 0.10) \times 10^{-9}\ \text{cm}^{-2}\ \text{s}^{-1}\,.$$

Calculations of the production rates of germanium isotopes in Ga for this muon flux [9] showed that the rate of the ^{71}Ge production at the laboratory location depth was less than 0.01 atoms per day, i.e., lower than 1% of the value predicted by the SSM (in the absence of attenuation of the electron neutrino flux due to, for example, oscillations or other effects).

Metal gallium is considerably less sensitive to fast neutrons than is the solution of its chloride in hydrochloric acid. According to estimate [12], the contribution of fast neutrons from surrounding rocks to the production rate of ^{71}Ge, even without shielding, in experiments with metal Ga is less than 1% of the contribution expected from solar neutrinos by neglecting their oscillations.

However, to maximally realize the potential of this unique arrangements for performing experiments requiring an extremely low radiation background, it was decided to reduce significantly the neutron flux in the gallium laboratory by applying for its construction special low-background concrete, which, apart from its direct function of strengthening rocks, can serve as a radiation shield. In addition, we took into account that the low-energy solar neutrino flux, to which the gallium experiment is primarily sensitive, can be suppressed and considerably lower than the expected flux, as had been found in the chlorine experiment for high-energy neutrinos.

The content (g g^{-1}) of radioactive elements in rocks surrounding the laboratory is as follows: ^{238}U — $(1.5-3.8)\times 10^{-6}$, ^{232}Th — $(1.9-2.5)\times 10^{-5}$, and ^{40}K — 3.4×10^{-6}.

The GGNT laboratory was embedded in concrete based on dunite, silica sand, and Portland cement, which was developed at the Central Research Laboratory of Orgproekt in cooperation with INR, USSR Academy of Sciences [13]. The average contents of uranium and thorium impurities in the basic concrete components were 1.58×10^{-7} and 6.73×10^{-7} g g^{-1}, respectively.

In December 1987, the laboratory was put into operation and work was started on GGNT adjustment. The first measurements of a solar neutrino flux in SAGE were performed in December 1989.

5. Soviet-American gallium experiment (SAGE)

The neutrino flux in SAGE is determined by measuring the rate of neutrino capture reaction $^{71}\text{Ga}(\nu_e, e)^{71}\text{Ge}$ on metal Ga in the GGNT. The reaction threshold, which was 233 keV, allows the detection of neutrinos produced in all neutrino-

production reactions proceeding in the Sun according to the SSM, including neutrinos produced in pp reactions (pp-neutrinos). The maximum energy of the pp-neutrino is 420 keV. The number of pp-neutrinos with energies exceeding the capture threshold by ^{71}Ga nuclei is more than half the total number of pp-neutrinos, and their contribution to the expected capture rate in experiments is about 54%.

The telescope target consists of approximately 50 t of metal gallium uniformly distributed in seven chemical reactors. Gallium is contained in reactors in the liquid form at a temperature of 31 °C (the melting point of gallium is 29.8 °C). Measurements are performed cyclically.

Each measurement of the capture rate of solar neutrinos begins with the addition of a carrier (≈ 250 μg of stable germanium) to the Ga target. The carrier is added in the form of tablets containing the gallium alloy with the known amount of germanium (about 2×10^{-4} mass percent). Germanium is uniformly distributed in the reactors over the entire gallium mass.

The neutrino capture rate in radiochemical experiments is expressed in SNU (Solar Neutrino Units): 1 SNU corresponds to one neutrino captured per second in a target containing 10^{36} atoms of isotope (in our case, ^{71}Ga) capturing neutrinos. The expected capture rate of solar neutrinos by gallium atoms amounts to 128 SNU [14]. For natural gallium containing 39.9% of ^{71}Ga isotopes, the capture rate of 128 SNU corresponds to the production rate of ^{71}Ge atoms in the 50-t target of about 1.9 atoms per day. Thus, for a long exposure time (the half-life of ^{71}Ge decay is $T_{1/2} = 11.43$ days), the average number of ^{71}Ge atoms in the target can be about 32.

Exposures used in the experiments lasted for 4 to 6 weeks. Then, the ^{71}Ge atoms produced are chemically extracted together with the germanium carrier from gallium by the method described in Ref. [15]. Germanium extracted from gallium (the carrier and ^{71}Ge atoms) is converted to the gaseous form GeH_4 (germane) and, after measuring its volume, is placed into a proportional counter.

The chemical properties of germanium isotopes are identical, and therefore the total extraction efficiency for ^{71}Ge atoms is equal to the extraction efficiency for stable germanium, which is defined as the ratio of the germanium mass in germane to the introduced mass of the germanium carrier. Germanium enriched with ^{72}Ge or ^{76}Ge isotopes is used as the carrier. After completing each extraction, the final extraction solution sample is analyzed with a mass spectrometer to determine the fractional composition of different Ge isotopes.

Molecules of germane are highly symmetrical and are not polarized, and therefore they can be used as a quenching addition in proportional counters. The main counting gas in counters is xenon having a large atomic number ($Z = 54$) and, consequently, a large enough cross section for interaction with soft X-rays produced upon the recovery of electron shells during the decay of ^{71}Ge nuclei.

The counting of ^{71}Ge decays extends over 5–6 months, which is related to the method of selecting pulses generated by the ^{71}Ge decay from all the pulses detected by the counter, a considerable fraction of them being background pulses. The pulses are analyzed after the termination of counting by the developed method of event selection and time analysis.

The capture rate of solar neutrinos by gallium is determined by the number of detected ^{71}Ge decays, taking into account the extraction and counting efficiencies.

Figure 3. GGNT chemical reactors.

Figure 4. General view of the GGNT reactor hall.

5.1 GGNT chemical reactors

The GGNT comprises ten chemical reactors (Figs 3, 4) connected with each other by a heated Teflon pipe with a Teflon liquid pump providing the circulation of metal gallium between reactors. The reactor (Fig. 5) represents a 2-m^3 Teflon tank with 40-mm-thick walls, which is heated with band heaters. The Teflon tank is placed inside a stainless steel tank. Gallium is mixed with a special mixer with the maximum rotation speed of 80 rpm. To provide the efficient mixing of reagent solutions (density of ≈ 1 kg l^{-1}) with metal gallium (density of 6.1 kg l^{-1}), the reactor has special cutters fastened on the inner side of the reactor lid. The cutters are made of Teflon, and the mixer and the inner side of the lid are also covered by a Teflon layer.

Reagents are fed into reactors by means of a system of controllable valves and pumps made of Teflon and borosilicate glass. The system allows one to feed the measured amounts of reagents to any of these reactors. The solution obtained after completing the extraction (the extraction solution) is decanted with the help of a vacuum system whose components are made of glass, Teflon, and zirconium. The reagent dosing and mixing processes are completely automated.

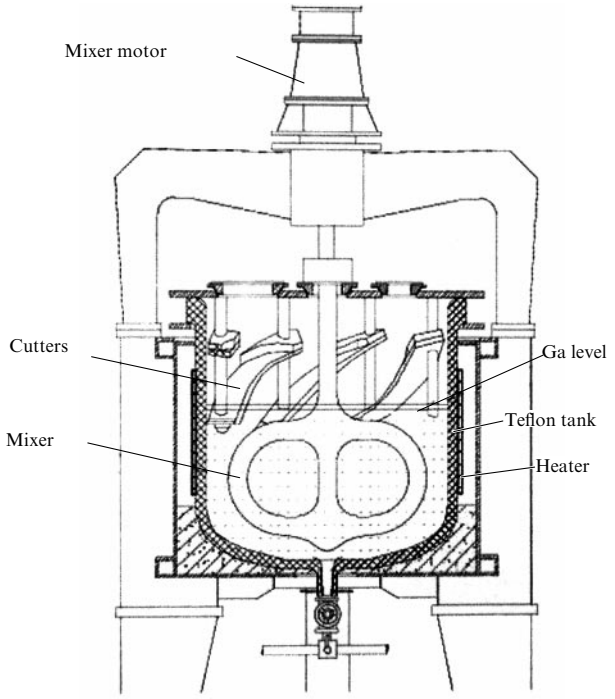

Figure 5. Chemical reactor for extracting germanium from gallium.

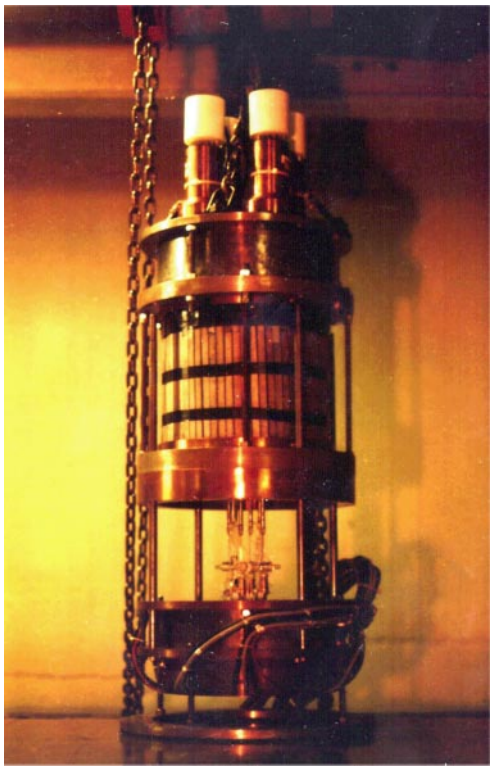

Figure 6. Part of the active shield of the detection system with an NaI detector and proportional counters inside it.

The germanium extraction efficiency depends on many parameters, and increases upon increasing the amount of oxidizer (hydrogen peroxide solution) added; at the same time, the amount of gallium dissolved during the oxidation reaction increases proportionally to the amount of hydrogen peroxide added. The extraction efficiency also depends on the aqueous phase volume, which determines the duration of the subsequent concentration of germanium — the longest stage of the entire extraction process.

Taking into account all the factors considered above, an extraction procedure was developed which provides a total extraction efficiency reaching $(95 \pm 3)\%$ for an amount of dissolved gallium smaller than 0.1%.

5.2 Counting ^{71}Ge atoms

The ^{71}Ge nuclei decay back into ^{71}Ga nuclei due to purely electron capture with a half-life period of 11.4 days. A proportional counter gives two peaks: the K peak at 10.4 keV, and the L peak at 1.2 keV.

Beginning from April 2001, completely reconstructed proportional YCT (Yants–Carbon–Thin) type counters [16] have been used in the experiment. These counters were developed by V E Yants at the Laboratory of Radiochemical Methods for Neutrino Detection at the INR, RAS. Unlike the solid cathode used in counters earlier, a cathode in new counters represents a thin carbon layer deposited onto the inner surface of a quartz flask upon thermal decomposition of hexane or acetone vapor. This excluded the 'dead' volume behind the cathode. The dead volume was also diminished by eliminating edge effects due to the specific design of these counters.

The contacts of the cathode and anode are brought out from the counter with the help of a molybdenum band, which provides air tightness and a high stability of the counter. The cathode is so thin that the counter walls are transparent, allowing the visual observation of its internal structure. The measured volume efficiency of all new counters reached 96%, with a spread in values of only 1%. The increase in the volume efficiency resulted in a considerable increase in the efficiency of counters: by approximately 25% in the K peak, and 10% in the L peak.

The output pulses of a proportional counter are fed into a digital oscilloscope, where they are digitized in the 800-ns interval after the pulse onset with two different amplifications for the K and L peaks. The digital oscilloscope is used to separate fast rising ^{71}Ge pulses from (predominantly) slowly rising background pulses.

Proportional counters filled with a gas mixture are set up in the GGNT detection system, which is designed so that the detection of the ^{71}Ge decays in counters is provided with maximum efficiency. For this purpose, a number of measures were taken for suppressing noise and background pulses. The detection system is placed in a specially equipped room of the underground laboratory. The external walls of the room are made of 10-mm-thick sheet steel and a 70-cm-thick low-radioactive concrete layer protecting from fast neutrons and γ-radiation of the surrounding rocks. The inner walls are coated with 1-mm-thick sheets of zinc-plated iron for screening from radio interference.

A counter containing GeH_4 obtained from gallium-extracted germanium is placed into an NaI detector well (Fig. 6) located inside a large passive shield, and decay pulses from ^{71}Ge are detected with the counter for 5–6 months. The NaI detector well can simultaneously accommodate up to eight counters.

To reduce the action of ^{223}Ra nuclei, the volume inside the shield around the counters is blown out with liquid nitrogen evaporated from a Dewar. The shield consists of successive iron, lead, copper, and tungsten layers. All the components of

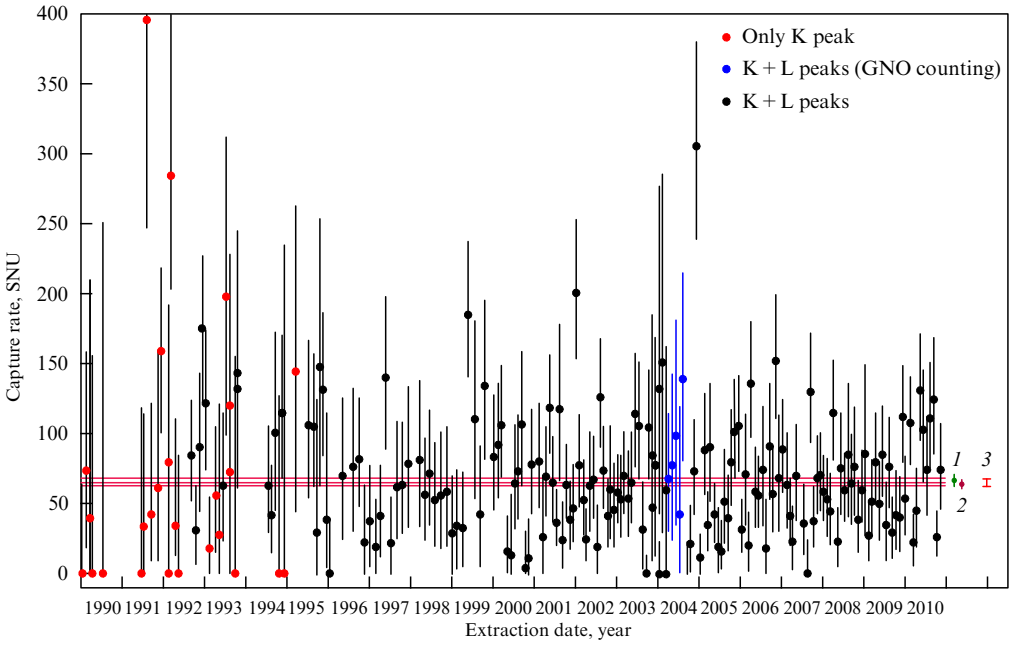

Figure 7. Neutrino capture rate for all SAGE extractions as a function of time. The vertical bars at each point correspond to a statistical error of 68%. Results of processing with the L peak (*1*), the K peak (*2*), and the combined result for all data (*3*). The horizontal bars correspond to the combined SAGE result (65.4 ± 2.7 (stat.)) SNU.

the shield are made of low-radioactive materials which were preliminarily selected with the help of a low-background germanium semiconductor detector.

5.3 Data analysis and SAGE results

Based on selection criteria described in Ref. [15], candidate events from ^{71}Ge nuclei decays are selected from the counter data for each germanium extraction. The time distribution of these selected events is approximated by the maximum likelihood function [17], assuming that they occur from the unknown background constant in time and from decays of ^{71}Ge atoms whose number exponentially decreases.

The measurement of the capture rate of solar neutrinos on a metal gallium target in SAGE was started in December 1989. Since then, the measurements have been performed mainly monthly, with only a few short interruptions. The results of 200 individual measurements performed between January 1990 and August 2010 are presented in Fig. 7. Because only a few decays of ^{71}Ge nuclei are detected in each extraction, the results of individual measurements have a large statistical uncertainty and, therefore, a small significance. The results of analysis of the SAGE data combined over years for the same period are given in Fig. 8.

The neutrino capture rate obtained from the analysis of 200 measurements is (65.4 ± 2.7) SNU. If the data obtained for the L and K peaks are analyzed separately, the results will be (66.9 ± 4.1) SNU and (64.2 ± 3.6) SNU, respectively (here and above, only statistical uncertainties are indicated). The agreement between the results of the independent analysis of data in the two peaks well confirms the reliability of the criteria for selecting events. As another argument that we are counting namely ^{71}Ge atoms, we introduce into the likelihood function, along with the combined production rate of ^{71}Ge atoms and all background counting rates, the decay constant as a free variable. The half-life period found in such a way for all events selected in the L and K peaks amounts to (11.5 ± 0.9 (stat.)) days, in good agreement with the half-life

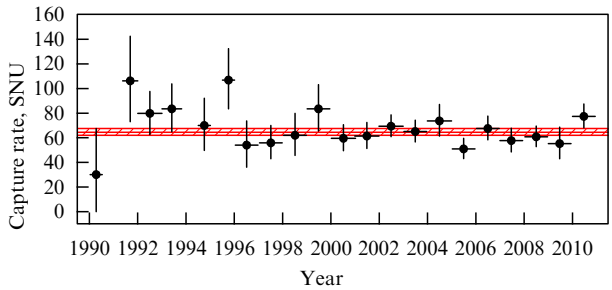

Figure 8. Results of measurements combined by years. The shaded region corresponds to the combined SAGE result (65.4 ± 2.7 (stat.)) SNU. The vertical bars at each point correspond to a statistical error of 68%, and the horizontal bars correspond to the time interval of the combined analysis of measurements.

period of (11.43 ± 0.03) days for ^{71}Ge decays measured in Ref. [18].

The combined analysis of the SAGE data for the entire measurement period, taking into account the statistical and systematic uncertainties, gives a capture rate of solar neutrinos by gallium at [65.4 ± 2.7 (stat.) ±2.7 (sist.)] SNU or (65.4 ± 3.8) SNU, where the statistical and systematic errors are combined quadratically. The systematic uncertainties of the experiment were considered in detail in papers [15, 19, 20].

5.4 Results of gallium experiments

The measurements of solar neutrinos in the GALLium EXperiment (GALLEX) at the underground laboratory in Gran Sasso [21] were performed with a 103-t target consisting of a $GaCl_3$ solution in hydrochloric acid containing 30 t of gallium. For 5.4 years, from May 1991 to January 1997, 65 measurements were performed, the final analysis of which gave the capture rate of (73.1 ± 7.2) SNU.

After some interruption, the experiment was continued under the new name GNO (Gallium Neutrino Observatory);

from May 1998 to April 2003, 58 measurements were performed which gave the capture rate of (62.9 ± 5.1) SNU.

The combined result of solar neutrino measurements in two Gran Sasso experiments gives the neutrino capture rate in gallium equal to (67.6 ± 5.1) SNU, which is in excellent agreement with the SAGE result of (65.4 ± 3.8) SNU. The agreement between the results of two independent gallium experiments using Ga targets of different shapes considerably increases their reliability.

The weighted-mean neutrino capture rate obtained from SAGE and GALLEX/GNO experiments is (66.1 ± 3.1) SNU, which is about 50% of the value predicted by the SSM. Thus, gallium experiments have demonstrated a considerable suppression of the solar neutrino flux over the entire energy range, which excluded the possibility of solving the solar neutrino problem within the framework of solar physics only, and proved the change in the flavor of neutrinos traveling from the center of the Sun to Earth.

6. The pp-neutrino flux from the Sun

As mentioned above, the radiochemical gallium experiment with its low energy threshold (233 keV) is sensitive to all the components of the solar neutrino spectrum — from low-energy pp-neutrinos to high-energy neutrinos produced in the ^{8}B nucleus decay. Thus, the neutrino capture rate measured in gallium experiments, which is the sum of capture rates from all the components of the solar neutrino flux, can be expressed in the form

$$[\mathrm{pp} + {}^7\mathrm{Be} + \mathrm{CNO} + \mathrm{pep} + {}^8\mathrm{B}|\mathrm{Ga}] = 66.1(1 \pm 0.047)\ \mathrm{SNU},$$

where the left-hand side presents the capture rates in gallium from the components of the solar neutrino flux. Here, we neglected the insignificant contribution of the *hep*-neutrino and combined neutrino fluxes from the ^{13}N, ^{15}O, and ^{17}F decays into one component of the solar neutrino flux, denoted CNO.

By using the results of measurements of neutrino fluxes in the Borexino [21] and SNO (Sudbury Neutrino Observatory) [23] experiments and the neutrino capture rates obtained in the chlorine experiment [24], we determined the contribution from each component of the solar neutrino flux to the capture rate measured on Ga targets [20]:

$$[{}^7\mathrm{Be}|\mathrm{Ga}] = 19.1(1 \pm 0.12)\ \mathrm{SNU},$$

$$[{}^8\mathrm{B}|\mathrm{Ga}] = 3.6(1^{+0.32}_{-0.16})\ \mathrm{SNU},$$

$$\left[(\mathrm{CNO} + \mathrm{pep})|\mathrm{Ga}\right] = 3.68(1 \pm 1.0)\ \mathrm{SNU},$$

$$[\mathrm{pp}|\mathrm{Ga}] = 39.7(1 \pm 0.14)\ \mathrm{SNU}.$$

The capture rate of the pp-neutrino on Ga equal to $39.7(1 \pm 0.14)$ SNU corresponds to the pp-neutrino flux $\Phi_{\mathrm{pp}} = 3.38(1 \pm 0.14) \times 10^{10}$ cm^{-2} s^{-1}. This is a fraction of the flux of pp-neutrinos with the electron flavor that falls on Earth.

The magnitude of the pp-neutrino flux obtained for the first time in experiments directly demonstrates the existence of the proton–proton chain in the thermonuclear fusion reactions proceeding in the Sun.

Taking into account the survival factor $\langle P^{\mathrm{ee}} \rangle = 0.561(1^{+0.030}_{-0.042})$ for neutrino oscillations with a large mixing angle (LMA solution), the total pp-neutrino flux arriving on Earth from the Sun is $\Phi_{\mathrm{pp}} = 6.01(1 \pm 0.14) \times 10^{10}$ cm^{-2} s^{-1} [20]. This value agrees well with the pp-neutrino fluxes predicted by the two existing solar models differing in the concentrations of heavy elements in the Sun: $\Phi_{\mathrm{pp}} = (5.97 \pm 0.04) \times 10^{10}$ cm^{-2} s^{-1} and $\Phi_{\mathrm{pp}} = (6.04 \pm 0.03) \times 10^{10}$ cm^{-2} s^{-1} [14].

7. Experiments with artificial neutrino sources

The first SAGE [25] and GALLEX [26] measurements performed in 1990 already revealed the low neutrino flux which could not be explained by the SSM. Because this result leads to the important conclusions that the neutrino changes its flavor and has mass, it was necessary to confirm that we correctly estimated the efficiency of all the procedures followed in experiments.

The total verification of the SAGE and GALLEX measurements as a whole (i.e., the chemical extraction efficiency, the counting of ^{71}Ge atoms, and the data analysis technique) was performed by utilizing artificial neutrino sources. Gallium targets were irradiated by artificial neutrino sources based on isotopes produced in atomic reactors with the activity close to 1 MCi. In SAGE, approximately 25% of the target was irradiated by the ^{51}Cr [27] and ^{37}Ar [28] sources. In GALLEX, the ^{51}Cr source was twice used for irradiating the entire target [29]. The weighted-mean ratio R of the measured production rate of ^{71}Ge isotopes to the expected rate, calculated from the source power, proved to be unexpectedly low for all four experiments, $R = 0.87 \pm 0.05$, less than unity by more than two standard deviations.

To prove the correctness of the efficiencies of all the procedures followed in running SAGE and GALLEX, numerous investigations were performed [15]. The extraction efficiency was determined from various chemical and volume measurements based on the introduction and subsequent extraction of the known amount of the carrier of stable Ge. Also, the verification was performed by adding to a Ga target the Ge carrier in a mixture with a known number of ^{71}Ge atoms in SAGE and ^{71}As atoms in GALLEX. As a result, it was shown that the extraction efficiencies of the stable carrier and ^{71}Ge isotopes are very close.

The results of all auxiliary verifications, especially those of the GALLEX experiment with ^{71}As [16], showed that all the efficiencies were most likely determined correctly, and it was concluded that the low neutrino capture rate observed in gallium experiments with different sources is not caused by erroneous experimentation.

The possible reasons for such a low neutrino capture rate were considered in detail in paper [20]. One of the hypotheses is that the cross sections for neutrino capture into the two lowest excited levels in ^{71}Ge nuclei, which can be reached when using the ^{51}Cr or ^{37}Ar source, are overestimated [31]. Other possible reasons can be a statistical fluctuation, which has a low probability (about 5%), or a real physical effect of an unknown nature, such as the hypothetical transition of active neutrinos to the sterile state.

8. The potential of SAGE in the investigation of oscillation transitions of active neutrinos into sterile states

The most relevant issues in neutrino physics at present are whether sterile neutrinos exist and whether there are *CP* and *CPT* violations in the neutrino sector of physics? The

question of the existence of sterile neutrinos with $\Delta m^2 \sim 1$ eV^2 appeared in the analysis of results obtained in the LSND (Liquid Scintillator Neutrino Detector) and MiniBooNE (Booster Neutrino Experiment) accelerator experiments, in a number of reactor experiments, and in gallium experiments with artificial neutrino sources [32].

The question of the existence of sterile neutrinos has aroused considerable interest in the last few years. This is explained by both some refinement of cosmological data and the appearance of new 'anomalous' results obtained in experimental studies of neutrino oscillations. New estimates of reactor antineutrino fluxes have confirmed the hypothesis about the oscillations of neutrinos with a mass of ~ 1 eV. On the other hand, the absence of specific features in the spectrum of atmospheric neutrinos with energies of about 1 TeV in the first data from the IceCube neutrino telescope suggests the absence of neutrino transitions with large Δm^2.

To study the oscillation transitions of active neutrinos to sterile states, it is planned at present to perform, along with known experiments, new experiments by using both existing and specially projected atomic reactors and accelerators.

We propose using the unique possibilities of the GGNT for studying the oscillation transitions of active neutrinos to sterile states. For this purpose, a ^{51}Cr source with an activity of 3 MCi is placed at the center of a metal Ga target of the 50-t telescope divided into two independent, internal and external, zones containing 8 and 42 t of Ga, respectively (Fig. 9), with equal neutrino mean free paths, and the neutrino capture rates are measured simultaneously in each zone. During transitions to sterile states with the oscillation parameter $\Delta m^2 > 0.5$ eV^2 (it is these transitions that are of special interest at present), the capture rate in one of the zones or in both zones of the target should be suppressed (Fig. 10). In the case of the statistically ensured difference between neutrino capture rates in each zone or the statistically ensured difference between the mean capture rate in both zones and the expected value, we obtain direct confirmation of the existence of unusual properties of the neutrino. The ratios of capture rates measured in zones to the expected values will give the allowed regions of parameters of the observed oscillations.

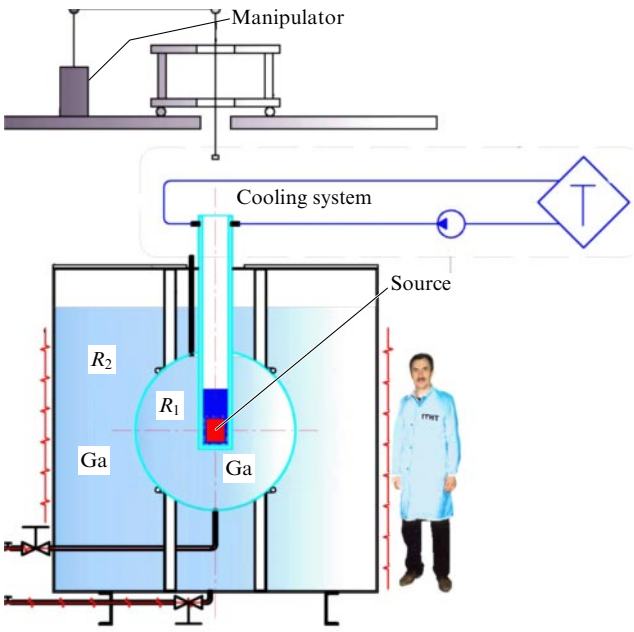

Figure 9. Schematics of the proposed experiment with an artificial neutrino source. R_1 and R_2 are the ratios of the capture rates measured in the internal and external zones, respectively, to the expected capture rate.

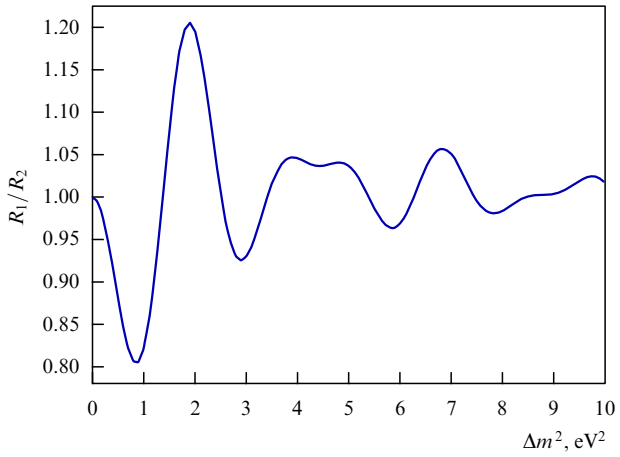

Figure 10. Ratio of neutrino capture rates in the external and internal zones as a function of Δm^2 for $\sin^2 2\theta = 0.3$.

The experiment on Ga with an artificial electron neutrino source offers significant advantages compared to other projects. These advantages are provided due to the employment of: a compact, almost monochromatic neutrino source with a well-known activity; a metal Ga target with a density providing a high interaction rate; targets with a special geometry allowing the study of the dependence of the neutrino capture rate on the distance to the source, and a well-developed method for measuring the neutrino capture rate on gallium target in the GGNT.

Another obvious advantages of such experiments are a large signal-to-noise ratio and the simplicity of the interpretation of results. The point is that the main contribution to the background will be made by solar neutrinos whose flux is well known from GGNT measurements performed for many years, while the source activity should provide the number of interactions in the detector exceeding by a few dozen times that which can be caused by solar neutrinos. The results can be simply interpreted because the artificial source emits a monochromatic neutrino flux and, therefore, systematic uncertainties related to the uncertainty in the neutrino spectrum are absent.

Taking into account the cross section for neutrino capture on Ga calculated by Bahcall [33], we determine that, in the absence of oscillations to sterile neutrinos, the production rate from the source at the beginning of the first irradiation will be ~ 65 ^{71}Ge atoms per day in each zone. We plan to perform 10 irradiations of Ga, for 9 days each, with the 1-day interruption between irradiations. The standard procedure for extracting and counting ^{71}Ge atoms, which was well developed in solar measurements, will be used. ^{71}Ge decays from each zone will be detected in individual counters. The production rate of ^{71}Ge atoms at the beginning of the first irradiation by the source will be higher than that from solar neutrinos by approximately 64 times for the external zone, and by almost 340 times for the internal zone.

The statistical uncertainty for the irradiation series, obtained by the Monte Carlo method based on the proposed program of irradiations, the extraction and counting efficiencies, the background rate, and the production rate from solar

neutrinos is equal to 3.7% in each zone and ±2.6% for the entire target.

Thus, the expected total number of ^{71}Ge atoms accumulated over ten exposures in such experiments will be ~ 840 (±4.5%) in each zone, and ~ 1680 (±3.7%) on the entire target (the statistical and systematic uncertainties are combined quadratically).

9. Conclusion

The capture rate of solar neutrinos on a Ga target obtained in SAGE is (65.4 ± 3.8) SNU. The weighted average capture rate of neutrinos on Ga in three gallium experiments (SAGE, GALLEX, and GNO) is (66.1 ± 3.1) SNU, where the statistical and systematic uncertainties are combined quadratically.

By using the results of other solar neutrino experiments and the theory of large-mixing-angle (LMA) neutrino oscillations, we obtained in SAGE for the first time the value of pp-neutrino flux reaching $(3.40 \pm 0.46) \times 10^{10}\,\mathrm{cm}^{-2}\,\mathrm{s}^{-1}$ for neutrinos with the electron flavor arriving on Earth, and the value of total pp-neutrino flux amounting to $(6.0 \pm 0.8) \times 10^{10}\,\mathrm{cm}^{-2}\,\mathrm{s}^{-1}$.

The gallium solar neutrino experiments have shown for the first time that most of the solar neutrinos arriving on Earth are low-energy neutrinos created in the proton–proton reaction and directly confirmed the correctness of the SSM and the LMA solution for solar neutrino oscillations.

To elucidate the reasons for the unexpectedly low neutrino capture rate on Ga in experiments with artificial sources, we developed the concept of a new experiment with a high-intensity neutrino source and the optimized geometry of a Ga target [34].

Up to now, SAGE remains to be the sole experiment in which the pp-neutrino flux has been measured. We plan to pursue the monitoring of solar neutrino fluxes and to make preparations for a new experiment with a high-intensity neutrino source and the optimized geometry of a Ga target.

Acknowledgments. On behalf of SAGE, the author wishes to express his appreciation to M Baldo-Ceolin, G T Garvey, W Haxton, H Ejiri, R G H Robertson, A Yu Smirnov, A Suzuki, and our colleagues from the GALLEX and GNO collaborations for their constant interest in our work and fruitful and stimulating discussions. We thank especially V A Matveev and V A Rubakov for their active support throughout the experiment and their attention to many important aspects of our studies. Our experiment was supported for many years by the Russian Foundation for Basic Research.

References

1. Allen J S *The Neutrino* (Princeton, N.J.: Princeton, Univ. Press, 1958)
2. Bahcall J N *Neutrino Astrophysics* (Cambridge: Cambridge Univ. Press, 1989) [Translated into Russian (Moscow: Mir, 1993)]
3. Markov M A *Neitrino* (Neutrino) (Moscow: Nauka, 1964)
4. Davis R (Jr.), Harmer D S, Hoffman K C *Phys. Rev. Lett.* **20** 1205 (1968)
5. Pontecorvo B, Report PD-205 (Chalk River: National Research Council of Canada, Division of Atomic Energy, 1946)
6. Pontecorvo B M *Zh. Eksp. Teor. Fiz.* **53** 1717 (1967) [*Sov. Phys. JETP* **26** 984 (1968)]
7. Kuz'min V A *Zh. Eksp Teor. Fiz.* **49** 1532 (1965) [*Sov. Phys. JETP* **22** 1051 (1966)]
8. Barabanov I R et al. *Pis'ma Zh. Eksp. Teor. Fiz.* **32** 384 (1980) [*JETP Lett.* **32** 359 (1980)]
9. Gavrin V N, Zakharov Yu I, Preprint P-560 (Moscow: INR, Acad. Sci. USSR, 1987)
10. Zakharov Yu I, Ph.D. Phys. Math. Sci. Thesis (Moscow: INR, Acad. Sci. USSR, 1987)
11. Gavrin V N et al., Preprint P-698 (Moscow: INR, Acad. Sci. USSR, 1991)
12. Glotov V I, Ph.D. Phys. Math. Sci. Thesis (Moscow: INR, Acad. Sci. USSR, 1979)
13. Panchenko V P et al. *Vopr. Atom. Nauki Tekh.* **21** (3) 21 (1989)
14. Peña-Garay C, Serenelli A M, arXiv:0811.2424
15. Abdurashitov J N et al. (SAGE Collab.) *Phys. Rev. C* **60** 055801 (1999); astro-ph/9907113
16. Danshin S, Kopylov A, Yants V *Nucl. Instrum. Meth. Phys. Res. A* **349** 466 (1994)
17. Cleveland B T *Nucl. Instrum. Meth. Phys. Res.* **214** 451 (1983)
18. Hampel W, Remsberg L P *Phys. Rev. C* **31** 666 (1985)
19. Abdurashitov J N et al. (SAGE Collab.) *Zh. Eksp. Teor. Fiz.* **122** 211 (2002) [*JETP* **95** 181 (2002)]
20. Abdurashitov J N (SAGE Collab.) *Phys. Rev. C* **80** 015807 (2009); arXiv:0901.2200
21. Kaether F et al. *Phys. Lett. B* **685** 47 (2010); arXiv:1001.2731
22. Arpesella C et al. (Borexino Collab.) *Phys. Rev. Lett.* **101** 091302 (2008)
23. Aharmim B et al. (SNO Collab.) *Phys. Rev. Lett.* **101** 111301 (2008)
24. Cleveland B T et al. *Astrophys. J.* **496** 505 (1998)
25. Abazov A I et al. *Phys. Rev. Lett.* **67** 3332 (1991)
26. Anselmann P et al. (GALLEX Collab.) *Phys. Lett. B* **285** 376 (1992)
27. Abdurashitov J N et al. (SAGE Collab.) *Phys. Rev. C* **59** 2246 (1999)
28. Abdurashitov J N et al. *Phys. Rev. C* **73** 045805 (2006)
29. Hampel W et al. (GALLEX Collab.) *Phys. Lett. B* **420** 114 (1998)
30. Hampel W et al. (GALLEX Collab.) *Phys. Lett. B* **436** 158 (1998)
31. Haxton W C *Phys. Lett. B* **431** 110 (1998)
32. Giunti C, Laveder M *Phys. Rev. D* **82** 053005 (2010); arXiv:1005.4599
33. Bahcall J N *Phys. Rev. C* **56** 3391 (1997); hep-ph/9710491
34. Gavrin V N et al., arXiv:1006.2103

PACS numbers: 29.40.Ka, 95.55.Vj
DOI: 10.3367/UFNe.0181.201109h.0984

BAIKAL neutrino experiment

G V Domogatsky

1. Introduction

The Baikal neutrino experiment is rooted in 1959–1960, when M A Markov [1] proposed the idea of large-scale underground and deep-sea experiments for studying the properties of neutrinos and the natural sources of their origin. The idea proved to be extremely fruitful. Investigations performed under conditions of the drastically reduced background of penetrating cosmic radiation, when huge volumes of the surrounding soil or water themselves serve as targets for high-energy neutrinos, made it possible to achieve a fundamentally new sensitivity level of experiments, allowing the study of rare processes which cannot be virtually detected in ground-based laboratories. The underground investigations

Domogatsky G V Institute for Nuclear Research,
Russian Academy of Sciences, Moscow, Russian Federation
E-mail: domogats@pcbai10.inr.ruhep.ru

Uspekhi Fizicheskikh Nauk **181** (9) 984 – 989 (2011)
DOI: 10.3367/UFNr.0181.201109h.0984
Translated by M Sapozhnikov; edited by A Radzig

Table 1. Cherenkov high-energy neutrino detectors in natural media (water and Antarctic ice). The effective masses of detectors are presented for 100-TeV events.

Detector*	Optical modules	Effective mass, Mt	Depth, m	Construction years	State
'Baikal'	230	10	1100 – 1300	1993 – 1998	Operating
AMANDA	677	15	1350 – 1850	1994 – 2000	Closed (2009)
ANTARES	900	10	2050 – 2400	2002 – 2008	Operating
IceCube	900	10	1350 – 2250	2005 – 2011	Operating
KM3NeT (NEMO)	≈ 10000	≈ 1000	2300 – 3300	≈ 2017	Being developed
KM3NeT (NESTOR)	≈ 10000	≈ 1000	2000 – 4000		
KM3NeT (ANTARES)	≈ 10000	≈ 1000	1400 – 2400		
'Baikal NT-1000'	≈ 2500	600 – 800	800 – 1300	≈ 2018	Being developed

* AMANDA — Antarctic Muon And Neutrino Detector Array, ANTARES — Astronomy with a Neutrino Telescope and Abyss environmental RESearch, KM3NeT — KM3 Neutrino Telescope, NEMO — NEutrino Mediterranean Observatory, and NESTOR — Neutrino Extended Submarine Telescope with Oceanographic Research.

were rapidly developed, and they have already given a number of outstanding results, such as the detection of the neutrino radiation burst accompanying a supernova (SN 1987a) explosion in the Large Magellanic Cloud, the establishment of the restriction on the proton lifetime, the study of solar neutrinos and detection of neutrino oscillations, and the reliable observation of the first events produced by neutrinos created in the decay of uranium and thorium series radionuclides in the interior of Earth.

The development of the deep-sea area was initiated about 15 years later and gathered momentum rather slowly because of the unusual engineering problems encountered in solving the issues of the stationary installation of recording instruments at large depths in natural basins or in ice and in the construction of stable systems for data control and transmission. The history of the development of this area of research up to the present time is traced in Table 1.

In this table listing the created, operating, and projected large-scale neutrino telescopes, the DUMAND (Deep Underwater Muon and Neutrino Detection) project, well known in the past, is absent. This project for the construction of a deep-sea Cherenkov high-energy neutrino detector with an efficient volume of about 1 km^3 or more in the Pacific Ocean near the Hawaiian Islands was actively discussed in 1970s–1980s by physicists in the USA, USSR, Japan, and West Germany. On the initiative of outstanding American physicists F Reines and J Learned, the world community began to discuss particular ways for realizing Markov's idea. The technical possibilities were studied for the installation of recording instruments at a depth of about 5 km in the ocean for obtaining reliable information on the energies and propagation directions of neutrinos or, more exactly, charged particles created in the interaction of neutrinos with the target material (i.e., oceanic water). The first deep-sea recording modules based on large-cathode-area photomultipliers were developed and fabricated. The strings of such modules submerged from a ship were tested as the base element of a future detector; however, attempts to install the string at the ocean bottom for operating in the stationary regime failed. The researchers had no time to overcome the encountered deep-sea engineering problems because they lost credit from financers, and for this reason the project was closed down in the mid-1990s.

The direct participation of Soviet physicists and oceanologists in this project ended much earlier, about 1980, which was related to the well-known events in Afghanistan. At the suggestion of A E Chudakov, supported by M A Markov, a start was made on the development of the method for deep-sea neutrino recording in Lake Baikal as a proving ground for testing and constructing the prototypes of future large-scale detectors. The first deep-sea NT-200 detector was constructed in Baikal over the period between 1993 and 1998, and the first events produced by neutrinos were detected in 1994. By 2005, the effective detector volume was increased to 10^7 m^3 due to the installation of the external strings of deep-sea recording modules. To date, the scientific and technical project has been developed and the program for testing the basic elements of the NT-1000 [Baikal-GVD (Gigaton Volume Detector)] detector with the effective volume of about 1 km^3 is being completed [2]. The results of investigations performed with the NT-200 and NT-200 + detectors and the story about basic elements of the project of the future NT-1000 detector are presented in this report.

In concluding the story of work on the DUMAND project, the first and rather adventurous head-on storm of the problem, it is necessary to emphasize that this experience proved to be far from useless. On the one hand, this project has distinctly demonstrated the difficulties encountered in the deployment of stationary systems in natural basins, and, on the other hand, many problems regarding the construction of deep-sea recording instruments have been solved and theoretical studies of the problems of high-energy neutrino astrophysics have been developed. All this initiated the formation of the NESTOR, ANTARES, and NEMO research groups setting as a goal the drawing up of the projects and the creation of large-scale detectors with an effective volume of about 1 km^3 in the Mediterranean Sea [3], and as the intermediate stage, the creation of detectors with a volume of about 10^7 m^3. The ANTARES collaboration advanced more than the others and completed the deployment of the first such detector in Toulon Bay near the French coast in 2008 [4] (see Table).

The idea of creating large-scale detectors with recording instruments located directly in a transparent natural medium, being initially a purely 'deep-sea' idea, acquired a new sense in the early 1990s, after the ingenious proposal of J Learned and

F Halzen to locate the equipment in deep layers of Antarctic ice. The optical properties of ice at depths of more than 1.5 km proved to be adequate for solving this problem, and the AMANDA detector was constructed at the American Amundsen–Scott South Pole Station in the 1990s [5]. The recording instruments were sunk and frozen into holes specially melted in the ice using a hot water drill. The successful development of the project allowed the researchers to persuade the US Congress to invest about $300 billion for the construction of the next-generation IceCube neutrino telescope with an effective volume close to 1 km^3 [6]. The drawing up of this project and the construction and assembling of the detector equipment took approximately ten years, and the detector was assembled in accordance with the design version on 18 December 2010. The 'inauguration' of this project is planned for the end of April 2011.

This short introduction is written to demonstrate the background against which the Baikal neutrino project developed and continues to develop. The story about this project is presented below.

2. Baikal NT-200 and NT-200+ neutrino telescopes

We can assume that the Baikal neutrino experiment was initiated on 1 October 1980, when the Institute for Nuclear Research (INR), USSR Academy of Sciences announced its decision to found a Laboratory of High-Energy Neutrino Astrophysics, which later became the core of the Baikal collaboration also including Irkutsk State University, Moscow State University, the Joint Institute for Nuclear Research (Dubna), the DESY-Zeuthen Research Center (Germany), Nizhny Novgorod State Technical University, and St. Petersburg State Marine Technical University. The researchers from Tomsk Polytechnical University, the Russian Research Centre 'Kurchatov Institute', the Limnology Institute, RAS Siberian Branch, the Academician Andreev Acoustic Institute, and a number of other Russian and foreign (Hungary, Italy, France) institutions also participated in the experiment at some of its stages.

Lake Baikal was chosen as a place for the development of experimental studies for the following obvious reasons: good transparency (comparable to ocean water transparency) of deep waters; the presence of places with sufficiently steep shore slopes in which a depth of about 1 km, required for protection from penetrating cosmic rays, is located at distances of 4–5 km from the shore; the presence of an ice crust allowing the mounting of deep-sea instruments and laying down cable communications from it for two months per annum, and a low expected level of the intrinsic emission of deep waters caused by bioluminescence and radioactivity. Based on the experience and results of Baikal studies performed for many years by researchers at the Limnology Institute, Siberian Branch of the RAS, a concrete site was chosen for starting the work — an area of the lake adjacent to the 106th km of the Krugobaikal railway.

The design of the project, the mounting and startup of the detector were preceded by investigations of experimental hydrooptical, hydrophysical, and hydrological conditions in Baikal, which were performed for about a decade. In these experiments, the intrinsic emission of deep waters in the lake, which is caused by the oxidation of particles a few micrometers in size, was discovered. This emission is typical of the Baikal bacteria that dominate in amount and of many phyto- and zooplankton species. In collaboration with the 'Ekran' Special Design Bureau in Novosibirsk, the high-sensitive hybrid Kvazar-370 photodetector with a photocathode 370 mm in diameter was developed exclusively for the Baikal neutrino telescope [7]. Deep-sea pilot Cherenkov detectors were installed for prolonged operation to try out the method of data acquisition and perform the first physical experiments.

The next task of the Baikal collaboration was the construction of the first large-scale deep-sea NT-200 neutrino telescope [8] with an effective detection area of (2–10) $\times 10^3$ m^2 (depending on the particle energy) and carrying out a wide program of physical studies with it. This telescope was assembled and deployed from 1993 to 1998.

2.1 The NT-200 neutrino telescope

The NT-200 telescope, located at a depth of about 1100 m at a distance of 3.6 km from the shore, is connected by bottom communication lines with a shore data control and acquisition center. The telescope represents a three-dimensional lattice of optical modules mounted on vertical load-bearing cables with the lower ends fastened to bottom anchors, and the upper ends fastened to buoys. Each vertical cable with optical modules forms a structural unit of the telescope — a string of optical modules. The telescope contains 192 optical modules mounted pairwise on eight strings, each 68 m in length. The central string is surrounded by peripheral strings located uniformly on a circle 21.5 m in radius (Fig. 1).

An optical module contains a hybrid Kvazar-370 photodetector placed in a low-radioactive glass housing. To suppress the dark counting rate of PMTs and the background emission of the deep waters of the lake, the optical modules are combined in pairs and are switched in a coincidence circuit, detecting signals within a time window of $\sim$ 15 ns. Two pairs of optical modules, having a common electronic system module, form a functional unit of the string,

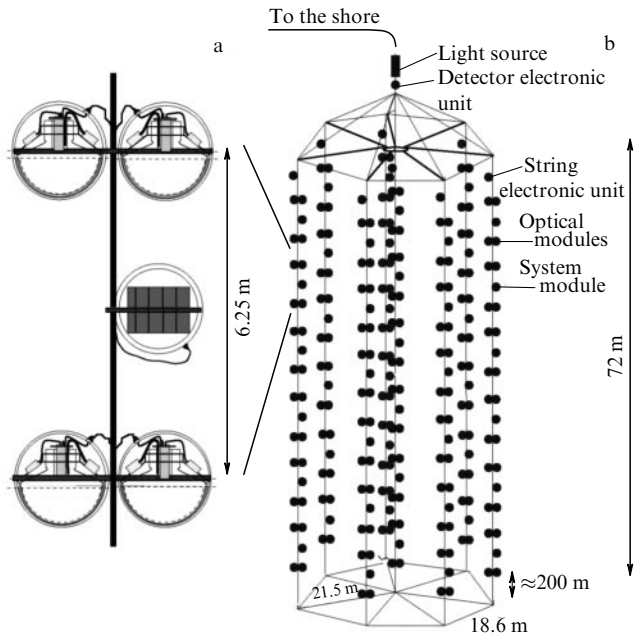

Figure 1. (a) Structural element of the NT-200 telescope ('bundle') consisting of two pairs of optical modules connected in a coincidence circuit and an electronic module providing their operation. (b) Schematic of the NT-200 telescope.

a 'bundle'. The system module contains two units generating a local signal, an amplitude conversion unit, a light-diode triggering unit, and a control unit. The system module generates the output signals (local triggers) of two bundle channels with durations proportional to input charges and the leading edge determining the channel response time.

Local triggers from all the system modules of a string are fed to the string electronic units (SEUs). These electronic units have six measurement channels, a controller, and modems of the data and control channels. Each string has two SEUs connected with the detector electronic unit (DEU). Information from each measurement channel is digitized in the SEU, a local trigger is generated, and a request signal is formed in the DEU. If a sufficient number of request signals are accumulated in the DEU from string electronic units within a 500-ns time interval, a confirmation signal is generated, which is fed to all the string electronic units. Then, a number is assigned to the event in string electronic units and the data accumulated are transferred to the shore data acquisition and control center.

2.2 The NT-200+ telescope

To increase the efficiency of detecting high-energy neutrinos, the NT-200 telescope was modernized in 2004–2005. The new facility, called NT-200+ neutrino telescope [9], provided both an increased efficient volume for recording cascades produced by neutrinos and a considerably improved telescope energy resolution as a whole. The NT-200+ detector represents the initial version of the structural unit of the future Baikal neutrino telescope with an efficient volume of order 1 km^3.

The telescope consists of the central part (NT-200) and three additional external strings located at a distance of 100 m from the central part of the detector (Fig. 2). Each external string contains 12 optical modules grouped in pairs, similarly to the optical modules of the NT-200 telescope. The distances between the channels of the external strings are 20, 50, 20, 30, and 20 m from the channel top.

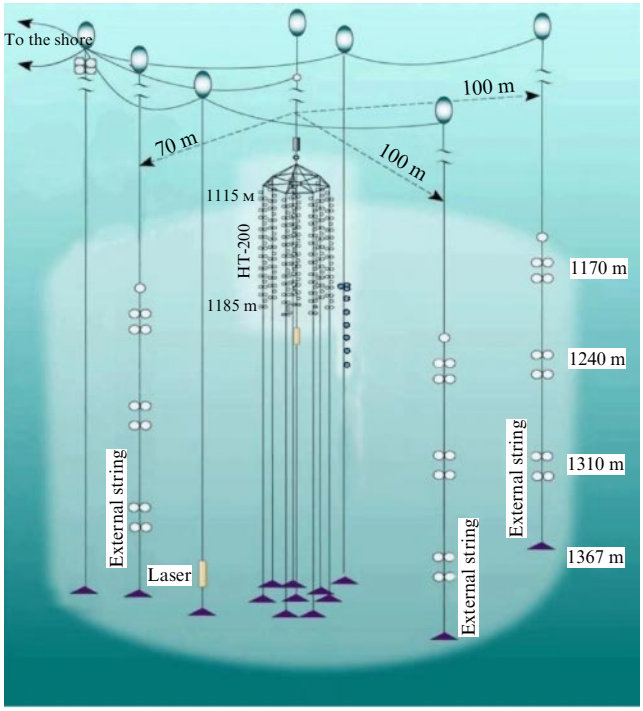

Figure 2. NT-200+ detector.

While optical modules, system modules, and measurement channels of each external string are the same as those in the NT-200 telescope, the electronics of the SEU controller were considerably modernized. Each measurement channel of the SEU contains a time–code converter, a duration–code converter, and an event number recording circuit. A string request signal is formed by the SEU controller for double coincidences of the channel request signals within the 0.5-μs time window. Requests from all the external strings are fed to the central commutation module [data acquisition (DAQ) center], where a confirmation signal is generated and fed back to all the external strings. In the presence of the confirmation signal, information on each local trigger (time, amplitude, event number, measurement channel number, and global event number) is delivered through the SEU controller to the DAQ center. The DAQ center provides the combination of data flows and translation of all obtained information to the shore center.

2.3 Basic results obtained in NT-200 neutrino telescope experiments

The Baikal deep-sea neutrino telescope is one of the three largest high-energy neutrino detectors (along with ICeCube at the South Pole, and the underwater ANTARES detector in the Mediterranean Sea). The important results of the first stage of Baikal project investigations obtained with intermediate setups between 1980 and 1998 concerned both the study of the parameters of detectors and atmospheric muon fluxes, the selection of events produced by neutrinos, and the search for magnetic monopoles. The upper intensity limit for the flux of superheavy magnetic monopoles was found from the catalysis of baryon decay, which was at that time one of the strongest theoretical and experimental restrictions. In experiments with the NT-36 and NT-96 detectors, the first neutrino events were recorded and one of the strongest restrictions on the muon flux was found, which was caused by the annihilation of dark matter massive particles (neutralinos) at Earth's center [10]. In addition, the restriction on the intensity of the superhigh-energy (above 10 TeV) natural neutrino flux was established [11].

The most important results were obtained in 2005–2008 in experiments with the Baikal telescope. The analysis of these experiments has demonstrated the existence of new restrictions (one of the strongest at present) on the intensity of the natural flux of fast ($v/c > 0.8$) magnetic monopoles, 4.6×10^{-17} cm^{-2} s^{-1} sr^{-1} (for $v/c = 1$) [12], on muon fluxes accompanying the annihilation of dark matter massive particles (neutralinos) at Earth's center, 4.2×10^{-15} cm^{-2} s^{-1} [13], and at the Sun's center, 3×10^3 km^{-2} year^{-1}, in the region of neutralino masses above 500 GeV [14], on the neutrino flux from gamma bursts in the energy range up to 10^7 GeV [15], on the neutrino flux from local galactic sources located in the Southern Celestial Hemisphere depending on the declination, $E^2F < 5 \times 10^{-10}$ TeV cm^{-2} s^{-1}, and, finally, the restriction on the intensity of the natural diffusion neutrino flux, which is $E^2F < 2.9 \times 10^{-7}$ GeV cm^{-2} s^{-1} sr^{-1} for the total flux of neutrinos of all types in the energy range from 2×10^4 GeV to 2×10^7 GeV and lies in the region of theoretically predicted values [16]. In addition, the strongest at present restriction $F < 3.3 \times 10^{-20}$ cm^{-2} s^{-1} sr^{-1} GeV^{-1} on the electron antineutrino flux in the region of the

6.3×10^6-GeV resonance was established [17]. The implementation of the NT-200+ detector project provided approximately a threefold increase in the sensitivity of experiments on searching for the natural diffusion neutrino flux and made it possible to begin the study of their energy spectrum at energies up to 10^{18} eV.

The fortunate combination of natural factors along with the well-studied place for experimentation and the experience acquired in the deployment and operation of the first-generation NT-200/NT-200+ neutrino telescope provided the required prerequisites for the beginning of work on the designing and construction of the deep-sea Baikal NT-1000 neutrino telescope with an efficient volume of order 1 km^3.

3. The NT-1000 neutrino telescope (Baikal-GVD)

The successful operation of NT-200/NT-200+ and AMANDA neutrino telescopes for more than ten years and the results obtained in these experiments stimulated the development and building of next-generation telescopes IceCube, NT-1000, and KM3NeT with characteristic scales on the order of 1 km^3. The Baikal NT-1000 telescope and Mediterranean KM3NeT telescope both located in the Northern Hemisphere and the IceCube telescope located at the South Pole will supplement each other due to their different geographical positions, and will form the world network of telescopes for searching for and studying neutrino sources in the entire celestial sphere. Detectors located in the Northern Hemisphere have an important advantage because they can perform virtually continuous observation of the Galaxy center and galactic plane where a significant part of the potential sources of high-energy cosmic rays are concentrated.

The deep-sea NT-1000 neutrino telescope [2] is intended for solving a variety of problems in astrophysics, cosmology, and elementary particle physics: the search for local neutrino sources, the study of the diffusion neutrino flux, the search for dark matter manifestations, and the search for magnetic monopoles and other hypothetical particles. The next-generation deep-sea Baikal NT-1000 telescope will be an experimental complex intended to study natural neutrino fluxes at energies above 10 TeV by detecting the Cherenkov radiation of secondary muons and showers generated in neutrino interactions.

The concept of the NT-1000 neutrino telescope is based on a number of quite obvious requirements for the construction and deployment of the recording system of the new detector: the maximum possible use of the advantages of mounting the recording system from the ice crust of Lake Baikal; the possibility of building up the facility and providing its efficient operation already at the first stages of deployment, and the potential of using different variants of the arrangement and number density of photodetectors within one measuring system.

Taking into account the requirements mentioned above and estimates of the sensitivity and energy resolution of the NT-1000 neutrino telescope obtained in the large-scale simulation of the telescope response to Cherenkov radiation from muons and showers, the architecture of the measurement and communication systems was developed and the basic configuration of the telescope was chosen (Fig. 3). Radiation is detected with 2304 Hamamatsu-7081HQE photomultipliers with a hemispherical photocathode 250 mm in diameter. Photomultipliers, together with control electronics, are encased in deep-sea glass housings, forming optical modules. The optical modules mounted on vertical cables form strings.

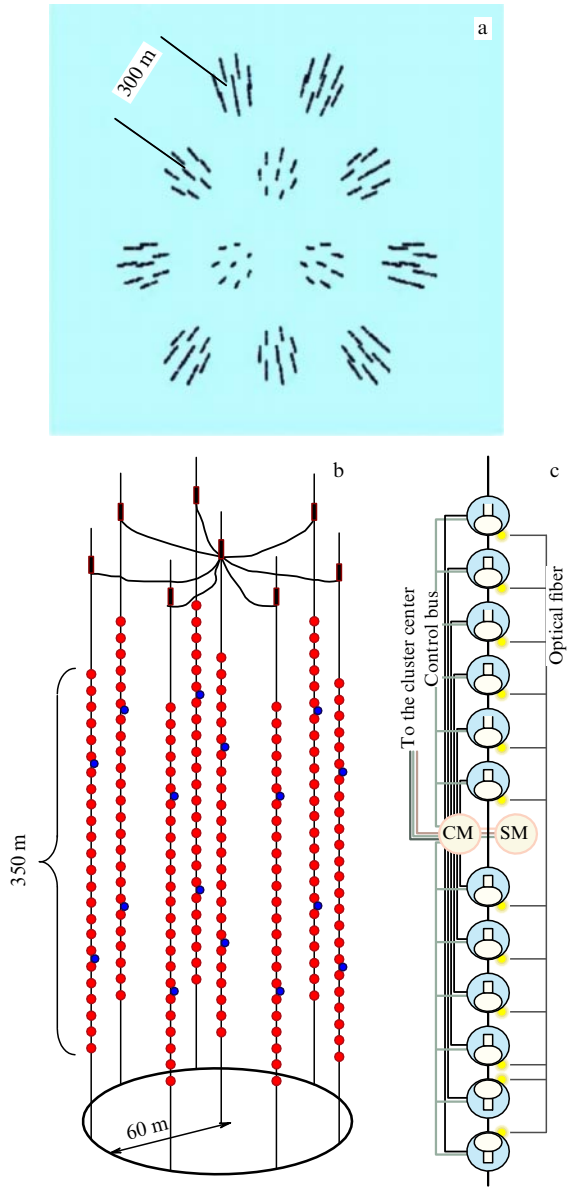

Figure 3. Schematic view of the km3-scale NT-1000 neutrino telescope in Lake Baikal: (a) top viw; (b) telescope cluster; (c) string of optical modules.

The basic structural unit of a string is the section of optical modules. The section comprises a functionally complete detector unit including systems for radiation detection, signal processing and calibration, trigger formation, and data transfer. The section contains 12 optical modules arranged 15 m apart along the string, and the central and service modules. Analog signals from all optical modules of the section are fed to the central module over coaxial cables. The low-voltage supply is fed to optical modules over the same cables. The analog signals from optical modules are converted in the central module to a digital code and information is transferred over an Ethernet line. The service module is designed for calibrating the time channels of the setup, and determining the string position and electrical feeds of the optical modules. The string position is determined with a hydroacoustic coordinate measurement system. The synchronization, power supply,

and data transfer channels of the sections are combined in the switching module of the string, which is connected with the central control unit of a cluster.

The basic configuration of each of the 12 clusters in the NT-1000 neutrino telescope contains eight strings, each including 24 optical modules (two sections in a string) separated from each other by 60 m. The distance between adjacent clusters reaches 300 m. The string clusters are connected with the shore center by combined electrooptical cables about 6 km in length. Each cluster of the NT-1000 telescope is a functionally complete detector (with the detection volume on the scale of NT-200+ or ANTARES detector), which can operate both incorporated into the setup and independently. This provides the simplicity of expanding up the telescope instrumented volume and the possibility of bringing into operation its separate parts during the deployment of NT-1000.

The basic configuration of the telescope provides an efficient volume of 0.2–0.7 km^3 for recording showers in the energy range from 10^5 to 10^9 GeV, and an efficient area of 0.2–0.5 km^2 for recording muons in the energy range from 10^4 to 10^6 GeV. The accuracy of recovering the muon propagation direction ranges $0.4° - 0.6°$, and that for showers is $5° - 7°$. The relative accuracy of the shower energy recovery comes to 20–35%.

Long-term full-scale tests of the equipment of the NT-1000 section were successfully performed in Lake Baikal between 2008 and 2010. A prototype of the NT-1000 cluster was already constructed and tested under laboratory conditions and will be deployed in Lake Baikal in the continuous data acquisition regime during the winter expedition in 2011.

4. Conclusions

Thus, the method of deep-sea recording of elementary particles (and its ice modification) proved its efficiency for studying natural high-energy neutrino fluxes. The modern knowledge of the diffusion neutrino flux in the energy range from 10^{13} to 10^{18} eV, local sources of neutrinos with energies above 10 GeV, the natural flux of fast magnetic monopoles, and dark matter massive particles manifestations is mainly determined by the results of experimental studies performed with the Baikal NT-200/NT-200+ neutrino telescope, the AMANDA detector at the South Pole, and (in late 2009 and 2010) the ANTARES detector in the Mediterranean Sea. Bringing the IceCube detector into operation at the South Pole will provide the increase in the sensitivity of some experimental studies by one–two orders of magnitude.

On the agenda is the problem of the construction of a detector (or detectors) in the North Hemisphere for studying the center of our Galaxy with a sensitivity comparable to that of the IceCube detector. The Baikal collaboration, which developed, constructed, and prepared for full-scale tests a prototype of the basic element — an autonomous cluster of deep-sea strings of recording modules for the km3-scale NT-1000 detector (Baikal-GVD) — is considerably ahead of all on the part to constructing the operating project of such a detector.

Acknowledgments. The author gratefully acknowledges his colleague Zh-A M Dzhilkibaev for the substantial help in the preparation of this paper.

References

1. Markov M A, in *Proc. of the 1960 Annu. Intern. Conf. on High-Energy Physics, Rochester, New York, 25 August – 1 September 1960* (Eds J Prentki, J Steinberger) (Rochester, N.Y.: Univ. of Rochester, 1960) p. 572
2. Baikal Collab. "Nauchno-tekhnicheskii proekt glubokovodnogo neitrinnogo teleskopa kubokilometrovogo masshtaba na oz. Baikal" ("Scientific and technical project of the km^3-scale neutrino telescope in the Lake Baikal"), http://baikalweb.jinr.ru/GVD/ (2010)
3. Katz U F (for the KM3NeT Consortium) *Nucl. Instrum. Meth. Phys. Res. A* **602** 40 (2009)
4. Circella M (for the ANTARES Collab.) *Nucl. Instrum. Meth. Phys. Res. A* **602** 1 (2009)
5. Andres E et al. *Astropart. Phys.* **13** 1 (2000)
6. Abbasi R et al. (and the IceCube Collab.) *Nucl. Instrum. Meth. Phys. Res. A* **601** 294 (2009)
7. Bagduev R I et al. *Nucl. Instrum. Meth. Phys. Res. A* **420** 138 (1999)
8. Baikal Collab. "The Baikal neutrino telescope NT-200", Preprint No. 92-03 (Moscow: INR RAS, 1992)
9. Avrorin A V et al., Preprint No. 1265/2010 (Moscow: INR RAS, 2010)
10. Balkanov V A et al. *Yad. Fiz.* **62** 1015 (1999) [*Phys. At. Nucl.* **62** 949 (1999)]
11. Balkanov V A et al. *Astropart. Phys.* **14** 61 (2000)
12. Aynutdinov V et al. *Astropart. Phys.* **29** 366 (2008)
13. Antipin K et al. *Proc. of the First Workshop on Exotic Physics with Neutrino Telescopes: EPNT'06, Uppsala, Sweden, September 20 – 22, 2006* (Ed. C P de los Heros) (Uppsala: Uppsala Univ., 2007)
14. Avrorin A et al., in *Proc. of the 31st ICRC, Lodz, Poland, July 2009*; arXiv:0909.5589
15. Avrorin A V et al., Preprint No. 1211/2009 (Moscow: INR RAS, 2009)]
16. Avrorin A V et al. *Pis'ma Astron. Zh.* **35** 723 (2009) [*Astron. Lett.* **35** 651 (2009)]
17. Aynutdinov V *Astropart. Phys.* **25** 140 (2006)

PACS numbers: 95.55.Vj, 96.50.sb, 96.50.sh
DOI: 10.3367/UFNe.0181.201109i.0990

Telescope Array Observatory observations of the Greisen–Zatsepin–Kuzmin effect

I I Tkachev

1. Introduction

The enigma of the origin of ultrahigh-energy cosmic rays (UHECRs) is one of the most interesting and important unsolved problems of particle astrophysics. The center of attention in this research field is the Greisen–Zatsepin–Kuzmin (GZK) effect. Recently, the Telescope Array (TA) observatory, the largest observatory in the northern hemisphere of Earth, studying the origin of UHECRs, began to operate in the state of Utah (USA). In this report, we consider the fundamentals of the GZK effect, its history and present observational status, and preliminary results obtained at the

I I Tkachev Institute for Nuclear Research,
Russian Academy of Sciences, Russian Federation
E-mail: tkachev@m12.inr.ac.ru

Uspekhi Fizicheskikh Nauk **181** (9) 990 – 997 (2011)
DOI: 10.3367/UFNr.0181.201109i.0990
Translated by M Sapozhnikov; edited by A Radzig

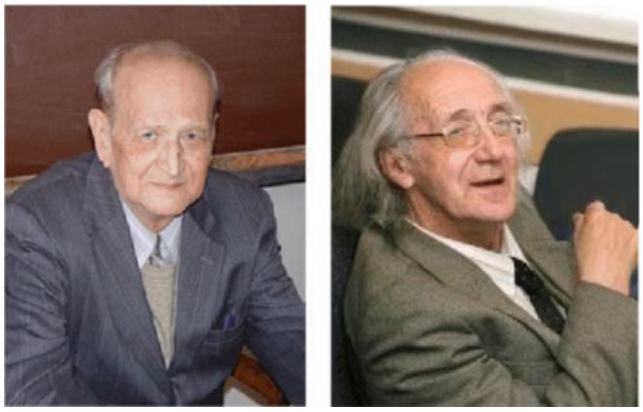

G T Zatsepin (at the left) and V A Kuzmin became staff members of INR, RAS from the first days of its foundation.

TA observatory, including the energy spectrum, composition, and the results of investigations of the arrival directions of initial UHECR particles.

Soon after the discovery of the cosmic microwave background (CMB) radiation of the Universe, Greisen [1], and Zatsepin and Kuzmin [2] pointed out that highest-energy protons propagating over cosmological distances from a source to an observer should catastrophically loose their energy in the threshold reactions of the photoproduction of pions in interactions with the universal background radiation. This process considerably limits the possible distance to the sources of detected UHECRs, which, according to the GZK limit, cannot exceed 100 Mpc, and should lead to the cutoff of the high-energy part of the spectrum.

The discovery made by Greisen, Zatsepin, and Kuzmin is based on physical observations and laws, which were well investigated and verified under laboratory conditions, in particular, on the cross sections for interactions between particles measured for energies of order 1 GeV (in the center-of-mass system) and on the validity of the general relativity theory and Lorentz's transformations. Thus, the question of whether the GZK flux suppression exists in the observed spectrum of cosmic rays is one of a number of fundamental questions because the absence of such a cutoff in the spectrum would be an unambiguous signal of 'new physics'.

On the other hand, the observational verification of the GZK cutoff of the high-energy part of the spectrum would suggest that the optical thickness of the cosmic medium for initial high-energy particles becomes comparable to a scale at which the Universe is noticeably inhomogeneous because the distribution of matter is inhomogeneous on scales of a few hundred megaparsec (and smaller). This means that the anisotropy of the UHECR flux can be anticipated in this case. It should be emphasized here that it is not only variations of the flux on large angular scales that are expected. It is also possible that we are standing at the threshold of discovering UHECR point sources. The astronomy of charged particles originating before our eyes may have a bright future if a noticeable fraction of initial particles consists of protons. This means that the study of the mass composition of initial UHECR particles is very important.

It is no wonder that great efforts in recent decades have gone into careful measurements of the spectrum of ultrahigh-energy cosmic rays, while the GZK effect is a source of growing interest in investigations conducted in the field of cosmic ray physics.

2. Effects of propagation of ultrahigh-energy cosmic rays

In this section, we consider the influence of different cosmological factors on the propagation of UHECRs and manifestations of this influence in observational data.

2.1 The Greisen–Zatsepin–Kuzmin cutoff

2.1.1 Optical depth. Ultrahigh-energy cosmic rays do not freely propagate in space and on cosmological scales. Their energy is sufficient for producing massive secondary particles in collisions with relic photons and also, depending on the nature of an initial particle, with radio photons and infrared photons.

The most important reaction is the photoproduction of pions during the propagation of protons (or neutrons) in the cosmic microwave background radiation left over from the hot Universe epoch. The threshold energy of this reaction in the laboratory reference system is defined as

$$E_{\rm th}({\rm p}+\gamma\to{\rm n}+\pi)=\frac{(m_{\rm p}+m_\pi)^2-m_{\rm p}^2}{2E_\gamma(1-\cos\theta)}\,. \qquad (1)$$

It should be noted that this expression was derived using standard Lorentz transformations and standard dispersion relations $E^2=k^2+m^2$ between the energy and momentum of particles. If these assumptions are incorrect in the ultrahigh-energy region, the threshold conditions in the laboratory coordinate system can be different. For the black-body spectral distribution of relic photons at the temperature $T=2.7$ K, reaction (1) becomes efficient for

$$E_{\rm GZK}\gtrsim 5\times10^{19}\ {\rm eV}\,. \qquad (2)$$

The pion photoproduction reaction has a large cross section and reaches a maximum at the Δ resonance. At the resonance half-width, this cross section equals

$$\sigma\sim 300\ \mu{\rm b}\approx 3\times10^{-28}\ {\rm cm}^2\,. \qquad (3)$$

The number density of relic photons is $n\sim T^3\sim 400\ {\rm cm}^{-3}$. This corresponds to the proton mean free path

$$L_\sigma=(\sigma n)^{-1}\approx 8\times10^{24}\ {\rm cm}\approx 2.7\ {\rm Mpc}. \qquad (4)$$

In each collision, an initial proton loses about 20% of its energy (corresponding to the pion–proton mass ratio). The proton energy decreases exponentially (by a factor of e) in a series of successive collisions after propagation over the distance $L_{\rm A}$, called the decay length. For energies exceeding the resonance energy $E\approx 5\times10^{20}$ eV, the decay length is $L_{\rm A}\approx 10$ Mpc. Thus, energy decreases to values close to the threshold at 10^{20} eV after propagation over distances of order 100 Mpc, virtually independently of the initial energy (Fig. 1).

Thus, *protons detected with energies* $E\gtrsim 10^{20}$ eV *should be accelerated in sources located at the distance* $R\lesssim R_{\rm GZK}$, $R_{\rm GZK}\equiv 100$ Mpc. The corresponding spatial volume is called the GZK sphere (or the GZK distance).

2.1.2 Spectral cutoff. We assume that the injection spectrum for initial photons exhibits a power form, $J_{\rm in}(E)\propto E^{-\alpha}$, and $n(r)$ is the density of sources. The particle flux from an individual source decreases as r^{-2}, which is compensated for by the integration volume $r^2\,{\rm d}r$. Therefore, the cosmic ray

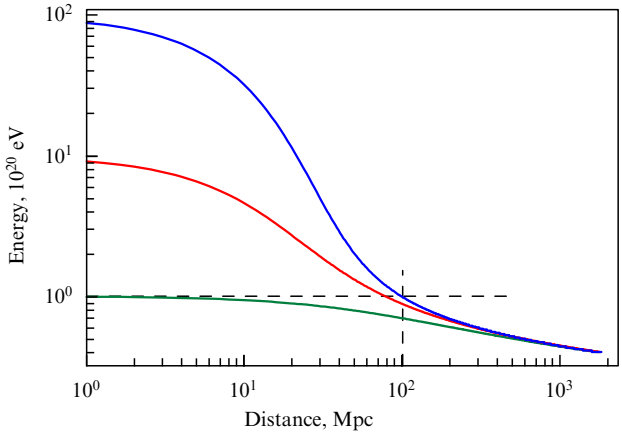

Figure 1. Initial proton energy as a function of the distance travelled from a source.

flux with energy E should increase proportionally to the radius of the integration sphere:

$$J(E) \propto \int_0^{R(E)} n(r)\,\mathrm{d}r \propto R(E)\,, \tag{5}$$

if the density of sources remains invariable. Here, $R(E)$ corresponds to the decay length, i.e., the maximum distance to the sources of initial particles detected with energy E. The decay length for protons with energies $E < 5 \times 10^{19}$ eV is 10^3 Mpc, whereas for $E > 5 \times 10^{20}$ eV, the decay length is 10 Mpc.

Thus, *the UHECR flux should change by two orders of magnitude at the GZK energy if the distribution of sources is homogeneous* (Fig. 2).

2.2 Magnetic fields

Let us estimate a typical angle $\sim L/R_{\mathrm{g}}$ through which the trajectories of charged particles deflect after passing over the distance L in galactic and intergalactic magnetic fields. Here, R_{g} is the Larmor radius, and the angle of deflection is assumed small.

(1) For particles intersecting a galactic disc transversely to a galactic magnetic field, we have

$$\frac{\Delta\theta}{Z} \approx 2.5^\circ\,\frac{10^{20}\,\mathrm{eV}}{E}\,\frac{B}{3\,\mu\mathrm{G}}\,\frac{L}{1.5\ \mathrm{kpc}}\,, \tag{6}$$

where Z is the electric charge of the initial particle, 3 μG is the value of the regular component of the magnetic field, and 1.5 kpc is the galactic disc thickness. (The weaker deflections in the turbulent component of the galactic magnetic field are discussed, for example, in paper [3].) Protons with energies $E > 10^{18}$ eV intersect the galactic disc during one passage. The trajectories of protons with lower energies 'become entangled' and escape from the Galaxy, diffusing through its boundary.

Cosmic rays with energies $E > 10^{18}$ eV should have an intergalactic origin if the initial particles comprise protons. Even if the UHECR composition corresponds to iron nuclei, cosmic rays for $E > 2 \times 10^{19}$ eV should enter the Galaxy from outside, otherwise the anisotropy of a particle flux on the galactic disc should be observed, which is not the case.

(2) The deflection angle of UHECR trajectories in a homogeneous random intergalactic field with the coherence

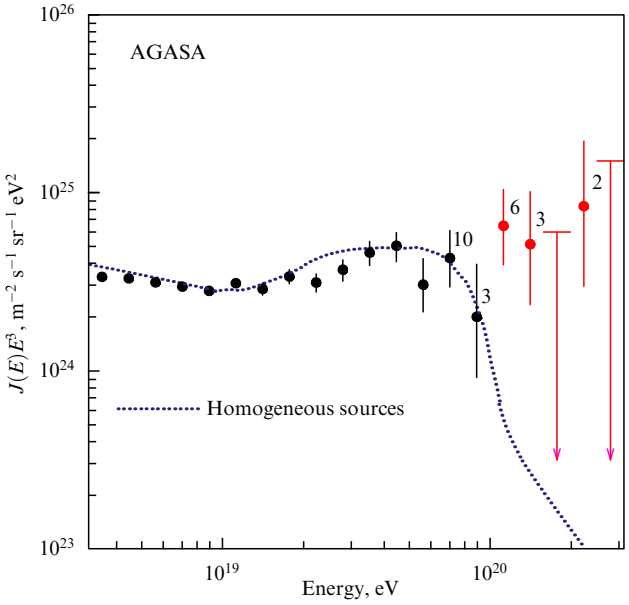

Figure 2. Energy spectrum of cosmic rays. The dotted curve fits the GZK expectation; dots show AGASA data (Akeno Giant Air Shower Array); numbers alongside the dots indicate the number of detected events (current data are discussed in Section 3).

length λ is determined by the relation

$$\frac{\Delta\theta}{Z} < 0.4^\circ\,\frac{10^{20}\ \mathrm{eV}}{E}\,\frac{B}{10^{-10}\ \mathrm{G}}\,\frac{(L\lambda)^{1/2}}{10\ \mathrm{Mpc}}\,. \tag{7}$$

Intergalactic magnetic fields have not been measured to date, except for the central regions of galactic clusters. The observational restrictions on their value and correlation length are presented in Ref. [4]. The numerical simulation of the magnetic field generation processes in galactic clusters gives the upper theoretical limit for inductions of these fields on the order of $B \lesssim 10^{-12}$ G [5]. The lower limit of $B \gtrsim 3 \times 10^{-16}$ G was recently obtained in Ref. [6]. This limit follows from the fact of nonobservation of secondary gamma radiation from electromagnetic cascades induced by initial TeV photons.

Because the sources of highest-energy cosmic rays should be located inside the GZK sphere, the trajectories of protons with $E > 10^{20}$ eV are not deflected considerably by galactic or intergalactic magnetic fields, the deflections being comparable with the angular resolution of modern telescopes.

Thus, *the arrival directions of initial protons with energies exceeding the GZK energy should indicate their sources. The astronomy of charged particles is principally practicable.*

3. Observational status

For particle energies below 10^{14} eV, the cosmic ray flux is intense enough, so that direct observations are possible with the use of high-altitude balloons or satellites. For an energy of 10^{15} eV, the flux is one particle per 1 m^2 over a year, which excludes the possibility of direct orbital observations. For an energy of 10^{20} eV (the energy region where the GZK flux suppression should be manifested), the flux decreases to one particle per km^2 over a century, which, notably, is a reason for the slow progress in UHECR physics. However, difficulties involved in the direct observation of UHECRs would be

caused not only by their negligibly small flux but also by the extremely high energy being measured (recall that detectors of modern colliders weigh a few hundred thousand tons).

Fortunately for physicists working in this field, most of the detector has already been created by Nature — Earth's atmosphere being a suitable calorimeter. The atmosphere thickness is such that extended air showers (EASs), consisting of secondary particles induced by the incident initial particle, reach a maximum near Earth's surface. For an energy of 10^{19} eV, the transverse size of the air shower on the Earth surface achieves a few kilometers.

Thus, air showers can be detected by placing an array of particle detectors on Earth's surface, typically separated by a distance of a few hundred meters. Such a setup will accumulate data continuously. Other methods for detecting EASs are also possible, for example, based on the measurement of the fluorescence of the atmosphere caused by the passage of EASs. Such detectors can accumulate data only during clear, moonless nights. However, their advantages include the possibility of direct observations of important parameters, such as the longitudinal profile of a shower and the atmospheric altitude at which this profile reaches its maximum and the possibility of using the calorimetric method to estimate the energy of the initial particle.

In early experiments in the GZK energy region, such as Volcano Ranch [7], SUGAR (Sydney University Giant Air Shower Recorder) [8], Haverah Park [9], Yakutsk [10, 11], and AGASA [12, 13], the first method for detecting EASs based on detector arrays was utilized. Later on, the Fly's Eye [14] and HiRes [15] 'telescopes' appeared, which measured the fluorescent glow of the atmosphere. The results of earlier experiments were impressive but contradictory, and required verification and confirmation. It became clear that hybrid setups are required which use simultaneously a surface detector array and fluorescence telescopes for detecting the same EASs. Such a hybrid approach, which allows the reduction of systematic errors and determining more accurately the physical characteristics of the initial particle, because many EAS parameters are measured simultaneously, was applied to the development of the newest generation of observatories detecting cosmic rays, such as the Pierre Auger Observatory in the southern hemisphere of Earth [16], and the Telescope Array in the northern hemisphere [17].

3.1 Early results and theorists' growing interest in the GZK problem

To emphasize the importance of the discovery of Greisen, Zatsepin, and Kuzmin, we present here the historical review of early experimental results and describe briefly the considerable excitement generated by these results among theorists in the field of high-energy and particle physics.

Over four decades after the publication of papers by Greisen, Zatsepin, and Kuzmin [1, 2], the number of events detected with energies exceeding the GZK limit increased; however, no signs of the spectral cutoff or indications of possible particle sources were found. In particular, the spectrum measured with AGASA, the largest facility for recording EASs and which accumulated the most complete statistics by the time of the appearance of the last generation of observatories, is illustrated in Fig. 1.

These experimental results proved to be a puzzle because, unlike expectations based on the Standard Model, it was found that:

— the GZK cutoff was absent in the UHECR spectrum. Notice that the assumption that initial particles consist of heavy nuclei or photons does not solve this problem, and

— the arrival directions of particles with energies $E \gtrsim 10^{20}$ eV do not lead to the identification of astrophysical sources inside the GZK sphere.

This attracted interest and attention to this problem, and theorists proposed many possible solutions to this puzzle. Consider below some of them.

• *Invisible sources*. To explain the second part of the puzzle related to the arrival directions of initial particles, a hypothesis was advanced that the UHECR sources are not unique, bright astrophysical objects, which usually attract attention, but *something* that was located (or is located) inside the GZK sphere, but is invisible today and does not reveal itself as a source, except for the presence of luminosity in UHECRs. As objects of this type, 'dead' quasars were proposed [18]. The model assumes that quasars, which were bright and powerful in the past, preserve their capability to accelerate protons near the horizon of a supermassive black hole, even when the matter accretion process has terminated and the quasar is quenched in the electromagnetic spectral range. However, this model is intrinsically contradictory. The acceleration of protons up to ultrahigh energies in such a compact object is inevitably accompanied by intense gamma radiation in the TeV-energy range, and more recent results obtained with Cherenkov gamma telescopes exclude this model [19].

• '*Local*' *models*. The GZK cutoff will be absent in the UHECR spectrum if the sources of cosmic rays are located in the galactic halo. Such a scenario is implemented in the hypothesis of decomposing superheavy dark matter [20, 21]. The problem of generating superheavy, but long-lived (and, therefore, noninteracting) particles is solved quite simply. Dark matter particles in the required mass range $M_X \sim 10^{13}$ GeV are created at the right cosmological concentration due to the Universe expansion process itself [22–24]. The model of decomposing superheavy dark matter has an unambiguous signature: the anisotropy of the UHECR flux at the galactic center [25, 26]. This characteristic is not observed in real data.

• *Models with 'intermediary' particles*. It is possible that intermediary particles exist beyond the framework of the Standard Model, which are immune with respect to interactions with relic radiation and therefore can fly to us from remote sources with energies lying above the GZK limit. Such hypothetical hadrons (the bound states of light gluino and usual quarks) were proposed in paper [27]. Being hadrons, these particles could reproduce the development of EASs [28]. However, this model gives rise to contradictions related to the results of acceleration experiments and the absence of observation of exotic isotopes [28]. The role of an intermediary particle was also ascribed to a hypothetical axion [29–31]. This scenario assumes that high-energy photons oscillate into axions in the magnetic field of a source and, having propagated over cosmological distances without energy loss, oscillate back into photons in the magnetic field of the Galaxy.

• *Violation of the Lorentz invariance*. Threshold energy (1) was obtained assuming the standard Lorentz kinematics. Its violation at high energies could lead to a larger threshold for photomesonic reactions and, therefore, the UHECR spectrum could continue without the GZK flux suppression [32, 33].

3.2 New Telescope Array experiments

The Telescope Array project is a collaboration of several institutions and universities in Japan, the USA, Korea, Russia, and Belgium. From Russia, the Institute for Nuclear Research, RAS participates in the project.

The experimental facility of the Telescope Array (TA) Collaboration is located in the west Utah desert. At present, it is operated with three observation stations using fluorescence detectors (FDs) and arrays of 507 surface detectors (SDs) (Fig. 3), which together form the largest hybrid facility recording UHECRs in the northern hemisphere of Earth. The SDs form an array with a distance of 1.2 km between detectors, which covers an area of 700 km^2. Three FD stations surrounding the SD array are called Middle Drum (MD), Black Rock Mesa (BR), and Long Ridge (LR). The MD station (Fig. 4) comprises 14 telescopes which were earlier employed in the HiRes experiment. All the equipment at the BR and LR stations was made especially for the TA experiment. Observations with FD stations started in November 2007, and with the surface array in March 2008.

3.2.1 Energy spectrum. By now, the UHECR energy spectra have been obtained by using the TA facility for each of the three data sets: SD data (the SD spectrum), MD station data (which were used to construct the monocular FD spectrum), and hybrid data.

Figure 3. One of the surface detectors in the west Utah desert (USA).

Figure 4. Middle Drum station comprising 14 telescopes recording fluorescent emission of the atmosphere. The long-exposure night shot was contributed by B Stokes.

The SD spectrum is constructed using data gathered between May 2004 and February 2010. The exposure is 1500 km^2 sr per year, which is approximately equal to the total AGASA exposure for the entire observation time. The SD events are reconstructed by fitting the EAS front geometry and the transverse (to the EAS axis) energy density distribution. The number density S_{800} of particles at a distance of 800 m from the EAS axis is utilized to estimate the energy of the initial particle. The relation between S_{800} and energy, as well as the effective aperture are retrieved by the Monte Carlo method. The resulting (preliminary) energy spectrum is presented in Fig. 5.

The obtained SD spectrum was fitted with power functions on the segments. The two break points are found at the values of $\log(E\,[\mathrm{eV}])$ equal to 18.71 and 19.75, which corresponds to the 'ankle' [1] and the onset of the GZK cutoff. For energies exceeding the energy $E = 10^{19.75}$ eV of the break point, five events were recorded, whereas in the case of the continuous power extension of the spectrum, 18.4 events would be expected. Thus, the suppression of the UHECR flux at energies exceeding the GZK limit was found at a confidence level of 3.5σ. The details of the SD analysis are presented in paper [35].

It should be noted that the GZK cutoff was first observed by the FD method in HiRes experiments [36] and was confirmed by the Pierre Auger Observatory [37]. The absence of the GZK cutoff would mean the emergence of new physics which can be manifested differently in various detectors [38]. In this connection, it is important to note that the TA SD detectors are identical to those used in the AGASA facility.

The spectrum obtained at the MD station includes data accumulated for almost three years, from December 2007 to September 2010. The preliminary result is shown in Fig. 5.

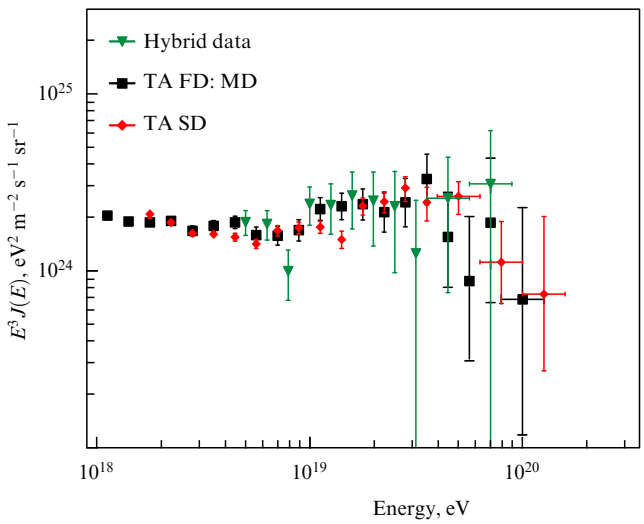

Figure 5. UHECR spectrum obtained at the Telescope Array Observatory (preliminary results). The spectrum suppression at high energies is statistically meaningful and begins in the GZK energy range.

[1] A spectral feature whose position and shape correspond to the theoretically predicted [34] change in the power spectrum, taking into account losses for creation of e^+e^- pairs in the interaction of initial protons with relic radiation.

This TA energy spectrum is consistent with the one obtained in the HiRes experiments [36], and also demonstrates the GZK cutoff. The details of the analysis of these data are presented in the thesis [39].

Hybrid events, i.e., those recorded simultaneously with an SD array and some of the FD stations, have smaller statistics, but nevertheless are preferable for spectral measurements because the energy of the initial particle can be determined calorimetrically using the FD data, while the exposure is accurately determined by means of the SD array. In addition, hybrid events are reconstructed more reliably because more information is available for each event. The preliminary energy spectrum obtained in the hybrid analysis of the TA data accumulated over a year and a half of observations is depicted in Fig. 5; the corresponding details can be found in Ref. [40].

3.2.2 Mass composition. The longitudinal development of an EAS depends both on the initial particle energy and the particle nature. The atmospheric depth, at which the number of particles in the shower reaches its maximum $X_{\max}$, is a good indicator of the initial particle type. The longitudinal development of the EAS is directly observed by means of fluorescence detectors. Because of this, the FD technique is most convenient for determining the mass (or as the saying is — chemical) composition of UHECRs.

Analyzing EASs by this method, the HiRes Collaboration presented results consistent with the proton-dominated composition of UHECRs in the energy range from 1.6 to 64 EeV (10^{18} eV) [41]. On the other hand, both the average value of $X_{\max}$ and the root-mean-square value of its fluctuations, measured at the Pierre Auger Observatory, point to the growing masses of initial particles at energies above 3 EeV, reaching values typical of iron [42].

We are studying the mass composition of UHECRs by measuring $X_{\max}$ in a set of the FD stereo data. The analysis presented here is based on the data obtained between November 2007 and September 2010. For events detected simultaneously at two FD stations, the geometry and longitudinal development of the air shower were reconstructed. The energy dependence of the average value of $X_{\max}$ obtained in the range from $10^{18.2}$ to 10^{20} eV is plotted in Fig. 6. This figure also shows the Monte Carlo expectation for different models of nuclear interactions. The TA data are in good agreement with the QGSJET-01 prediction for the purely proton composition, and inconsistent with the iron composition for all the interaction models considered. Details of the analysis of the mass composition of UHECRs are presented in Ref. [43].

3.2.3 Constrains on photons. The suppression of the particle spectrum at the highest energies is not necessarily caused by the GZK effect. It can also be related to an attainment of the acceleration limit by sources, together with the random coincidence of corresponding limiting energies. These alternatives can be distinguished by detecting the photon component of initial particles. The latter appears here as the product of photonuclear reactions. The expected fraction of photons is small, and photons have not yet been observed in UHECRs. The experimental limit of the photon flux for $E > 10$ EeV obtained in TA experiments is [44]

$$F_\gamma < 3.4 \times 10^{-2}\ \mathrm{km}^{-2}\ \mathrm{sr}^{-1}\ \mathrm{year}^{-1}\ (95\%\ \mathrm{CL}).$$

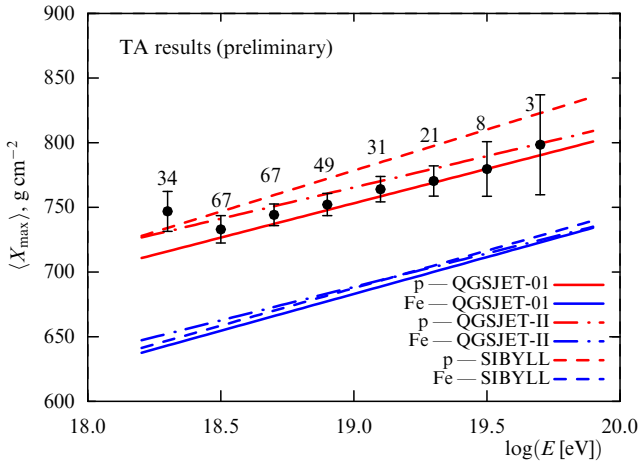

Figure 6. Average value of $X_{\max}$ as a function of energy (preliminary TA results). Dots are the FD stereo data (the numbers of recorded events are indicated alongside the dots). The three upper lines correspond to predictions of different interaction models for the purely proton composition: QGSJET-01 (solid line); QGSJET-II (dashed-dot line), and SIBYLL (dashed line). The three lower lines correspond to UHECRs consisting of iron nuclei.

This constrain is the strongest in the northern hemisphere of Earth, exceeding constrains found earlier [45]. The method applied to searching for the photon component was developed in Ref. [46].

3.2.4 Arrival directions. It may be said without exaggeration that UHECR investigations open a window on the high-energy Universe. The measurement of the arrival direction anisotropy for initial particles is one of the most important scientific issues facing the TA Collaboration. The discovery of such anisotropy will be a key to the identification of UHECR sources, and an important step in the establishment of the chemical composition of UHECRs and measurements of the important parameters of the intergalactic medium, such as the strength and structure of its magnetic fields.

If the discovered suppression of the UHECR spectrum is indeed caused by the GZR effect, then, as discussed in Section 2.1.1, the sources of highest-energy rays should be located inside a sphere 100 Mpc in radius from us. The distribution of matter in the Universe at such spatial scales is strongly inhomogeneous, and therefore the anisotropy of the UHECR flux can be expected. Both variations in the flux at large angular scales and the appearance of point sources on the celestial sphere are expected.

Here, we present the results of correlation analysis [47] of the arrival directions of initial particles with the large-scale structure of the Universe and correlations with active galactic nuclei (AGNs), and also consider autocorrelations on small angular scales. This analysis covers data accumulated for 28 months with a surface detector array, from March 2008 to September 2010. With the cutoff over a zenith angle of 45°, the data set contains 655 events with energies exceeding 10 EeV, 35 events with energies greater than 40 EeV, and 15 events with energies exceeding 57 EeV.

(1) *Autocorrelations.* The arrival directions of initial particles in the AGASA data formed clusters (doublets and triplets) with an angular size of 2.5° [48, 49]. These results can be treated as the formulation of the statistical hypothesis according to which the arrival directions are anisotropic. Here, we will verify this hypothesis by utilizing TA data. By

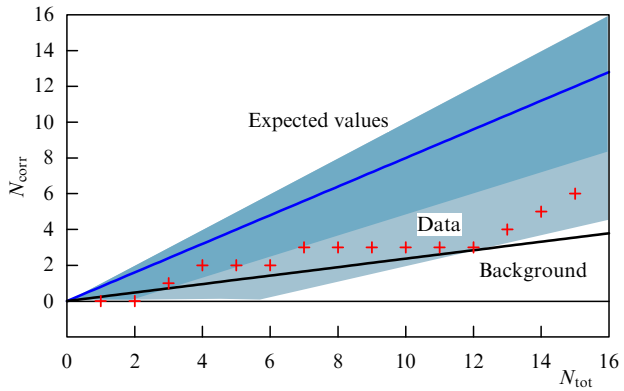

Figure 7. Result of a correlation test with AGNs. On the abscissa, the number of recorded events with $E > 57$ EeV is plotted in chronological order; on the ordinate is the number of correlating events. According to the Auger hypothesis, the expectation is shown by the line surrounded by confidence intervals 1σ and 2σ. The lower thick line is the expectation for the isotropic distribution. Crosses mark TA data.

following the AGASA analysis, we will use the energy cutoffs $E > 10$ EeV and $E > 40$ EeV in the data set. Then, all the events are counted in which arrival directions form pairs with the angular distance smaller than 2.5°. The number obtained is compared with that expected for the isotropic distribution of arrival directions. In a data set with $E > 10$ EeV, we found 311 such pairs, whereas 323 pairs are expected for the isotropic distribution. A set with $E > 40$ EeV contains one pair, whereas the expected value is 0.838. Thus, data redundancy is absent. Then, we weakened the formulation of the hypothesis and performed such a test at all angular scales from 0 to 30° and again obtained a negative result. Thus, no anisotropy of the TA data was observed at small angular scales.

(2) *Correlations with active galaxies*. The Pierre Auger Observatory reported correlations [50] of UHECRs with energies exceeding 57 EeV with near (a distance of less than 75 Mpc) AGNs. Correlations were observed at angular scales of 3.1%. In a control data set consisting of 13 events, 9 events correlated, which amounts to 69%. Here, we will verify the corresponding statistical hypothesis.

The TA exposure, unlike the Auger Observatory exposure, is concentrated in the northern celestial hemisphere, where the catalogue [51] used for analysis contains many AGNs, and therefore a greater fraction of correlating events can be expected. Assuming that the luminosities of AGNs in UHECRs are the same, we estimate this fraction as 73% for the TA observation. The result of the corresponding correlation analysis is given in Fig. 7. So far no certain conclusions can be made because the available statistics are very scarce, making the TA data consistent with both the isotropic distribution and the AGN hypothesis.

(3) *Correlation with the structure*. In this case, we verify the hypothesis that TA events occur in sources which follow the distribution of matter in the Universe. Such a correlation should inevitably exist if initial particles are protons and the intergalactic magnetic fields are not too strong. We perform our analysis by the method developed in Ref. [52] and used earlier to analyze the HiRes data [53]. In this method, first the expected distribution of the UHECR flux in the sky is calculated, assuming that sources follow the distribution of visible matter. Then, the expected distribution of sources is compared with real data.

Correlation with the large-scale structure of the Universe was verified for energies $E > 40$ EeV and $E > 57$ EeV. Both data sets were found to be consistent with this hypothesis. The data set with $E > 40$ EeV is also in agreement with the isotropic distribution, whereas the data set with $E > 57$ EeV is inconsistent with the isotropic distribution at a confidence level of 95%. To distinguish reliably these two hypotheses, statistics exceeding in number the existing ones by several times is required.

4. Conclusion

The Telescope Array is the largest observatory in the northern hemisphere of Earth for studying ultrahigh-energy cosmic rays. The TA detectors began to operate in March 2008. The spectrum of cosmic rays has been measured, and the GZK cutoff has been found at energies exceeding $10^{19.75}$ eV at a confidence level of 3.5σ. The mass composition in the energy range from $10^{18.2}$ to 10^{20} eV is consistent with the purely proton one. The arrival direction distribution for initial particles is still consistent with the isotropic distribution of their sources.

Acknowledgments. The Telescope Array experiment is supported by the Ministry of Education, Culture, Sports, Science and Technology of Japan through Kakenhi grants on priority area (431) 'Highest Energy Cosmic Rays', and basic research awards 18204020(A), 18403004(B), and 20340057(B); by the U.S. National Science Foundation awards PHY-0307098, PHY-0601915, PHY-0703893, PHY-0758342, and PHY-0848320 (Utah), and PHY-0649681 (Rutgers); by the Korea Research Foundation (KRF-2007-341-C00020); by the Korean Science and Engineering Foundation (KOSEF, R01-2007-000-21088-0); by the Russian Academy of Sciences through the Russian Foundation for Basic Research (grants Nos 10-02-01406a, 11-02-01528a); by the grant NSh-5525.2010.2 of the President of the Russian Federation; by the Ministry of Education and Science of the Russian Federation through the state contract 02.740.11.0244, and through the IISN contract 4.4509.10.

References

1. Greisen K *Phys. Rev. Lett.* **16** 748 (1966)
2. Zatsepin G T, Kuz'min V A *Pis'ma Zh. Eksp. Teor. Fiz.* **4** 114 (1966) [*JETP Lett.* **4** 78 (1966)]
3. Tinyakov P G, Tkachev I I *Astropart. Phys.* **24** 32 (2005); astro-ph/0411669
4. Neronov A, Semikoz D V *Phys. Rev. D* **80** 123012 (2009); arXiv:0910.1920
5. Dolag K, Grasso D, Springel V, Tkachev I *Pis'ma Zh. Eksp. Teor. Fiz.* **79** 719 (2004) [*JETP Lett.* **79** 583 (2004); astro-ph/0310902
6. Neronov A, Vovk I *Science* **328** 73 (2010); arXiv:1006.3504
7. Linsley J *Phys. Rev. Lett.* **10** 146 (1963)
8. Winn M M et al. *J. Phys. G Nucl. Phys.* **12** 653 (1986)
9. Lawrence M A, Reid R J O, Watson A A *J. Phys. G Nucl. Part. Phys.* **17** 733 (1991)
10. Afanasiev B N et al., in *Proc. Intern. Symp. on Extremely High Energy Cosmic Rays: Astrophysics and Future Observatories* (Ed. M Nagano) (Tokyo: Univ. of Tokyo, 1996) p. 32
11. Antonov E E et al. *Pis'ma Zh. Eksp. Teor. Fiz.* **69** 614 (1999) [*JETP Lett.* **69** 650 (1999)]
12. Takeda M et al. *Phys. Rev. Lett.* **81** 1163 (1998)
13. Hayashida N et al., astro-ph/0008102
14. Bird D J et al. *Astrophys. J.* **441** 144 (1995)
15. Jui C H et al., in *Proc. 27th Intern. Conf. on Cosmic Rays: ICRC 2001, Hamburg* Vol. 1 (Göttingen: Copernicus Gessellshaft, 2001) p. 354

16. Mantsch P (for the Pierre Auger Collab.) "The Pierre Auger Observatory progress and first results", astro-ph/0604114
17. Tokuno H et al. *AIP Conf. Proc.* **1238** 365 (2010)
18. Boldt E, Ghosh P *Mon. Not. R. Astron. Soc.* **307** 491 (1999); astro-ph/9902342
19. Neronov A, Tinyakov P, Tkachev I *Zh. Eksp. Teor. Fiz.* **127** 744 (2005) [*JETP* **100** 656 (2005)]; astro-ph/0402132
20. Berezinsky V, Kachelrieß M, Vilenkin A *Phys. Rev. Lett.* **79** 4302 (1997); astro-ph/9708217
21. Kuzmin V A, Rubakov V A *Yad. Fiz.* **61** 1122 (1998) [*Phys. At. Nucl.* **61** 1028 (1998); astro-ph/9709187
22. Chung D J H, Kolb E W, Riotto A *Phys. Rev. D* **59** 023501 (1999)
23. Kuzmin V A, Tkachev I I *Pis'ma Zh. Eksp. Teor. Fiz.* **68** 255 (2005) [*JETP Lett.* **68** 271 (1998)]
24. Kuzmin V, Tkachev I *Phys. Rev. D* **59** 123006 (1999)
25. Dubovsky S L, Tinyakov P G *Pis'ma Zh. Eksp. Teor. Fiz.* **68** 99 (1998) [*JETP Lett.* **68** 107 (1998); hep-ph/9802382
26. Berezinsky V, Mikhailov A A *Phys. Lett. B* **449** 237 (1999); astro-ph/9810277
27. Chung D J H, Farrar G R, Kolb E W *Phys. Rev. D* **57** 4606 (1998); astro-ph/9707036
28. Berezinsky V, Kachelrieß M, Ostapchenko S *Phys. Rev. D* **65** 083004 (2002); astro-ph/0109026
29. Gorbunov D S, Raffelt G G, Semikoz D V *Phys. Rev. D* **64** 096005 (2001); hep-ph/0103175
30. Csáki C et al. *JCAP* (05) 005 (2003); hep-ph/0302030
31. Fairbairn M, Rashba T, Troitsky S V, arXiv:0901.4085
32. Coleman S, Glashow S L *Phys. Rev. D* **59** 116008 (1999); hep-ph/9812418
33. Dubovsky S L, Tinyakov P G *Astropart. Phys.* **18** 89 (2002); astro-ph/0106472
34. Berezinsky V, Gazizov A Z, Grigorieva S I *Phys. Lett. B* **612** 147 (2005); astro-ph/0502550
35. Stokes B et al. (for the Telescope Array Collab.), in *Proc. of the Intern. Symp. on the Recent Progress of Ultra-High Energy Cosmic Ray Observation*: *UHECR, Nagoya, Japan, December 10–12, 2010*
36. Abbasi R U et al. (HiRes Collab.) *Phys. Rev. Lett.* **100** 101101 (2008); astro-ph/0703099
37. Abraham J et al. (Pierre Auger Collab.) *Phys. Rev. Lett.* **101** 061101 (2008); arXiv:0806.4302
38. Kalashev O E, Rubtsov G I, Troitsky S V *Phys. Rev. D* **80** 103006 (2009); arXiv:0812.1020
39. Rodriguez D C, Ph.D. Thesis (Salt Lake City, UT: Univ. of Utah, 2011)
40. Ikeda D et al. (for the Telescope Array Collab.), in *Proc. of the Intern. Symp. on the Recent Progress of Ultra-High Energy Cosmic Ray Observation*: *UHECR, Nagoya, Japan, December 10–12, 2010*
41. Abbasi R U et al. (HiRes Collab.) *Phys. Rev. Lett.* **104** 161101 (2010); arXiv:0910.4184
42. Abraham J et al. (Pierre Auger Collab.) *Phys. Rev. Lett.* **104** 091101 (2010); arXiv:1002.0699
43. Tameda Y et al. (for the Telescope Array Collab.), in *Proc. of the Intern. Symp. on the Recent Progress of Ultra-High Energy Cosmic Ray Observation*: *UHECR, Nagoya, Japan, December 10–12, 2010*
44. Rubtsov G I et al. (for the Telescope Array Collab.), in *Proc. of the Intern. Symp. on the Recent Progress of Ultra-High Energy Cosmic Ray Observation*: *UHECR, Nagoya, Japan, December 10–12, 2010*
45. Glushkov A V et al. *Pis'ma Zh. Eksp. Teor. Fiz.* **85** 163 (2007) [*JETP Lett.* **85** 131 (2007)]; astro-ph/0701245
46. Gorbunov D S, Rubtsov G I, Troitsky S V *Astropart. Phys.* **28** 28 (2007); astro-ph/0606442
47. Tinyakov P et al. (for the Telescope Array Collab.), in *Proc. of the Intern. Symp. on the Recent Progress of Ultra-High Energy Cosmic Ray Observation*: *UHECR, Nagoya, Japan, December 10–12, 2010*
48. Hayashida N et al. *Phys. Rev. Lett.* **77** 1000 (1996)
49. Tinyakov P G, Tkachev I I *Pis'ma Zh. Eksp. Teor. Fiz.* **74** 3 (2001) [*JETP Lett.* **74** 1 (2001)]; astro-ph/0102101
50. Abraham J et al. (Pierre Auger Collab.) *Science* **318** 938 (2007); arXiv:0711.2256
51. Veron-Cetty M P, Veron P "Quasars and active galactic nuclei", ESO Scientific Report 19, 9th ed. (2000)
52. Koers H B J, Tinyakov P *JCAP* (04) 003 (2009); arXiv:0812.0860
53. Abbasi R U et al., arXiv:1002.1444

PACS numbers: 14.60.Pq, 25.30.Pt
DOI: 10.3367/UFNe.0181.201109j.0997

T2K neutrino experiment: first results

Yu G Kudenko

1. Introduction

The discovery of neutrino oscillations became direct experimental evidence of the existence of new physics beyond the framework of the Standard Model and simultaneously marked the beginning of the study of this physics. As follows from the oscillations, neutrinos possess a small nonzero mass, they mix, and neutrino flavors (lepton numbers) are not conserved. Neutrino oscillations are described by the so-called neutrino Standard Model (νSM), which is the minimal model describing the mixing of three neutrino types. The physics of neutrino oscillations is described by a unitary matrix U [1] that relates three types of active neutrinos with left-handed helicity, ν_e, ν_μ, and ν_τ, to the mass eigenstates ν_1, ν_2, and ν_3 with the respective masses m_1, m_2, and m_3. In a form convenient for physical analysis, the matrix U can be represented as follows:

$$U=\begin{pmatrix}1 & 0 & 0\\ 0 & c_{23} & s_{23}\\ 0 & -s_{23} & c_{23}\end{pmatrix}\begin{pmatrix}c_{13} & 0 & s_{13}\exp(-\mathrm{i}\delta)\\ 0 & 1 & 0\\ -s_{13}\exp(\mathrm{i}\delta) & 0 & c_{13}\end{pmatrix}\times\begin{pmatrix}c_{12} & s_{12} & 0\\ -s_{12} & c_{12} & 0\\ 0 & 0 & 1\end{pmatrix}. \quad (1)$$

In this expression, $s_{ij}\equiv\sin\theta_{ij}$ and $c_{ij}\equiv\cos\theta_{ij}$ $(i,j=1,2,3)$. Neutrino oscillations are described by six parameters: two independent mass squared differences: $\Delta m_{12}^2=m_2^2-m_1^2$ and $\Delta m_{23}^2=m_3^2-m_2^2$; three mixing angles: θ_{12}, θ_{23}, θ_{13}, and a CP-odd phase δ.

Experiments with atmospheric [2], solar [3–8], reactor [9], and accelerator [10, 11] neutrinos measured four parameters θ_{12}, θ_{23}, Δm_{12}^2, and Δm_{23}^2: $\tan^2\theta_{12}=0.47^{+0.06}_{-0.05}$, $\Delta m_{12}^2=7.59^{+0.21}_{-0.21}\times10^{-5}$ eV^2, $\sin^2 2\theta_{23}>0.92$ for a 90-percent confidence interval (90% CL), and $\Delta m_{23}^2=(2.43\pm0.13)\times10^{-3}$ eV^2. It is pertinent to note that the sign of Δm_{23}^2 is unknown, i.e., the neutrino mass hierarchy has not been determined. Both the normal hierarchy, $m_3\gg m_2>m_1$, and inverse hierarchy, $m_2>m_1\gg m_3$, are possible. Furthermore, the parameters θ_{13} and δ have not been measured. The best limit, $\sin^2 2\theta_{13}<0.15$ (90% CL) for $\Delta m_{23}^2=2.43\times10^{-3}$ eV^2, was obtained in the ChOOZ experiment [12].

Since $|\Delta m_{12}^2|\ll|\Delta m_{13}^2|\simeq|\Delta m_{23}^2|$ and the typical baselines of accelerator experiments for studying neutrino oscillations in the region of 'atmospheric' parameters ($\Delta m_{23}^2\sim(2-3)\times10^{-3}$ eV^2) amount to several hundred kilometers, the contribution of Δm_{12}^2-bearing terms to the oscillation probability is small, so that approximate expressions for muon neutrino

Yu G Kudenko Institute for Nuclear Research,
Russian Academy of Sciences, Moscow, Russian Federation
E-mail: kudenko@inr.ru

Uspekhi Fizicheskikh Nauk **181** (9) 997–1004 (2011)
DOI: 10.3367/UFNr.0181.201109j.0997
Translated by E N Ragozin; edited by A Radzig

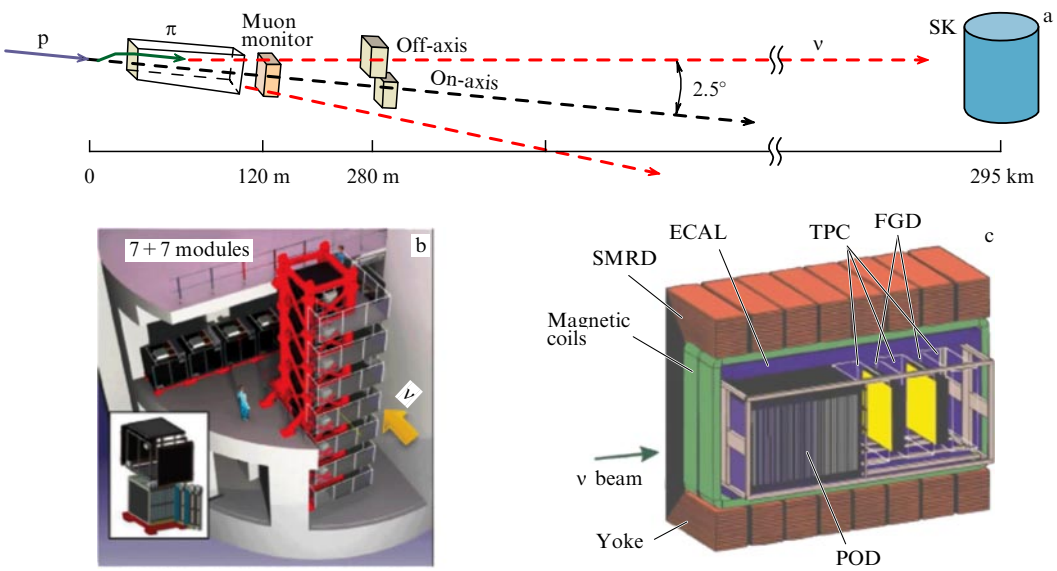

Figure 1. Layout of the T2K experiment: (a) main elements of the facility — neutrino beam, neutrino beam monitor, ND280 near neutrino detector located 280 m away from the target, and Super-Kamiokande far neutrino detector (SK); (b) general view of the INGRID on-axis neutrino beam monitor, and (c) near off-axis neutrino detector, which comprises a neutral-pion detector (POD), an electromagnetic calorimeter (ECAL), a side muon range detector (SMRD), and a tracking detector, which consists of three time-projection chambers (TPCs) and two (scintillation) fine-grained detectors (FGDs).

oscillations may be written in the following form [13, 14]:

$$P(\nu_\mu \to \nu_e) \simeq \sin^2 2\theta_{13} \sin^2 \theta_{23} \sin^2 \frac{\Delta m^2_{13} L}{4E_\nu}\,, \tag{2}$$

$$P(\nu_\mu \to \nu_\mu) \simeq 1 - \sin^2 2\theta_{23} \cos^4 \theta_{13} \sin^2 \frac{\Delta m^2_{13} L}{4E_\nu} - P(\nu_\mu \to \nu_e)\,. \tag{3}$$

When the neutrino energy and the experiment baseline are selected in such a way that the oscillation probability $P(\nu_\mu \to \nu_e)$ is at its maximum, i.e. $(\Delta m^2_{13} L)/(4E_\nu) = \pi/2 + n\pi$, then

$$P(\nu_\mu \to \nu_e) \approx \frac{1}{2} \sin^2 2\theta_{13}\,. \tag{4}$$

The primary goal of the T2K (Tokai-to-Kamioka) second-generation long-baseline experiment [15] performed in Japan is the quest for $\nu_\mu \to \nu_e$ oscillations and the measurement of the θ_{13} angle with a sensitivity of up to $\sin^2 2\theta_{13} \sim 0.006$ (90% CL), and precision measurements of other oscillation parameters with an accuracy of $\delta(\sin^2 2\theta_{23}) \sim 0.01$ and $\delta(\Delta m^2_{23}) \sim 10^{-4}$ eV^2. More than 500 scientists from 12 countries are members of the T2K collaboration. Participating in the experiment on the part of Russia is the Institute for Nuclear Research (INR), Russian Academy of Sciences. The conception of this experiment, the experimental facility, first results, its status, and short-term prospects are outlined below.

2. T2K experimental facility

The general layout of the experiment is shown in Fig. 1. The main elements of the facility are the neutrino channel, the array of near neutrino detectors (ND280) located 280 m away from the target, and the far Super-Kamiokande detector (SK) located 295 km from the target. The near detector ND280 [16–18] consists of two neutrino detectors stationed in a 40-m-deep pit about 18 m in diameter. It is employed for measuring the parameters of the neutrino beam near the target (prior to oscillations), monitoring its properties, and measuring the neutrino–nuclei interaction cross sections. One detector [the neutrino beam monitor INGRID (Interactive Neutrino GRID)] is located on the beam axis, i.e., at a zero angle to the direction of the proton beam, and the other (off-axis) near neutrino detector is located on the axis connecting the decay volume and Super-Kamiokande detector, i.e., at an angle of 2.5°.

2.1 Neutrino beam

For the first time, the T2K experiment uses a quasimonoenergetic off-axis neutrino beam whose energy is tuned to the first oscillation maximum. As follows from the $\pi \to \mu + \nu$ decay kinematics, the neutrino energy E_ν depends only slightly on the pion energy E_π for a small angle θ between the pion and neutrino momenta. This off-axis muon-neutrino beam concept was implemented at the 30-GeV high-current proton synchrotron Japan Proton Accelerator Research Complex (J-PARC). The accelerator power is designed to be 0.75 MW, which affords a proton beam intensity of 3.3×10^{14} protons per pulse for a pulse duration of about 3.0 μs and a fast beam extraction and its delivery to the target every 3.2 s. The experiment uses a graphite target 30 mm in diameter and 900 mm in length (≈ 2 nuclear lengths), in which about 80% of the protons participate in nuclear interactions. The target is cooled by gaseous helium. Three toroidal pulsed magnets focus the generated pions into the 94-m-long decay volume which is filled with helium at a pressure of 1 atm to reduce pion absorption and production.

The spectra of muon neutrinos calculated for several θ angles are displayed in Fig. 2. The basic version of the experiment corresponds to the angle of 2.5° that can be varied between 2.0° and 3.0°, which allows changing the average neutrino energy from 0.5 to 0.9 GeV and optimizing the experimental sensitivity to the oscillation parameters [19, 20]. For neutrino energies corresponding to the intensity

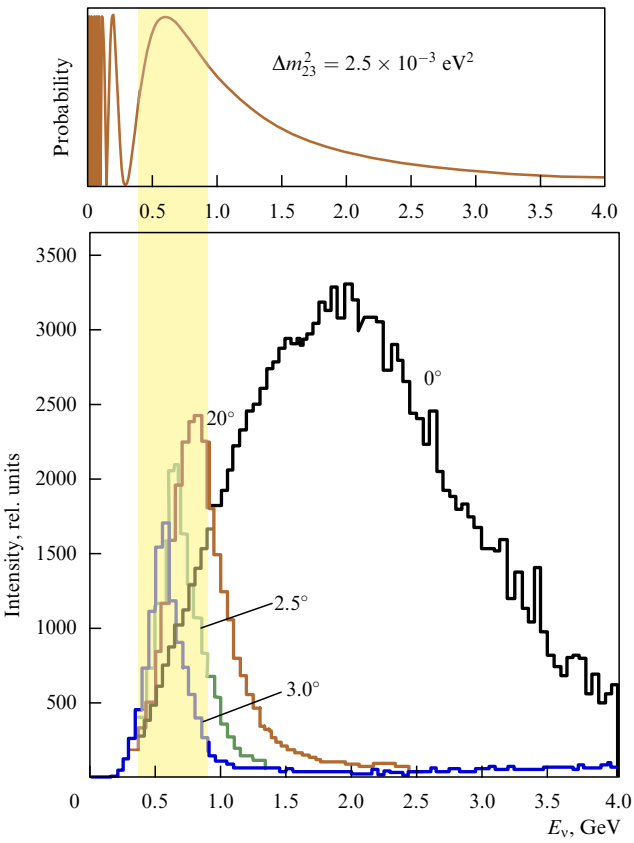

Figure 2. Neutrino spectra for different angles relative to the proton beam axis: 0°, 2.0°, 2.5°, and 3.0°. The T2K experiment uses the beam at an angle of 2.5°, tuned to the first oscillation maximum for $\Delta m^2_{23} = 2.5 \times 10^{-3}$ eV^2, as is evident from the oscillation probability curve depicted in the upper part of the figure.

maximum, the admixture of electron neutrinos from the $\pi \to \mu \to e$ decay chain and the decay of kaons is about 0.4% for the angle of 2.5°. It is noteworthy that the off-axis neutrino beam parameters, which depend strongly on the angle, as is clear from Fig. 2, should be carefully monitored in the course of the experiment.

2.2 Near neutrino detector

To achieve the main experiment goals, the near neutrino detector must provide the measurement of the neutrino energy spectrum near the target with an accuracy of 2%. To obtain the neutrino energy with this accuracy, the spectrum of muons from the quasielastic neutrino scattering should be measured with a momentum resolution $\Delta p/p \leqslant 10\%$, and the absolute value of the muon momentum should be determined with a precision better than 2%. Furthermore, the detector should have a low proton detection threshold (≈ 200 MeV/c). The admixture of electron neutrinos to the muon neutrino spectrum has to be measured with an accuracy of $\approx 10\%$. One of the main detector tasks also involves the measurement of neutrino scattering cross sections on nucleons and light nuclei for neutrino energies from 500 to 1500 MeV. The principal function of the neutrino beam monitor consists in measuring the beam profile and monitoring the direction of the neutrino beam with an uncertainty of less than 1 mrad, which ensures monitoring the neutrino energy in the SK direction to better than 15 MeV at the maximum of the spectrum.

Neutrino beam monitor. The monitor of the neutrino beam, the Interactive Neutrino GRID (INGRID), consists of 7 + 7 identical modules arranged in the form of a cross, and two additional modules, as shown in Fig. 1b. Each module of lateral size 1×1 m^2 has a steel–scintillator sandwich structure and consists of 10 alternating steel layers 6.5 cm thick and of 11 scintillating planes. The active plane is made up of two scintillating layers, each being an assembly of scintillating bars which are arranged vertically in one layer and horizontally in the other. A wavelength-shifting fiber transmits the scintillation signal to a photodetector Multi-Pixel Photon Counter (MPPC) developed by Hamamatsu, Japan, which is made up of multiple avalanche photodiode pixels operating in the limited Geiger mode. A description of these devices, their parameters, and the test data are given in Refs [21–24]. The total weight of the monitor is about 160 t.

Off-axis detector. The near (off-axis) neutrino detector is composed of a UA1 magnet which houses a pi zero detector (π^0 detector, or P0D), a tracking detector which comprises three time projection chambers (TPCs) and two highly segmented scintillation detectors (fine-grained detectors, or FGDs), an electromagnetic calorimeter (ECAL), and a side muon range detector (SMRD), as shown in Fig. 1c. With the exception of the TPCs, scintillation detectors with wavelength-shifting fibers are used for active elements in all of these detectors, with MPPCs serving as photodetectors. The pi zero detector is optimized for measuring the π^0 production cross section via neutral currents:

$$\nu_\mu + N \to \nu_\mu + \pi^0 + N\,, \tag{5}$$

where $N = \mathrm{n}, \mathrm{p}$. Measuring these processes plays an important role in determining the level of the physical background in the spectrum of electron neutrinos emerging in Super-Kamiokande due to $\nu_\mu \to \nu_e$ oscillations (if $\theta_{13} \neq 0$), because an event in which only one photon from the $\pi^0 \to \gamma\gamma$ decay is detected is identified as a single electron from the quasielastic scattering of an electron neutrino. The P0D consists of alternating water layers, each 3 cm thick, and tracking planes. One tracking plane, in turn, consists of two XY planes, in which scintillating bars are arranged perpendicular to each other. For the efficient detection of photons, thin brass foils are placed between the scintillating bars in the central part of the detector, and lead plates are inserted in the front and rear parts of the detector. The total P0D weight is about 17 t, and the water target weight is about 3 t. Since the active element of the far detector comprises water, reducing systematic errors calls for measurements of the cross section for neutral pion production on oxygen for neutrino energies less than 1 GeV. The P0D will also be employed for solving this problem.

The tracking detector measures the flux and spectrum of muon and electron neutrinos by detecting charged leptons produced in the quasielastic neutrino scattering. The principal muon neutrino–nucleon interaction process for T2K energies is the quasielastic scattering via charged current:

$$\nu_\mu + \mathrm{n} \to \mu^- + \mathrm{p}\,. \tag{6}$$

Precisely measuring the neutrino spectrum requires detecting and reconstructing the kinematic parameters of both the muon and the proton. The proton is identified and measured by the FGDs, and the muon momentum is measured by the TPC with the addition of information provided by FGDs.

The first FGD is a full-active scintillation detector consisting of 30 layers of scintillating bars with the 1×1 cm^2 cross section, which form alternating XY layers perpendicular to the neutrino beam direction. The second FGD contains 3-cm-thick water layers between scintillating layers. The total water weight is 0.44 t. This configuration allows simultaneously measuring the cross sections for neutrino interactions in water and carbon by comparing the events occurring in both detectors.

Three time-projection chambers, which are embedded in a 0.2-T magnetic field, should provide a momentum resolution of about 10% in the 1-GeV/c muon momentum range. High resolution ($< 10\%$) was also achieved in measuring the specific energy loss $\mathrm{d}E/\mathrm{d}x$, which will enable a reliable (at a level of 5σ) identification of muons and electrons in the 0.3–1.0 GeV/c momentum range.

The tracking detectors and the P0D are surrounded by an electromagnetic calorimeter whose primary function lies in the detection and identification of the particles that escape from the volume of these detectors. The calorimeter, which has an effective thickness of about 10 radiation lengths, consists of alternating layers of lead and plastic scintillator, and exhibits an energy resolution of $7.5\%/\sqrt{E\,[\mathrm{GeV}]}$ for electromagnetic showers. The muons escaping from the tracking detector at large angles cannot be measured by the TPC. They enter the magnet yoke and their momentum can be measured from their range determined using the SMRD, which was developed and built at INR, RAS. The active elements of this detector are 2100 scintillation detectors [25, 26] located in the air gaps between magnet sections.

The near neutrino detector thus configured permits measuring the neutrino beam near the target (the spectrum and the intensity at the angles of 0° and 2.5°), the admixture of electron neutrinos that arise from the decays of muons and kaons, and the cross sections of neutrino interactions with nucleons and different nuclei via charged and neutral currents. Based on these measurements, predictions for the spectrum and number of muon and electron neutrinos in the SK far detector in the absence of oscillations are made.

2.3 Super-Kamiokande far detector

The Super-Kamiokande facility [27], which is a water Cherenkov detector 50,000 m^3 in volume, is located near Kamioka, Japan in a disused Mozumi mine under Mount Kamioka. Because the thickness of the rock is about 1 km, which corresponds to 2700 m of water equivalent, cosmic muons with energies below 1.3 TeV do not reach the detector, and the high-energy muon flux is suppressed by a factor of about 10^6.

The detector, a giant tank 39 m in diameter and 42 m in height filled with ultrapure water, consists of two detectors: an inner one, and an outer one. The entire volume of the inner detector is viewed by approximately eleven thousand spherical photomultiplier tubes (PMTs), with a 1–300 photoelectron dynamic range. The PMTs are arranged in a 70-cm pitch array on the walls, top, and bottom of the detector. The photocathode of each PMT measures 50 cm in diameter; the total photocathode area, i.e., the active part of the photomultiplier tubes, covers 40% of the entire detector surface. The optically isolated water volume with a weight of 18 kt surrounding the inner detector is viewed by 1885 PMTs 20 cm in diameter (the outer detector). In this detector, the average water layer thickness is equal to 2.7 m. The outer detector operates as an active 4π-veto-detector for charged particles and also serves as a passive shield from the neutrons and gamma-ray photons from the mountain rock. The water transparency in the detector is about 100 m for Cherenkov radiation at a wavelength of 420 nm.

The Super-Kamiokande detects neutrinos in the energy range from 4.5 MeV to 1 TeV. For low-energy events (primarily for the study of solar neutrinos), the energy of a charged particle is determined using the number of PMT hits, while high-energy events are measured from the total number of photoelectrons of all the PMTs actuated.

The dimension, shape, and direction of the Cherenkov cone are used for event identification: a single-ring muon-like, single-ring e-like, or multiple-ring event. The momentum resolution of the detector amounts to 2.4% for muons with a momentum of 1 GeV/c. The time synchronization between the pulse of the J-PARC proton accelerator and Super-Kamiokande was provided via the Global Positioning System (GPS) with a precision of 50 ns. This precision allows observing the beam microstructure in the neutrino events detected by the SK and enables suppressing the atmospheric neutrino background to a negligible level.

3. Status of the T2K experiment and preliminary results

The construction of the J-PARC accelerator complex was completed in 2008. In April 2009, the proton beam was injected into the neutrino channel and the muon monitor detected the muon signal from the $\pi^+ \to \mu^+ + \nu$ decay. In November 2009, the first neutrino events were recorded by the ND280 near detector, all of whose elements had been practically installed by that time. The accumulation of statistics commenced in January 2010, and the first neutrino event in Super-Kamiokande was detected in February 2010. The integral number of protons accumulated on the target during the first run (January–June 2010) amounted to 3.3×10^{19} at an average proton beam power of ≈ 50 kW. The operation efficiencies of Super-Kamiokande and ND280 detectors during data taking period exceeded 99% and 96%, respectively. The preliminary results of the first physical run are outlined below.

3.1 Neutrino beam properties

The near detector measured and monitored the initial neutrino beam parameters near the decay volume, i.e., prior to possible oscillations. The profile of the neutrino beam and its direction relative to the proton beam axis (0°) are measured by the INGRID detector. To this end, use is made of the reaction of the quasielastic muon neutrino scattering (6). The measured neutrino beam profile is plotted in Fig. 3a, and the position of the beam center during the accumulation of statistics for about a month is shown in Fig. 3b. The position of the beam center is stable within the range required, ± 1 mrad (± 28.5 cm). A graphic representation of the first neutrino event in the ND280 near detector in the Super-Kamiokande direction (2.5°) is given in Fig. 4a: a muon track arising from a neutrino interaction in the P0D was reconstructed in three TPCs and both FGDs. The time structure of neutrino events in the SMRD shown in Fig. 4d is in complete agreement with the structure of the proton beam in the first physics run, which had six microbunches spaced by 580 ns.

It is noteworthy that the events between microbunches are practically lacking, which testifies to a very good proton-

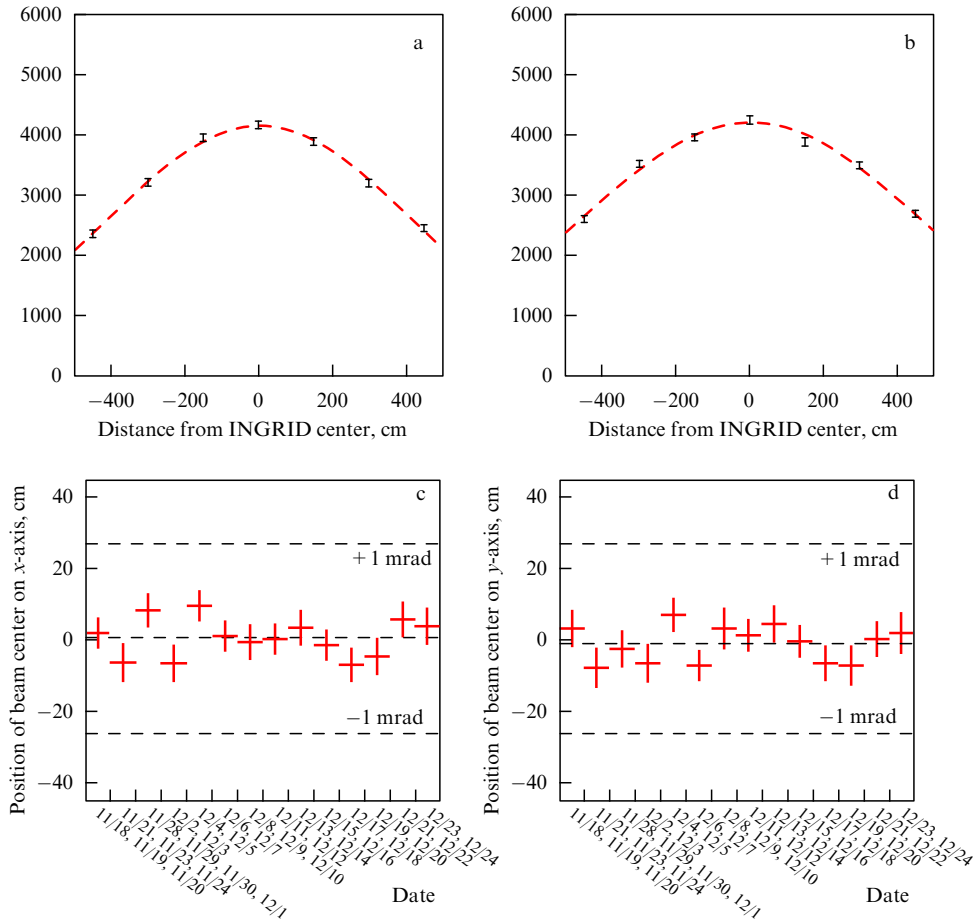

Figure 3. Neutrino beam measured by INGRID at an angle of 0°: horizontal (a) and vertical (b) profiles of the neutrino beam; horizontal (c) and vertical (d) position of the beam center over several months of measurements in 2010. Horizontal dashed lines indicate the admissible interval for beam center deviations, ±1 mrad, from the direction of the proton beam (0°).

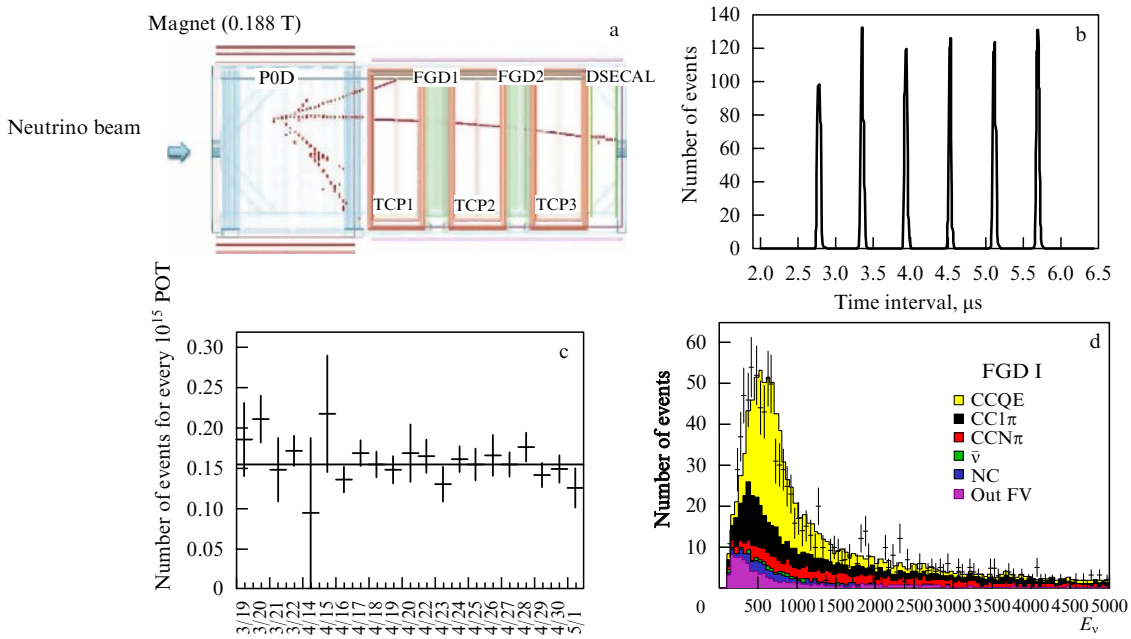

Figure 4. Neutrino events in the ND280 near detector. (a) The first neutrino event detected in the near detector. (b) Time distribution of neutrino events in SMRD: 6 peaks, which are spaced by 580 ns, correspond to 6 proton beam microbunches in the first physics run in 2010. (c) The number of neutrino events in FGD normalized to 10^{15} protons on target in 2010. (d) Neutrino spectrum in the near detector reconstructed from the neutrino events detected by FGD1; also shown are the spectra of different processes obtained by Monte Carlo simulations. Most important processes among them are quasielastic scattering (shown in yellow) and inelastic scattering with the production of a single pion (black). (See in color at www.ufn.ru.)

beam modulation structure without protons between the microbunches, and to a very low background level in ND280.

The number of neutrino events recorded in the near detector (FGD) for every 10^{15} protons on target (POT) is presented in Fig. 4c, which makes evident the good stability of detection of neutrino events over the period of accelerator operation. Figure 4d demonstrates the spectrum of muon neutrinos reconstructed from the events detected by FGD1. Also shown here are the characteristics of the main processes contributing to this spectrum, which were obtained by the Monte Carlo method. As is clear from this figure, the measured and calculated spectra of neutrinos near the target are in rather good agreement. A small excess of experimental events is seen at low energies, 350–2500 MeV, which is most likely attributable to the detection of secondary particles from neutrino events in the magnet and pit walls, which have yet to be completely included in the simulations. Of special note is the fact that the maximum of the spectrum falls in the 600–700 MeV neutrino energy range, i.e., the neutrino beam is tuned to the oscillation maximum, as initially planned in the design of the neutrino channel and off-axis angle selection.

3.2 Oscillation analysis

The first stage of the experiment is aimed at solving two main problems: precision measurements of $\nu_\mu \to \nu_\mu$ oscillation parameters, and the quest for the $\nu_\mu \to \nu_e$ transition and measurement of the θ_{13} angle.

3.2.1 $\nu_\mu \to \nu_\mu$. The basic process whereby muon neutrinos are detected at an energy of ≈ 700 MeV is their quasielastic scattering via charged current [see expression (6)]. Super-Kamiokande detects a muon and measures its energy with a resolution of about 2.5%, and the direction of its momentum with an angular resolution of about 1°. In this case, the uncertainty in determining the absolute value of the muon energy, i.e., the uncertainty in the energy scale of the detector, amounts to only about 2%. The expected neutrino flux $\Phi_{\rm SK}^{\rm expect}$ in Super-Kamiokande (without oscillations) is simulated by the Monte Carlo technique with the use of the initial flux $\Phi_{\rm ND}$ and neutrino spectrum near the decay volume measured in ND280:

$$\Phi_{\rm SK}^{\rm expect} = R_{\rm F/N}\,\Phi_{\rm ND}\,, \tag{7}$$

where $R_{\rm F/N}$ is the ratio between the neutrino fluxes in the far (F) and near (N) detectors. To minimize the uncertainties arising from the model description of hadron production processes, $R_{\rm F/N}$ simulations are performed with the use of the information about experimental cross sections of hadron production in proton-nuclear interactions measured with a graphite target, which is a copy of the T2K target, in the NA61 experiment at CERN [28]. The neutrino flux in the near detector is defined as follows:

$$\Phi_{\rm ND} = \frac{N_{\rm ND}^{\rm obs}}{\sigma_{\rm ND}\,\epsilon_{\rm ND}}\,, \tag{8}$$

where $N_{\rm ND}^{\rm obs}$ is the measured number of neutrino events in the near detector, and $\sigma_{\rm ND}$ and $\epsilon_{\rm ND}$ are the cross section of muon neutrino interaction and the efficiency of muon neutrino detection in ND280, respectively. Oscillation parameters (Δm_{23}^2 and $\sin^2 2\theta_{23}$) are obtained from the fitting of the measured spectrum and the number of neutrino events using expression (3).

Criteria for the selection of events were fixed beforehand on the basis of the simulations of neutrino processes at Super-Kamiokande, and they also relied on the techniques elaborated for the data analysis of K2K and Super-Kamiokande experiments. These criteria were as follows: (i) timing correlation with the J-PARC beam taking into consideration the time of flight to Super-Kamiokande correct to within ≈ 50 ns; (ii) the energy of a neutrino event is completely absorbed by the inner detector (the absence of any signal in the outer detector); (iii) the vertex of neutrino interaction is more than 2 m away from the walls of the inner detector; (iv) the number of rings is equal to unity; (v) the detected event energy > 100 MeV, and (vi) the ring should be muon-like. A typical muon-like ring is depicted in Fig. 5a.

As a result of the first physics run with 3.3×10^{19} POT, 33 muon neutrinos produced in the sensitive detector volume were detected at Super-Kamiokande; their energy was completely deposited in the inner detector. On the other hand, 49.5 events were expected for the same number of protons in the absence of oscillations.

Therefore, an event deficit typical of oscillations was observed, although the statistics are still poor. That these are accelerator neutrinos is confirmed by the temporal structure of these events, which is in perfect agreement with the proton beam structure, as seen from Fig. 5b. Special mention should be made of the absence of background prior to, after, and between microbunches, as well as of the high temporal resolution of the entire facility: $\sigma \approx 26$ ns (Fig. 5d). The background expected in the first session was about 0.01 events, i.e., it was negligible. The application of the Kolmogorov–Smirnov criterion for testing the correspondence between the event detection at Super-Kamiokande and the number of protons on target reveals that the probability of corresponding the distribution depicted in Fig. 5a to the expected linear dependence is equal to 8%.

3.2.2 $\nu_\mu \to \nu_e$. To measure the characteristics of this process and, in particular, determine the mixing angle θ_{13}, it is necessary to efficiently detect the electrons emerging in Super-Kamiokande as a result of the interaction of electron neutrinos with nucleons via charged currents, as well as to efficiently suppress those events in which neutral pions are produced via neutral currents. The problem consists in π^0 identification in the case of asymmetric $\pi^0 \to \gamma\gamma$ decay, when one of the photons has a low energy, resulting in the actuation of a small number of PMTs at Super-Kamiokande, with the identification of the Cherenkov ring of this photon being hindered.

To detect an electron from an electron neutrino, the of selection criteria 1–4 listed in Section 3.2.1 are applied using the following conditions: the detected event energy exceeds 30 MeV; the ring is electron-like, and there is no delayed electron signal from the decay of a muon produced in the course of neutrino interactions.

The last condition is applied to eliminate events in which a muon-like ring satisfies the selection criteria for an electron-like ring and might erroneously be taken as the electron-like one. To reduce the background from π^0, the second electron-like ring is looked for this event, the invariant mass is reconstructed, and the condition that it be no less than 105 MeV is imposed. It is also implied that the detected event constituted a quasielastic scattering via charged current and the reconstructed neutrino energy is lower than 1250 MeV. This permits eliminating the high-energy tail in the neutrino

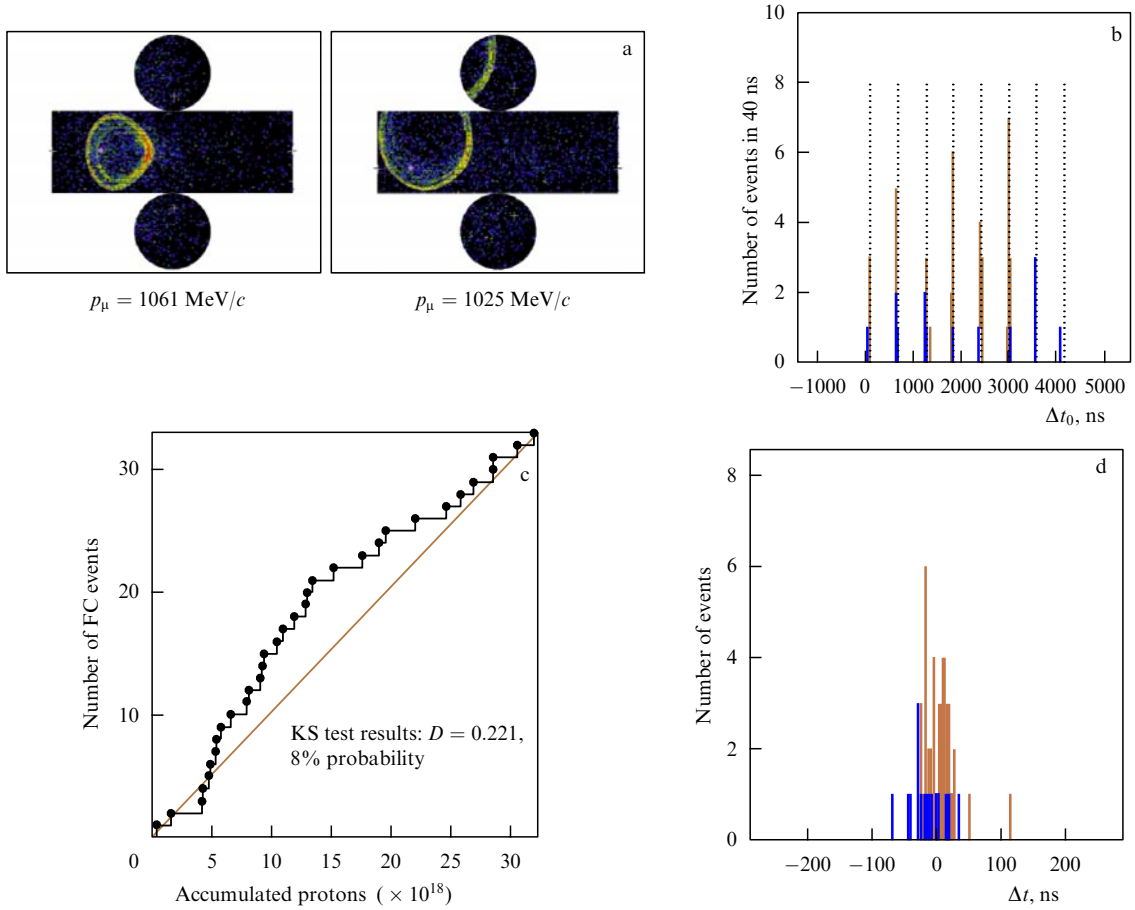

Figure 5. Neutrinos from the J-PARC proton accelerator detected by Super-Kamiokande. (a) Typical muon-like event. (b) Time distribution of recorded events, which corresponds to the accelerator time structure. There are no background events between the accelerator microbunches. (c) Number of events in the detector fiducial volume as a function of the number of protons on the target (FC events — events whose energy is completely absorbed in the Super-Kamiokande inner detector; KS — Kolmogorov–Smirnov criterion). (d) Time distribution of neutrino events ($\sigma = 26$ ns) relative to the center of the accelerator microbunch nearest to the event; Δt is the time interval between the event detection time and the center of the microbunch nearest to the event.

spectra, which contains a large fraction of electron neutrinos. As suggested by Monte Carlo simulations, a substantial lowering of the level of background events (suppression of $\pi^0 \to 2\gamma$ decays by about a factor of 100) is expected under these conditions, and a rather high detection efficiency, about 40%, for the expected signal may be obtained. During the first physics run, one event at Super-Kamiokande was recorded as a candidate for an electron neutrino produced in the detector fiducial volume. In this case, the expected background is estimated to be about 0.28 events.

4. Status of the experiment and immediate plans

The second T2K physical session, which commenced in November 2010, will continue for six months. It is planned to accumulate neutrino events for an integral proton beam power of 150 kW $\times 10^7$ s, which corresponds to $\approx 3 \times 10^{20}$ POT. It is anticipated that a sensitivity of 0.05 (90% CL) to $\sin^2 2\theta_{13}$ will be achieved.

The dependence of experimental sensitivity to θ_{13} (90% CL) on the integral number of protons on the target is plotted in Fig. 6 with the inclusion of possible systematic errors of 5%, 10%, and 20%. The following oscillation parameters were employed for these estimates: $\Delta m^2_{23} \approx 2.4 \times 10^{-3}$ eV^2, $\sin^2 2\theta_{23} = 1.0$, $\Delta m^2_{12} \sim 7.6 \times 10^{-5}$, $\sin^2 2\theta_{12} = 0.87$, and $\delta = 0$, as well as the normal hierarchy of neutrino masses. The dashed arrow shows the ultimate goal of the first experiment stage: $\sin^2 2\theta_{13} = 0.006$ (90% CL) for 8×10^{21} POT, which corresponds to five years of data taking for a proton beam power of 0.75 MW. This sensitivity is expected to be attained within the next two years. In this period, a measurement accuracy of $\delta(\Delta m^2_{23}) \approx 1 \times 10^{-4}$ and $\delta(\sin^2 2\theta_{23}) \approx 0.01$ will be attained in the $\nu_\mu \to \nu_\mu$ process as a result of measurements of event deficit and spectrum shape distortion [29].

Of special note is the paramount importance of the T2K experiment for subsequent investigations with accelerator neutrinos, because the discovery of $\nu_\mu \to \nu_e$ oscillations and a nonzero value of the θ_{13} angle furnish a unique possibility in the quest for *CP* violation in the leptonic sector in long-baseline accelerator experiments. These issues are considered at length in review [30].

In June 2011, the T2K collaboration published the first result [31] of the analysis of the data accumulated in the execution of the experiment from January 2010 to March 11, 2011 (the onset of an earthquake in Japan). Six events were discovered, which were candidates for electron neutrinos. Assuming the absence of $\nu_\mu \to \nu_e$ oscillations (at $\theta_{13} = 0$), the expected number of such events equaled 1.5 ± 0.3. The probability that the six events make up a fluctuation of

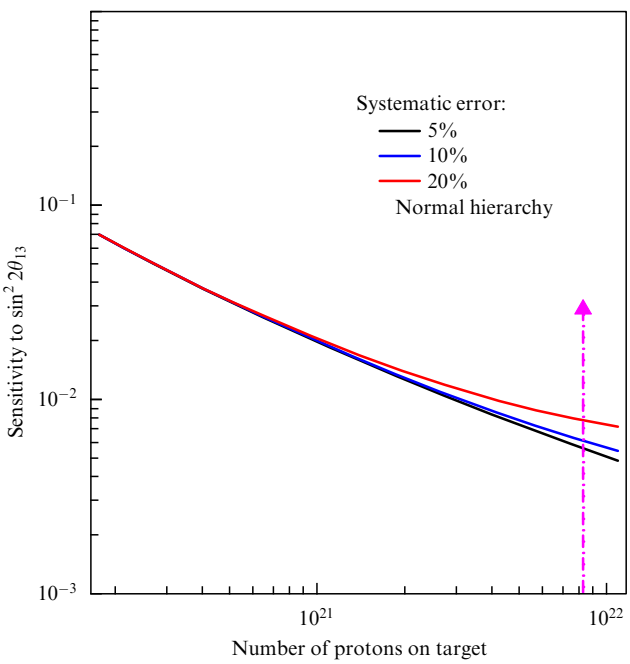

Figure 6. Dependence of the sensitivity to θ_{13} (90% CL) on the number of protons on the target. The three curves correspond to possible systematic errors of 5%, 10%, and 20%. The dashed arrow indicates the anticipated experimental sensitivity ($\sin^2 2\theta_{13} = 0.006$ at 90% CL) for 8.5×10^{21} POT.

background events rather than the result of neutrino oscillations is equal to 0.7%. Therefore, with a probability of 99.3% this result may be interpreted as an indication of $\nu_\mu \to \nu_e$ oscillations. The central value for $\sin^2 2\theta_{13}$ amounts to 0.11 for normal neutrino mass hierarchy, and to 0.14 for inverse hierarchy at $\delta = 0$.

Acknowledgments. This work was supported by the Neutrino Physics Program of the Presidium of the Russian Academy of Sciences, and the Program for Support of Scientific Schools (NSh-65038.2010.2).

References

1. Maki Z, Nakagawa M, Sakata S *Prog. Theor. Phys.* **28** 870 (1962)
2. Fukuda Y et al. (Super-Kamiokande Collab.) *Phys. Rev. Lett.* **81** 1562 (1998)
3. Fukuda Y et al. (Super-Kamiokande Collab.) *Phys. Rev. Lett.* **77** 1683 (1996)
4. Fukuda Y et al. (Super-Kamiokande Collab.) *Phys. Rev. Lett.* **81** 1158 (1998)
5. Abdurashitov J N et al. (SAGE Collab.) *Phys. Lett. B* **328** 234 (1994)
6. Anselmann P et al. (GALLEX Collab.) *Phys. Lett. B* **285** 376 (1992)
7. Ahmad Q R et al. (SNO Collab.) *Phys. Rev. Lett.* **87** 071301 (2001)
8. Ahmad Q R et al. (SNO Collab.) *Phys. Rev. Lett.* **89** 011301 (2002)
9. Eguchi K et al. (KamLAND Collab.) *Phys. Rev. Lett.* **90** 021802 (2003)
10. Ahn M H et al. (K2K Collab.) *Phys. Rev. D* **74** 072003 (2006)
11. Adamson P et al. (MINOS Collab.) *Phys. Rev. Lett.* **101** 131802 (2008); arXiv:0806.2237
12. Apollonio M et al. (CHOOZ Collab.) *Eur. Phys. J. C* **27** 331 (2003)
13. Fogli G L et al. *Prog. Part. Nucl. Phys.* **57** 742 (2006); hep-ph/0506083
14. Barger V, Marfatia D, Whisnant K *Phys. Rev. D* **65** 073023 (2002); hep-ph/0112119
15. Itow Y et al., hep-ex/0106019
16. "T2K ND280 Conceptual Design Report", T2K Internal Document, Version 1.0 (2005)
17. Karlen D (and the ND280 Group of the T2K Collab.) *Nucl. Phys. B Proc. Suppl.* **159** 91 (2006)
18. Kudenko Yu (and Representing the T2K Collab.) *Nucl. Instrum. Meth. Phys. Res. A* **598** 289 (2009)
19. Hayato Y (and the T2K Collab.) *Nucl. Phys. B Proc. Suppl.* **143** 269 (2005)
20. Yamada Y *Nucl. Phys. B Proc. Suppl.* **155** 28 (2006)
21. Yokoyama M et al., physics/0605241
22. Gomi S et al. *Nucl. Instrum. Meth. Phys. Res. A* **581** 427 (2007)
23. Yokoyama M et al. *Nucl. Instrum. Meth. Phys. Res. A* **610** 128 (2009); arXiv:0807.3145
24. Vacheret A et al. *Nucl. Instrum. Meth. Phys. Res. A* **656** 69 (2011); arXiv:1101.1996
25. Mineev O et al. *Nucl. Instrum. Meth. Phys. Res. A* **577** 540 (2007)
26. Izmaylov A et al. *Nucl. Instrum. Meth. Phys. Res. A* **623** 382 (2010); arXiv:0904.4545
27. Fukuda S et al. *Nucl. Instrum. Meth. Phys. Res. A* **501** 418 (2003)
28. Blondel A "Hadron production experiments", in *Neutrino 2010, June 14 – 19, 2010, Athens, Greece*
29. The T2K experiment, http://www.t2k.org
30. Kudenko Yu G *Usp. Fiz. Nauk* **181** 569 (2011) [*Phys. Usp.* **54** 569 2011)]
31. Abe K et al. (T2K Collab.) *Phys. Rev. Lett.* **107** 041801 (2011); arXiv:1106.2822

PACS numbers: **28.60.+s**, **29.20.–c**, 87.56.B–
DOI: 10.3367/UFNe.0181.201109k.1004

Isotope production at the Institute for Nuclear Research, Russian Academy of Sciences: current status and prospects

B L Zhuikov

1. Possibilities of producing radionuclides in intermediate-energy accelerators

It is likely that the idea of producing radionuclides for science and applications appeared when the Institute for Nuclear Research, USSR Academy of Sciences was founded in 1970 and it was decided to construct a linear accelerator of intermediate-energy protons — a meson factory. Beginning from the late 1980s, extensive research and development were performed aimed, first of all, at the construction of a facility for acceleration of heavy ions of radionuclides in a cyclotron specially built for this purpose [1]. It was assumed to produce radionuclides in the proton beam of a linear accelerator and to extract them expressively from irradiated targets. This project was aimed at fundamental studies in the field of nuclear physics. Simultaneously, it was planned to carry out the production of isotopes for medical and technical purposes. A similar program was accepted and is now being realized, for example, at the Legnaro National Laboratories (INFN-LNL) in Italy.

Because of a drastic reduction in financing, the program on heavy ions was not realized, and now the main focus is the

B L Zhuikov Institute for Nuclear Research, Russian Academy of Sciences, Moscow, Russian Federation
E-mail: bz@inr.ru

Uspekhi Fizicheskikh Nauk **181** (9) 1004 – 1011 (2011)
DOI: 10.3367/UFNr.0181.201109k.1004
Translated by M Sapozhnikov; edited by A Radzig

Table 1. Main operating intermediate-energy proton beam facilities for producing radionuclides.

Institution	Location	Proton energy used for producing radionuclides, MeV	Beam current used for producing radionuclides, μA
Institute for Nuclear Research, RAS	Troitsk, Moscow region, Russia	160	120
Los Alamos National Laboratory	New Mexico, USA	100	200
Brookhaven National Laboratory	Upton, New York, USA	200	90
TRIUMF: Canada' National Laboratory for Particle and Nuclear Physics	Vancouver, Canada	110	50
iThemba Laboratory for Accelerator Based Sciences	Faure, Republic of South Africa	66	150
ARRONAX (Accelerator for Research in Radiochemistry and Oncology at Nantes Atlantic) *	Nantes, France	70	2 × 375

* Being launched.

Table 2. Radionuclides produced at INR, RAS and the possibilities of producing them during one irradiation run at a current of 120 μA.

Radionuclide	Half-life period	Target	Energy range, MeV	Exposure time, h	Produced activity, Ci
Sr-82 *	25.5 d	Rb	40—100	250	5
Na-22 **	2.6 y	Mg, Al	35—150	250	2
Cd-109 **	453 d	In	80—150	250	2
Pd-103 **	15 d	Ag	50—150	250	50
Ge-68 **	288 d	Ga, GaNi	15—50	250	1
Sn-117m **	14 d	Sb, TiSb	40—150	250	3
Se-72 ***	8.5 d	GaAs	45—60	250	3
Cu-67 ***	62 h	Zn-68	70—150	100	10
Cu-64 ***	12.7 h	Zn	40—150	15	15
Ac-225 ***	10 d	Th	40—150	250	4
Ra-223 ***	11.4 d	Th	40—150	250	13

* Regularly produced.
** Technology is developed, test samples are delivered to a customer.
*** Production methods are developed, and technology is being developed.

production of radionuclides, predominantly for medicine. In 1991–1992, based on investigations and developments with minimal expenditures, a facility for the production of radionuclides in a diverted 160-MeV proton beam in a linear accelerator was built [2, 3], which became the word's highest facility for producing isotopes at that time. This facility, upgraded several times, continues to be one of the world's largest and is so far the only one operating in Europe and Asia. Today only a few such facilities exist in the world (Table 1).

We formulated the program of radioisotope studies based on principles which are quite obvious in the field of fundamental science, but have rarely been realized in Russia in applied studies to date:

— the development of only those areas in which we have an indisputable advantage over all other analogous developments in the world;

— the maximal optimization and permanent improvement of parameters to achieve the best efficiency;

— the combination of the results of our own scientific studies with technological developments, with the aim of their broad implication;

— the close scientific collaboration, as well as production and technical cooperation with leading world centers.

The specific feature of the linear accelerator at the Institute for Nuclear Research (INR), RAS is that it would simultaneously provide comparatively high-energy (160–600 MeV) protons and a high-intensity (100–500 μA) beam in the future. In principle, it can be used for producing not only various neutron-deficient isotopes but also neutron-excess isotopes. However, the production of only a few of these isotopes is expedient in such an expensive facility to be competitive with other methods and taking into account the volume of the potential market. Table 2 lists radionuclides which we produce or produced in the accelerator at INR, RAS. The facility provides radionuclides not only for medical and technical applications, but also for important fundamental studies, such as the investigation of high-spin isomers and the search for the neutrino mass [4–7].

The development of facilities for producing radionuclides was successful due to a close collaboration with colleagues from Canada's National Laboratory TRIUMF in Vancouver, and American specialists at the Los Alamos National Laboratory (LANL) and Brookhaven National Laboratory (BNL). Our foreign colleagues took part in the formation of the isotope program. The USA made a considerable investment for the development of medical isotope production in Russia within the framework of the program for Global Initiatives for Proliferation Prevention (GIPP). On the other hand, when a crisis in the production of strontium-82 for medicine occurred in the late 1990s due to the termination of operation of the isotope facility with an 800-MeV proton beam in Los Alamos, and the danger appeared that the continuous production of this very important radionuclide would cease, it was INR that played a decisive role in the solution to this critical problem [8–10]. The Institute supplied

targets irradiated at our accelerator for processing in the USA using Russian technology. In addition, we took part in the development of a new efficient facility on a diverted 100-MeV proton beam at the accelerator in Los Alamos laboratory [11]. Today, we are involved in a number of joint investigations, which are difficult or even impossible to perform without the participation of INR. The construction of the facility at Los Alamos in six to seven years was financed by the US government. According to estimates, about 150 thousand patients have already been diagnosed using isotopes prepared only in the accelerator at INR, RAS and recovered in the USA. It should be noted that the isotope produced in Los Alamos is supplied noncommercially to Russia for pre-clinical and clinical trials. In addition, American partners support the development of the independent production of selected radionuclides and radiopharmaceutical compounds in Russia. This collaboration, which is broadly discussed in the domestic press, is presented at a Nuclear Museum in Los Alamos as an example of fruitful international peaceful cooperation.

It is important that the unique accelerator at INR, which cannot be fully engaged in other domestic problems, is regularly in operation due to this work.

The methods elaborated in collaboration with Russian scientists are also used in Canada. At present, INR is involved in the development of a new powerful ARRONAX facility in Nantes (France) for the production of medical radionuclides. The construction of this facility is financed from several governmental sources.

2. High-intensity 160-MeV proton beam target facility

An accelerator beam facility at INR, RAS was constructed specially for the production of radionuclides with maximum efficiency [2, 3]. Some new, original developments were utilized in its construction. The facility control and safety systems are reliable and correspond to the highest world standards.

The laboratory spans five rooms in the beam zone and a control room located in an adjacent building. A proton beam with an energy of up to 160 MeV is directed to a separate underground room through an ion guide equipped with systems for beam and vacuum diagnostics. Targets are mounted in ultrastrong graphite slots at the edge of a horizontal rod (Fig. 1), which is inserted into a shielding cast iron cube about 180 t in weight. The targets are intensely cooled with water circulating in a closed loop. The construction of the beam entrance window between the accelerator vacuum and cooling water (metal lithium between two stainless steel sheets) allows using the window for many years and replacing it if necessary. A system of cooled graphite collimators with thermocouples provides an accurate control of the size and position of a high-intensity proton beam directly on a target.

The accelerator facility allows irradiating simultaneously several targets of different designs at different proton energies. The technical features of the INR linac allow the extraction of a 158-MeV proton beam, as well as beams of proton energies 143, 127, 113, 100, and 94 MeV, thereby minimizing the energy scattering of the beam. Already at present the shielding and the target cooling system permit the irradiation of targets with 120–140-μA beams.

The exploitation of the facility over the entire operation period has demonstrated that it is convenient to service, all its

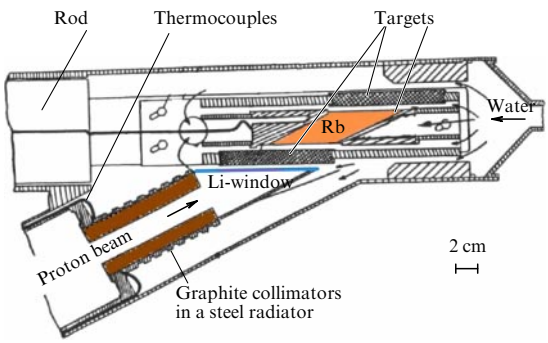

Figure 1. Target device in the proton beam of the INR, RAS accelerator.

systems operate reliably, and it can be used for fundamental studies and regular production of many important radionuclides for various applications.

3. Isotopes produced and production methods

3.1 Strontium-82

Among those isotopes for medical applications which can be produced using an intermediate-energy proton beam, strontium-82 (with the half-life period $T_{1/2} = 25.5$ days), obviously occupies the first place. This radionuclide is the most important product of all similar facilities (see Table 1). It is used in rubidium-82 medical generators applied in cardiologic diagnostics by means of positron-emission tomography (PET) (see section 3.2). At present, ^{82}Sr isotope is mainly produced in nuclear reactions Rb(p, 4n) and Rb(p, 6n) in the proton energy range from 40 to 100 MeV utilizing targets made of metallic rubidium or rubidium chloride. This radionuclide cannot be produced at small low-energy proton accelerators or in a nuclear reactor.

We use metal rubidium targets which are the most efficient for ^{82}Sr production. The targets irradiated at the INR accelerator are delivered to the LANL, where they are processed using radiochemical technology with rubidium dissolution. The extracted pure ^{82}Sr isotope is utilized in rubidium-82 generators mainly in clinics in the USA (Fig. 2).

Later on, we elaborated a new method for strontium extraction without rubidium dissolution, proceeding from ^{82}Sr sorption on different surfaces directly from melted rubidium [12]. The extraction of radionuclides from liquid metals is a complex and poorly studied physicochemical process involving the production of colloid particles in melted metal and chemical reactions on the surface. Our investigations have demonstrated the efficiency of this approach and the possibility of its application for extracting different radionuclides from the melts of other metals, for example, silver and lead. This makes the method promising for other applications, in particular, the recovery of valuable radionuclides from a lead–bismuth coolant upon transmutation of radioactive wastes.

Based on the investigations performed, a technology was developed for extracting ^{82}Sr nuclides from irradiated rubidium targets, which is utilized in hot cells at the Federal State Unitary Enterprise "State Scientific Center of the RF–Leypunsky Institute for Physics and Power Engineering" (SSC RF–IPPE) (Obninsk). It is planned in the future to built a new facility with a target made of circulating rubidium with the on-line extraction of produced ^{82}Sr, which will

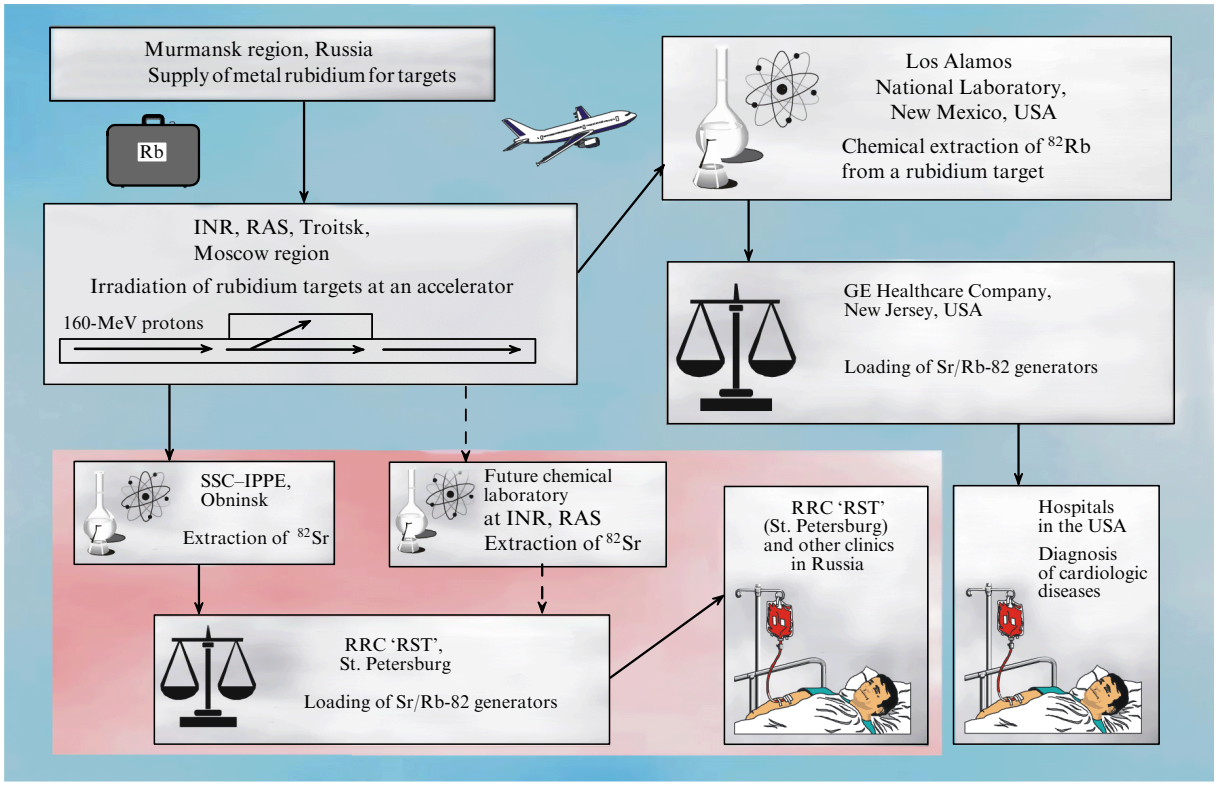

Figure 2. Production, transportation, and distribution of strontium-82.

drastically increase the efficiency. The INR, RAS holds patents on this technology [13].

The development of this new technology provided the production of proprietary pure ^{82}Sr and made it possible the fabrication of strontium/rubidium-82 generators for nuclear medicine in Russia and abroad (see Fig. 2).

3.2 Strontium/rubidium generator

The schematic of the generator's operation is illustrated in Fig. 3. Strontium-82 is absorbed on an ion-exchange column from hydrated tin dioxide. This radionuclide decays to short-lived ^{82}Rb ($T_{1/2} = 1.3$ min). A physiological solution (0.9% NaCl) is pumped through the column with the sorbent retaining Sr^{+2} ions, while Rb^{+} ions are washed out. The high ion-exchange properties are provided by the presence of microcrystallites (of size a few nanometers) on the sorbent surface [14].

^{82}Rb isotopes eluted from the column is introduced into the circulatory system of a patient for blood flow diagnostics. The decay of this radionuclide is accompanied by the emission of positrons, which annihilate, emitting two oppositely directed 511-keV gamma quanta. The blood supply of different organs, first and foremost of the heart, is measured with a PET scanner. This provides the effective diagnosis of the ischemia of the heart and other diseases. So far, such a generator (Cardiogen®) has regularly been produced only by the companies GE Healthcare and Nordion in North America. Our generator, developed in collaboration with Canadian researchers [15, 16], has much better parameters compared with its American counterpart. At present, our generator is successfully undergoing clinical trials at a laboratory equipped according to the GMP (Good Manufacturing Practice) standards at the Russian Scientific Center of Radiology and Surgery Technologies (St. Petersburg). However, numerous bureaucratic problems during transportation, customs formalities, and the receiving of licenses of different types have severely thwarted the adaptation process.

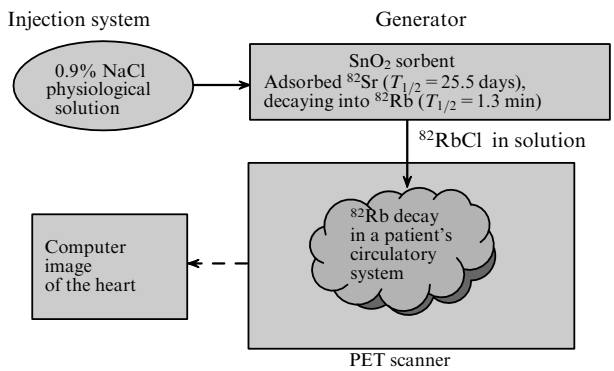

Figure 3. Operation principle of a strontium/rubidium-82 generator.

3.3 Tin-117m

This radionuclide is very promising for targeted immunotherapy in the medical treatment of atherosclerosis, bone cancer therapy, and other diseases [17]. Tin-117m emits monoenergetic Auger electrons with energies of 127 and 152 keV and fixed ranges of 0.22 and 0.29 mm, respectively, in water. This is the advantage of ^{117m}Sn over radionuclides emitting beta particles. The most efficient is a product with a high specific activity, which, unlike a product with a low specific activity, cannot be obtained by irradiation in a nuclear reactor.

^{117m}Sn with the high specific activity is produced in nuclear reactions of antimony with intermediate-energy protons: ^{121,123}Sb (p, 2p xn)^{117m}Sn. INR efficiently collaborates in this direction with BNL. This work is an example of utilizing fundamental studies in applied developments.

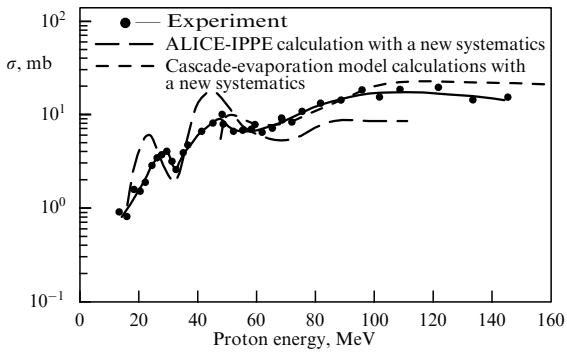

Figure 4. Calculated and experimental cross sections for ^{117m}Sn production upon irradiation of antimony by protons.

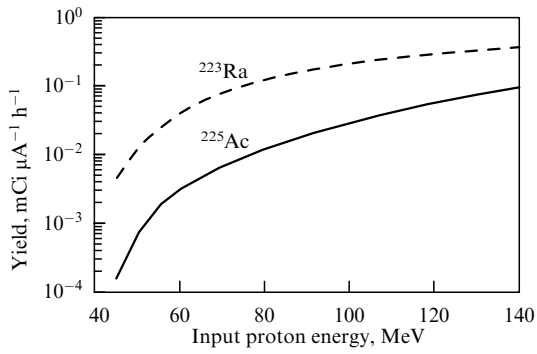

Figure 5. ^{225}Ac and ^{223}Ra yields in nuclear reactions of ^{232}Th as functions of the input proton energy in a thick target (calculations are performed for a 10-day exposure; the decay time after EOB is 10 days for ^{225}Ac, and 16 days for ^{223}Ra).

First of all, it was necessary to calculate the possible yield of ^{117m}Sn in nuclear reactions, its specific activity, and the level of radioactive impurities. The models that existed then could not provide the correct calculation of cross sections for isomeric states. We developed a new systematics which, in conjunction with the known ALICE-IPPE model (a version developed at the SSC–IPPE) and the Cascade–Evaporation–Fission (CEF) model (developed at INR, RAS), allows estimating isomeric ratios [5]:

$$\frac{\sigma_{\mathrm{m}}}{\sigma_{\mathrm{g}}} \approx a \exp\left[-b\left(J_{\mathrm{m}} - J_{\mathrm{t}}\right)\right],$$

where σ_{m} is the cross section for the isomeric nuclear state, σ_{g} is the ground-state cross section (it can be calculated from theoretical models), J_{m} and J_{t} are the spins of the produced isomeric nucleus and the target nucleus, respectively, and $a \approx 1.05$, and $b \approx 0.47$ are correlation coefficients. The experiments on production of high-spin isomers on different targets at different proton energies, on which a new systematics was developed, were conducted at the INR accelerator, the TRIUMF accelerator [4], and the cyclotron of the Joint Research Centre in Ispra (Italy) in collaboration with the scientists from the University of Milan.

The estimates of the ^{117m}Sn production cross sections, performed based on the developed systematics, were in good agreement with experimental cross sections [18] (Fig. 4). The specific activity in different irradiation regimes and the content of different impurities were also calculated.

We then developed technologies for manufacturing and irradiating targets containing antimony, and for the radiochemical recovery of ^{117m}Sn isotopes in hot chambers. Targets made of metal antimony in graphite or niobium shells [19] and of a TiSb intermetallic compound [20] were developed. The latter compound, which we produced for the first time in big amounts, is distinguished simultaneously by high thermal stability and high heat conduction and, therefore, constitutes a quite promising target material.

The methods for the production of ^{117m}Sn and its extraction from targets are protected by a number of Russian and foreign patents [19–22], and the technology is ready for mass production. Clinical trials are being undergone in the USA with the participation of BNL in collaboration with American commercial partners.

3.4 Actinium-225 and radium-223

Even more promising for radioimmunotherapy are alpha-active radionuclides [23]. The short ranges of alpha particles (smaller than 0.1 mm) and the high density of local energy release make alpha-emitters a rather efficient means for treating oncological diseases, which minimizes the irradiation dose of healthy organs and tissues. Alpha-radionuclides can be efficiently delivered to effected cells with the help of nanostructures based, in particular, on monoclonal antibodies [24].

Actinium-225 ($T_{1/2} = 10$ days) is one of the promising radionuclides for such a therapy, which can be used to destroy cancerous cells both directly and using daughter bismuth-213 ($T_{1/2} = 46$ min) obtained in an ^{225}Ac/^{213}Bi generator [25]. ^{223}Ra is also promising for nuclear medicine, and is already used as the drug Alpharadin® for medical treatment of the bone cancer diseases. The methods used earlier could not provide the production of ^{225}Ac and ^{223}Ra isotopes in big amounts.

Radionuclides ^{225}Ac and ^{223}Ra can be obtained irradiating thorium-232 by intermediate-energy protons [26]. Figure 5 presents the yields of ^{225}Ac and ^{223}Ra nuclides in thick thorium-232 targets as functions of the input proton energy, which were determined from the cross section measured in our experiments. Such high yields allow the production of these radionuclides in quantities of a few curies for only a week of irradiation at the accelerator. These amounts many times exceed the amounts produced by other methods. At the same time, due to nuclear spallation and fission reactions, numerous isotopes of other elements are produced in the target. We detected in the gamma and alpha spectra of irradiated Th-targets more than 80 radionuclides from which actinium and radium nuclides should be recovered by radiochemical methods. The method of actinium recovery was developed in collaboration with Moscow State University and the Frumkin Institute of Physical Chemistry and Electrochemistry, RAS by using liquid–liquid extraction and extraction chromatography, while radium was recovered by sublimation from a thorium–lanthanum melt and thermochromatographic separation in metal titanium columns (Fig. 6), followed by the additional purification of radium [27]. As a result, the opportunity opens for producing great amounts of radiochemically pure ^{225}Ac and ^{223}Ra isotopes valuable for nuclear medicine.

3.5 Other promising medical radionuclides

One of the advantages of the INR accelerator and the 160-MeV proton beam facility is the fact that several targets installed successively along the beam can be irradiated simultaneously. Thus, different targets are irradiated in

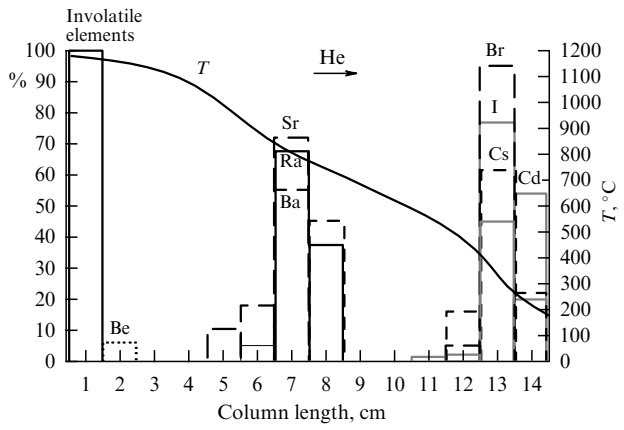

Figure 6. Thermochromatographic extraction of Ra with Sr and Ba from involatile (Th, Ac, Pa, La, Pm, Ce, Nd, Cr, Zr, Mo, Nb, Tc, Te, Sn, Sb, Ag, Ru, and Rb) and volatile elements, sublimated from a thorium–lanthanum melt, in a metal titanium column.

different proton energy ranges advantageous for the production of one isotope or another (see Table 1).

Simultaneously with a rubidium target irradiated in the energy range from 40 to 100 MeV, it is possible to irradiate metal silver at higher energies, and a gallium target at lower energies (see Table 1) to produce palladium-103 and germanium-68, respectively. These radionuclides are widely applied in medicine. ^{103}Pd is specifically tailored for prostate therapy in the form of special sources (Theragenics® seeds). Even more promising is the use of this radionuclide (as well as ^{117m}Sn) in the form of albumin microspheres [28] for the therapy of various diseases. ^{68}Ge finds use for calibration of positron-emission tomographs and manufacturing medical ^{68}Ga generators [29]. ^{103}Pd and ^{68}Ge nuclides can be produced more simply utilizing low-energy proton accelerators [30]. However, they can also be produced as by-products at the INR facility.

A new promising medical radionuclide, which cannot be obtained in low-proton energy accelerators, but can be produced in our accelerator, is selene-72 ($T_{1/2} = 8.5$ days), which serves as the generator of arsenic-72 ($T_{1/2} = 26$ h) emitting positrons and can find application in PET diagnostics. The high cross sections for the ^{75}As(p, 4n)^{72}Se nuclear reaction (which we measured for the first time) provide a high yield of ^{72}Se isotopes in targets containing arsenic. In accordance with our patent [31], a stable GaAs compound inserted into a niobium shell is utilized as a target. An efficient procedure was proposed for extracting ^{72}Se isotopes from the irradiated GaAs target by using sublimation and chemical reactions at high temperatures [3, 31]. Unfortunately, no efficient radiopharmaceutical drugs with ^{72}As radionuclides have been developed so far.

3.6 Isotopes for science and technology

Very important experiments are being carried out at INR, RAS on the search for the neutrino mass by analyzing the beta decay spectrum of tritium at the Troitsk-ν-mass installation [32]. To study volume charge effects in gaseous tritium, krypton-83m is of significance, emitting monoenergetic electrons with an energy close to the boundary electron energy in the beta decay of tritium. Krypton-83m is produced in the decay of ^{83}Rb ($T_{1/2} = 86.2$ days), which serves as the generator of ^{83m}Kr ($T_{1/2} = 1.86$ h).

We produced ^{83}Rb by irradiating strontium fluoride target with 100–120-MeV protons. Rubidium was extracted by the gas-chemical method: it was sublimated from an irradiated target at 1200 °C in a helium flow in a graphite apparatus and then deposited by a thin layer onto a metal foil. The foil was heated during experiments to evaporate ^{83m}Kr from a thin layer [6]. The use of this source contributed to the estimation of a new upper bound for the neutrino mass.

The INR accelerator can also be utilized for producing cadmium-109 from an indium target, and sodium-22 from an aluminium target (see Table 1). Both these isotopes are applied in science and technology: cadmium-109 is an important radionuclide used, in particular, in X-ray fluorescence analysis, while sodium-22 finds an application in Mössbauer spectrometry and in the physics of positronium. The experimental cumulative cross sections for the ^{109}Cd production from indium in the energy range from 80 to 140 MeV proved to be rather high. As a result, the yield of cadmium-109 upon irradiation of indium was many times higher than that in the previous method of producing this radionuclide by 800-MeV protons [33]. Both cadmium and sodium isotopes can easily be extracted from the irradiated target by the high-temperature sublimation methods [34] developed at INR, RAS.

4. New possibilities and outlook for the further development of isotope production

4.1 Modernization of the INR linear accelerator and the target irradiation facility

The linear accelerator at INR operates in the pulsed regime producing 200-μs, 14-mA pulsed beams at a pulse repetition rate of 50 Hz. The maximum admissible average beam current is determined in most cases by the target stability. The passage from a pulse repetition rate of 50 Hz to 100 Hz will provide an increase in the average current to the target by 20–30%. A beam sweeping system will ensure a more uniform distribution of pulsed thermal and radiation impacts over the target. Such systems were installed in other accelerators. As a result, the current can be approximately doubled, whereas the operational expenditures will increase insignificantly. Correspondingly, the amount of produced isotopes will increase. The target facility should also be modernized to improve the cooling of irradiated targets. Such a modernization can be performed during a short time, in one to two years.

4.2 Development of new efficient technologies and facilities for target processing

INR developed a number of techniques for the radiochemical extraction of radionuclides from different targets. Facilities based on radiochemical technologies of the ^{82}Sr and ^{117m}Sn recovery developed at INR in collaboration with SSC–IPPE operate in hot cells in Obninsk. Targets irradiated in the INR accelerator are processed in Obninsk and other institutions (LANL and BNL, Russian Scientific Center 'Applied Chemistry' in St. Petersburg, Tsiklotron Co., Ltd., Karpov Institute of Physical Chemistry in Obninsk, and Mayak Production Association in Ozersk, Chelyabinsk region). This involves large expenditures and considerable difficulties. The organization of a new production of ^{225}Ac and ^{223}Ra isotopes, which requires serious technological developments, is even more difficult.

The design of own radiochemical laboratory at INR, RAS with hot cells (an annex to operating building No. 17 with

waste processing plant) is completed. The project can be realized in four years, but this will require considerable expenditures.

4.3 Design of a new accelerator with target facilities

The INR accelerator is an efficient tool for producing various radionuclides. However, it is a complex and expensive facility which was constructed mainly for another purpose — investigations in the field of fundamental physics. In addition, facilities of this type cannot operate on a year-round basis and cannot provide the sufficient regularity of production of short-lived radioisotopes.

It is expedient to perform mass production of radionuclides at a special accelerator, probably of the cyclotron type. The ARRONAX accelerator (70 MeV, 750 μA) recently commissioned in France may cover the demand for ^{82}Sr isotopes for some time. However, the particle energy in this accelerator is too low for producing ^{225}Ac and ^{223}Ra in sufficient amounts (see Fig. 5). It is most appropriate to construct for this purpose a new H^- cyclotron with a particle energy of no less than 120 MeV, specially designed for the production of isotopes. It is assumed that such a cyclotron will have several beam lines with a total current of about 1 mA. It is reasonable to install it in the already existing building No. 25 of the experimental complex at INR, RAS.

The new accelerator can be used to realize a new technology for ^{82}Sr production from circulating rubidium with direct sorption from liquid metal. Many technical devices for systems with a liquid sodium coolant utilized in fast-neutron reactors have already been developed in Russia. As a result, it would be possible to produce ^{82}Sr isotopes in amounts of no less than 300 Ci per year, which exceeds the existing world's total ^{82}Sr consumption level. The rapidly increasing number of PET devices will provide a growing market for this radionuclide. Other beam lines in the cyclotron may serve for the regular production of ^{225}Ac, ^{117m}Sn, and other isotopes. In addition, the proton beam can find applications in proton therapy. The fulfillment of this project would make Russia a leading manufacturer of many important radionuclides, providing the diagnostics and therapy of many hundreds of thousands patients per year.

This project, including the modernization of the INR accelerator, the construction of the hot cell laboratory, the production of generators, and the construction of the new high-power cyclotron, has passed a scientific and technical expertise by the Russian Corporation of Nanotechnologies (RUSNANO)[1], and been approved. However, financing is still not allocated and when it will come through is still uncertain. The system of state regulation existing at present is becoming more complicated, hindering the development and commercialization of new technologies.

5. Conclusion

Based on our own scientific studies and technological developments, the researchers at INR, RAS have organized the production of radionuclides playing an important role for nuclear medicine in Russia and the world. To achieve further considerable progress, it is necessary to upgrade the existing facilities, to construct new facilities and buildings, and to develop new technologies. This would significantly increase the potential of nuclear medicine, most of all in the diagnosis of cardiological diseases and the medical treatment of oncological diseases. The scientific and technological problems are quite solvable. State financing all the world over always plays a great role in projects of this type; however, a considerable investment to provide progress in this field in Russia is rather problematic.

[1] On 21 March 2011, the State Corporation ROSNANO was transformed into Open joint-stock company RUSNANO (*Editor's footnote*).

References

1. Vyalov G N et al., Preprint No. 761/92 (Moscow: INR RAS, 1992)
2. Zhuikov B L et al. *Radiokhimiya* **36** 499 (1994) [*Radiochemistry* **36** 554 (1994)]
3. Zhuikov B L et al. *Nucl. Instrum. Meth. Phys. Res. A* **438** 173 (1999)
4. Zhuikov B L et al. *Phys. Rev. C* **68** 054611 (2003)
5. Zhuikov B L, Il'inov A S *Yad. Fiz.* **69** 766 (2006) [*Phys. At. Nucl.* **69** 739 (2006)]
6. Belesev A I et al. *Yad. Fiz.* **71** 449 (2008) [*Phys. At. Nucl.* **71** 427 (2008)]
7. Barabanov I R et al. *Yad. Fiz.* **73** 1144 (2010) [*Phys. At. Nucl.* **73** 1106 (2010)]
8. Wilson E *Chem. Eng. News* **76** (15) 13 (1998)
9. Phillips D R et al. *Radiochim. Acta* **88** 149 (2000)
10. Phillips D R, Zhuikov B L, Kolsky K L, in *The 4th Intern. Conf. on Isotopes, Cape Town, South Africa, 10–14 March, 2002* (Cape Town: NECSA, 2002) p. 32
11. Phillips D R et al., in *The 7th Intern. Conf. on Advanced Technology and Particle Physics, Villa Olmo, Como, Italy, 2001*, p. 76
12. Zhuikov B L, Kokhanyuk V M, Vincent J C *Radiokhimiya* **50** 162 (2008) [*Radiochemistry* **50** 191 (2008)]
13. Zhuikov B L, Ermolaev S V, Kokhanyuk V M, RF Patent No. 2356113 (2008); *Byull. Izobret.* (14) (2009); PCT Application RU 2009/000124 (2009)
14. Rumyantseva M N et al. *Vestn. Mosk. Univ. Ser. 2. Khim.* **42** 348 (2001)
15. Chudakov V M at al. in *The 5th Intern. Conf. on Isotopes, Brussels, Belgium, 25 – 29 April, 2005*, p. 9
16. Zhuikov B L et al., in *Fundamental'nye Nauki — Meditsine* (Fundamental Sciences for Medicine) (Moscow: Slovo, 2007) p. 105
17. Srivastava S C et al. *Clin. Cancer Res.* **4** 61 (1998)
18. Ermolaev S V et al. *J. Labeled Compounds Pharmaceut.* **50** 611 (2007)
19. Zhuikov B L et al., RF Patent No. 2313838 (2006); *Byull. Izobret.* (36) (2007); Zhuikov B L, Ermolaev S V, Kokhanyuk V M US Patent, Application No. 11/962851 (2007)
20. Seropegin Yu D, Zhuikov B L, Srivastava S, RF Patent No. 2403639 (2008); *Byull. Izobret.* (31) (2010); US Patent, Application No. 12/424944 (2010)
21. Zhuikov B L et al., RF Patent No. 2393564 (2008); *Byull. Izobret.* (18) (2010); US Patent, Application No. 12/424992 (2010)
22. Ermolaev S V et al., RF Patent No. 2398296 (2008); *Byull. Izobret.* (24) (2010); U.S. Patent Application No. 12/425038 (2010)
23. Mulford D A, Scheinberg D A, Jurcic J G *J. Nucl. Med.* **46** 199S (2005)
24. Sobolev A S *Usp. Biol. Khim.* **49** 389 (2009)
25. Dubinkin D O et al., Preprint IPPE-2927 (Obninsk: Institute for Physics and Power Engineering, 2001)
26. Zhuikov B L et al. *Radiokhimiya* **53** 66 (2011) [*Radiochemistry* **53** 73 (2011)]
27. Zhuikov B L, RF Patent No. 373589 (2008); *Byull. Izobret.* (32) (2009); Zhuikov B L, PCT Application RU 2009/000462 (2009)
28. Petriev V M et al., RF Patent No. 2359702 (2007); *Byull. Izobret.* (18) (2009)
29. Krasnov N N et al., RF Patent No. 2331439 (2008)
30. *Radioizotopnaya Produktsiya* (Radioisotope Production) (Obninsk: ZAO "Tsiklotron", 2003)
31. Zhuikov B L, Kokhanyuk V M, U.S. Patent No. 5987087 (1999)
32. Lobashev V M et al. *Phys. Lett. B* **460** 227 (1999)
33. Zhuikov B L et al. in *The VII Int. Workshop on Target and Target Chemistry, Heidelberg, Germany, 1997*, p. 210
34. Zhuikov B L *J. Radioanal. Nucl. Chem.* **263** 63 (2005)